

**MAGNETICALLY ACTUATED PHYSICAL  
IMPINGEMENT FOR ELUTION OF ARTIFICIAL  
MUCOUS FROM A SWAB**

**MAGNETICALLY ACTUATED PHYSICAL  
IMPINGEMENT FOR ELUTION OF ARTIFICIAL  
MUCOUS FROM A SWAB**

By SHUBHAM BANIK, B. Eng.

A Thesis Submitted to the School of Graduate Studies in Partial Fulfilment  
of the Requirements for the Degree Master of Applied Science

McMaster University © Copyright by Shubham Banik, March 2017

McMaster University

MASTER OF APPLIED SCIENCE (2017)

Hamilton, Ontario

Mechanical Engineering

TITLE:

MAGNETICALLY ACTUATED PHYSICAL  
IMPINGEMENT FOR ELUTION OF ARTIFICIAL  
MUCOUS FROM A SWAB

AUTHOR:

SHUBHAM BANIK, B.Eng.

SUPERVISOR:

Professor P. R. Selvaganapathy  
Department of Mechanical Engineering

NUMBER OF PAGES

xxii, 166

## **Abstract**

Swabs are used as a collecting device for many biological samples and its complete elution is a desired step for clinical and forensic diagnostics. Swabs are made of cotton, rayon, polyurethane, foam or polyester and come in a spun or flocked-tipped format. They are used to extract biological samples from a patient, which includes saliva, mucous, blood, semen or other body fluids. These body fluids then undergo the process of elution where the collected samples are extracted from the swabs into an elution fluid. Apart from biological samples, the importance of swabbing and elution also becomes more evident in forensics, when the concentration of available cells is very low. One such example is rape kit analysis. Another field of application is the capture and release of bacterial spores from environmental contact surfaces and food surfaces, which also indicate the use of swabs in non-biological areas.

The recovery of the biological material from the fibre matrix of the swab has a significant influence on diagnostic sensitivity of any assay. The recovery of microorganisms from a matrix of swab fibres depends on the nature of the body fluid, the type of the swab fibres and the process of elution. Various methods are used to elute samples from swab, including the use of chemicals to digest the cotton fibres to remove intact cells (~20% recovery), centrifugation (~58% recovery), piezoelectric vibration or pressurized fluid-flow (~60% recovery). These methods are either passive (chemical elution) or provides a gentle tangential shear force through associated flow (centrifugation,

piezoelectric and pressurized flow), resulting in a low recovery. The success of all the downstream processes of elution, like lysis, DNA amplification and detection, depends on the number of cells eluted from the swab fibre matrix. Hence, the recovery efficiency is an important parameter for determining the performance of elution, and higher value of the same is desired for most diagnostic assays.

This thesis reports a magnetically-actuated physical impingement method for elution and recovery of artificial sputum samples from cotton fibres. A device has been fabricated to induce a rotating magnetic field on smaller magnetic particles in a vial for striking the swab within a confined gap. Elution of samples from the swab using this device was demonstrated using artificial sputum prepared by mixing 2% methyl cellulose in deionised water, loaded with fluorescent-tagged polystyrene beads and *Escherichia coli* bacteria at various concentrations. The recovery efficiency was found to increase with both rotational speed and elution time, but plateaus after 400 RPM and 120s respectively. At higher concentration of polystyrene beads, a maximum recovery of ~85% was achieved at  $5 \times 10^8$  particles/ml sample. With lower concentration ( $10^6$  particles/ml), the maximum efficiency (~93%) was found to be almost twice of the static condition (46.7%), while using only 620 $\mu$ L of elution volume. Similar trends were found in experiments with artificial sputum loaded with *E. coli* cells, and the maximum recovery was found to be ~90% at  $10^5$  CFU/ml concentration.

The robust design and smaller size allows the device to be used in different clinical, forensic and laboratory settings. Also, due to cheaper means of manufacturing and assembly, the vials and smaller magnets can be discarded after every experiment, thereby

preventing contamination. The device is most suitable for recovering cells from different body fluids like saliva, mucous, semen or blood, absorbed by the swab fibres. Apart from body fluids samples, swabs holding biological agents from environmental surfaces can also be eluted. A higher recovery at lower concentration facilitates the use of this device where the available analyte concentration is low.

## **Acknowledgement**

First, I would like to thank Dr. P. Ravi Selvaganapathy for this wonderful opportunity to work in the Centre for Advanced Micro-Electro-Fluidics Lab of McMaster University. It has been a long, tedious journey to the finishing line of my MASc program and I am grateful that he has always been alongside me throughout this process. With all the invaluable instructions, guidance and learning procedure, the past two years have provided a lot of good memories.

My thesis was supervised by Dr. Ravi from Mechanical engineering. He had guided me throughout the entire length of my research project, on matters of both educational and professional development. Apart from various project directions, they also acted as a critique to my poster and oral presentation skills. They inspired me with their Engineering and Biological insights on my project and were always available to cater to my needs. I sincerely thank their efforts in putting up with me, with their calm and patient approach.

I would also like to thank Dr. Chan Ching and Dr. James Mahony for their inputs in all those glorious group meetings, that made me improve my presentational skills. My special thanks also to Dr. Robert H. Pelton and Mr. Doug Keller to let me use their research facilities and helping me in the process. Marta Prinz from the Bio-Interfaces Institute and Marcia Reid from Health science also deserves my utmost thanks for helping me out during my biological experiments.

Finally, my sincere thanks go to the guys from the Mechanical workshop, Ron Lodewyks, Mark Mackenzie, John Colebrander, Michael Lee and Dan Wright, without whose support I could not have created my device. I'm grateful to my colleagues, Leo Hsu, Aditya, Reza Ghaemi, Ali Shahid, Juncong Liu, Mohammadhossein Dabaghi, Ali Akbar, Pankaj Saini, Michael Zlatin, Shayan Liaghat, Kamrul Russel, Sondos Ayyash, Rana Attala, Melizeth Bolanos and Celine Ling for their continuous support and helping hands. I would specially like to thank Dr. Suvojit Ghosh, Dr. Souvik Pal, Dr. Rakesh Prasad Sahu and Priyanka Pal who always fed me with useful suggestions and ideas, since the very first day I landed in Canada and have become a part of my extended family.

Outside work, I would like to thank my parents and my sister for always believing in me. None of this would have been possible without them. An inspiring environment created by all these people helped me finish my journey as a Masters student. Maybe I didn't always find the right time and right words to show my gratitude but I'm grateful to all these people for providing me with a background to improvise myself.

## Table of Contents

<b>Abstract</b> .....	<b>iii</b>
<b>Acknowledgement</b> .....	<b>vi</b>
<b>Table of contents</b> .....	<b>viii</b>
<b>List of Figures</b> .....	<b>xii</b>
<b>List of Tables</b> .....	<b>xvi</b>
<b>List of Abbreviations and Symbols</b> .....	<b>xvii</b>
<b>Chapter 1: Introduction</b> .....	<b>1</b>
1.1 Motivation.....	1
1.2 Organization.....	3
1.3 Contributions.....	5
<b>Chapter 2: Literature review</b> .....	<b>6</b>
2.1 Introduction.....	6
2.2 Importance of elution in DNA analysis.....	9
2.3 Swabs.....	10
2.4 Body fluids.....	16
2.5 Elution techniques.....	20
2.5.1 Mechanical techniques.....	21
2.5.1.1 Vortexing.....	21
2.5.1.2 Abrasion.....	25

2.5.1.3 Sonication.....	26
2.5.1.4 Thermal elution.....	27
2.5.1.5 Pressurized flow.....	28
2.5.1.6 Indirect contact-based elution.....	29
2.5.1.6.1 Piezoelectric vibrations.....	29
2.5.1.6.2 Compression and squeezing.....	30
2.5.2 Chemical techniques.....	34
2.5.2.1 Effect of enzymes.....	36
2.5.2.2 Effect of detergents.....	37
2.5.2.3 Effect of buffers.....	39
2.6 Effect of nature of swabs on recovery.....	41
2.7 Summary.....	42
<b>Chapter 3: Conceptual design.....</b>	<b>44</b>
3.1 Introduction.....	44
3.2 Design criteria.....	45
3.3 Working principle.....	46
3.4 Acting forces and the motion of the magnetic particles.....	49
3.5 Nature of fluid motion.....	54
3.6 Device layouts.....	56
3.6.1 First design.....	58
3.6.2 Modifications of the device.....	60
3.7 Device fabrication.....	63

3.8 Electrical control.....	63
3.9 Motor calibrations.....	64
3.10. Advantages of the technique.....	66
<b>Chapter 4: Materials and Methods.....</b>	<b>68</b>
4.1 Swabs.....	68
4.2 Absorptivity.....	69
4.3 Actuating Magnet.....	70
4.4 Polystyrene beads.....	73
4.5 Bacterial Samples.....	74
4.6 Artificial Sputum.....	74
4.7 Device Characterizations.....	75
4.8 Experimental setup.....	76
4.9 Experimental procedure.....	78
4.10 Quantification of beads and cells.....	79
4.11 Quantification techniques.....	79
4.11.1 High concentration ( $10^9$ - $10^7$ /ml): Particle counting.....	80
4.11.2 Low concentration ( $10^7$ - $10^5$ /ml): Fluorescent Intensity measurements....	81
4.11.3 Very Low concentration ( $<10^5$ /ml): Plating technique.....	83
4.12 Recovery Efficiency.....	84
4.13 Summary.....	85

<b>Chapter 5: Results &amp; Discussions.....</b>	<b>87</b>
5.1 Effect of magnetic impingement.....	87
5.2 Effect of Sample Viscosity.....	94
5.3 Characterization.....	97
5.3.1 Effects of rotational speed of magnet.....	97
5.3.2 Effect of time.....	105
5.3.3 Effect of concentration.....	109
5.4 <i>E. coli</i> Samples.....	117
5.4.1 Effect of rotational speed.....	117
5.4.2 Effects of rotational speed at lower concentrations.....	121
5.4.2.1 Low concentration.....	126
5.5 Summary.....	127
<b>Chapter 6: Conclusion and Future Works.....</b>	<b>129</b>
6.1 Conclusions.....	129
6.2 Future works.....	132
Appendix A: Measurement of forces on the swab.....	134
Appendix B: Device design & fabrication.....	136
Appendix C: Machining processes.....	144
Appendix D: Ring magnets vs bar magnets.....	146
<b>References.....</b>	<b>150</b>

## List of Figures

Fig. 1 Types of swab tip: Cotton, Flocked, Polyester, Foam, Rayon and Calcium Alginate swabs. [Source: Puritan Swabs] .....	13
Fig. 2 Different types of swab heads: Flat top cylindrical, round top cylindrical, conical head, funnel. [Source: Cleanroom swabs Inc.] .....	16
Fig. 3 Specimen test unit with a blister end [80] .....	29
Fig. 4 Swab Elution Chamber in a Test Cartridge by actuated impact [12] .....	30
Fig. 5 Sampling deice with conditioning fluid [13] .....	31
Fig. 6 Liquid recovery device by wringing [81] .....	32
Fig. 7 Centrifuge tubes with squeezable bulges [82] .....	33
Fig. 8 Comparison of sperm cell recoveries for different detergents [87] .....	38
Fig. 9 Effect of DE buffer pH on recovery efficiency [89] .....	39
Fig. 10 Working principle: rotational motions induced by the diametrically magnetized magnet .....	48
Fig. 11 Variation of kinetic energy imparted to the swab by the magnetic particles and forces acting on the swab with RPM .....	52
Fig. 12 Variation of measured forces on the swab vs the number of impacts per minute by the particles .....	53
Fig. 13 Fluid motion generated by different trajectories of the magnetic particles .....	55
Fig. 14 Device layout .....	59
Fig. 15 Schematic of the modified device .....	61
Fig. 16 Modified vial to with internal helical groove .....	62

Fig. 17 Electrical connections of the motor to the controller .....	64
Fig. 18 Rotational speed (RPM) vs Voltage calibration curve .....	65
Fig. 19a Magnetic effect on the particle motion when magnetic particles are used .....	72
Fig. 19b Magnetic effect on the particle motion when ferromagnetic particles are used .....	72
Fig. 20 Schematic of the experimental setup to characterize the elution of particles and cells from the swab .....	76
Fig. 21 Experimental Setup: Second device .....	77
Fig. 22 RFU vs concentration for polystyrene samples, $5 \times 10^4 - 1.25 \times 10^6$ particles/ml range (Gain: 143) .....	82
Fig. 23 RFU vs concentration for polystyrene samples, $\sim 2.4 \times 10^3 - 7.8 \times 10^4$ particles/ml range (Gain: 196) .....	82
Fig. 24 RFU vs concentration for <i>E. coli</i> samples, $1.12 \times 10^5 - 7.16 \times 10^6$ particles/ml range (Gain: 100) .....	83
Fig. 25 RFU vs concentration for <i>E. coli</i> samples, $1.4 \times 10^4 - 8.9 \times 10^5$ particles/ml range (Gain: 158) .....	83
Fig. 26 Comparison of recovery efficiencies for elution without agitation and with magnetic impingement of swabs dipped in 10% v/v ( $\sim 10^9$ particles/ml) concentrated samples .....	89
Fig. 27 Comparison of recovery efficiencies for elution without agitation and with magnetic impingement of swabs dipped in 5% v/v ( $\sim 5 \times 10^8$ particles/ml) concentrated samples .....	90
Fig. 28 a) Distribution of polystyrene beads on swab fibres before elution, b) fibres post elution (no agitation) c) fibres post elution (magnetic beads agitation) – 1000x .....	94

Fig. 29 Distribution of polystyrene beads on swab fibres after elution with a) no agitation b) magnetic agitation – 5000x .....	94
Fig. 30 Comparison of recovery efficiencies for elution with artificial sputum and with DI water with 10% v/v ( $\sim 10^9$ particles/ml) bead concentration .....	96
Fig. 31 Number of eluted particles vs rotational speed for different elution times at 10% v/v ( $\sim 10^9$ particles/ml) concentration .....	99
Fig. 32 Recovery Efficiency vs rotational speed for different elution times at 10% v/v ( $\sim 10^9$ particles/ml) concentration .....	101
Fig. 33 No of eluted particles vs rotational speed for different elution times at 5% v/v ( $\sim 5 \times 10^8$ particles/ml) concentration .....	103
Fig. 34 Recovery Efficiency vs rotational speed for different elution times at 5% v/v ( $\sim 5 \times 10^8$ particles/ml) concentration .....	104
Fig. 35 Recovery Efficiency vs elution time for different rotational speeds at 10% v/v ( $\sim 10^9$ particles/ml) concentration .....	108
Fig. 36 Recovery Efficiency vs elution time for different rotational speeds at 5% v/v ( $\sim 5 \times 10^8$ particles/ml) concentration .....	109
Fig. 37 Effect of concentration on Recovery efficiencies at higher rotational speeds (120s elution time) .....	111
Fig. 38 Recovery Efficiency vs rotational speed for different elution times at 1% v/v ( $10^8$ particles/ml) concentration .....	113
Fig. 39 Recovery Efficiency vs Rotational speed for different elution time at 0.01% v/v ( $10^6$ particles/ml) concentration .....	115
Fig. 40 Recovery Efficiency vs Rotational speed for different elution time at 0.001% v/v ( $10^5$ particles/ml) concentration .....	115

Fig. 41 Recovery efficiency vs Rotational speed for $\sim 6 \times 10^9$ CFU/ ml concentration samples at different elution times .....	119
Fig. 42 Recovery efficiency vs Rotational speed for $\sim 6 \times 10^8$ CFU/ ml concentration samples at different elution times .....	120
Fig. 43 Recovery efficiency vs rotational speed for low concentration samples at 2 min elution time .....	123
Fig. 44 Recovery efficiency vs rotational speed for low concentration samples at 1 min elution time .....	124
Fig. 45 Recovery efficiency vs Rotational speed for high concentration samples at 2 min elution time .....	125
Fig. 46 Experimental setup for measuring forces with load cell .....	135
Fig. 47 Device and its parts .....	137
Fig. 48 Exploded view of the device .....	139
Fig. 49 Schematic of the modified device and its parts .....	141
Fig. 50 Exploded view of the modified device .....	142
Fig. 51 A) Ring with symmetric axis (z) and radial polarization, B) Infinitely long parallelepiped approach. [55] .....	147
Fig. 52 a) Different positions of the rotating bar magnet along the outer circumference. b) Magnetic remanence along the circular surface c) Acting forces on the magnetic particles when they are placed parallel to each other .....	148
Fig. 53 a) Different positions of the rotating ring magnet along the outer circumference. b) Magnetic remanence along the circular surface .....	149

## List of Tables

Table 1. Types, characteristics and usage of various swab heads .....	13
Table 2. Various vortexing techniques of elution .....	24
Table. 3 Effect of different swab tip materials on Recovery [90] .....	42
Table 4. Forces imparted to the swab by the particles and the total kinetic energy .....	51
Table. 5 Water absorptivity of the swab fibres .....	69
Table 6. Impact forces offered by the magnetic particles on the swab tip at different rotational speeds .....	100

## List of Abbreviations and Symbols

a	center distance
A	Surface area
AU	Arbitrary Units
B	Magnetic flux density
b	width
BA	<i>Bacillus anthracis</i>
B <sub>r</sub>	Residual Induction
BVAB	Bacterial vaginosis-associated bacteria
C	Coefficient
CFU	Colony Forming Unit
CTAB	Cetyl Trimethylammonium Bromide
CHAPS	3-[(3- <b>ch</b> olamidopropyl)dimethyl <b>ammonio</b> ]-1- <b>p</b> ropanesulfonate
C <sub>s</sub>	mass concentration of the substance on the surface
CSF	Cerebrospinal Fluid
C <sub>b</sub>	mass concentration of the substance in the bulk of the solvent
D	Diffusion coefficient

d	thickness of boundary layer
DC	Direct Current
DE	Differential Extraction
DI	Deionised water
DNA	Deoxyribonucleic acid
DS	Degree of Substitution
DTT	Dithiothreitol
E	Electromotive force
EBV	Epstein–Barr virus
<i>E. coli</i>	<i>Escherichia coli</i>
EDTA	Ethylenediaminetetraacetic Acid
F	Force
GFP	Green Fluorescence Protein
HCMV	Human cytomegalovirus
H	Magnetic field strength
h	height
HSV	Herpes simplex virus

i	gear ratio
I	Moment of Inertia
$I_m$	mass imbalance
KE	Kinetic energy
LB	Lysogeny broth or Luria-Bertani
LCST	Lower Critical Solution Temperature
m	module
MNV	Murine Norovirus
MSA	Mannitol Salt Agar
N	Rotational speed
NEC	Nucleated Epithelial Cells
PBS	Phosphate-buffered saline
PBST	Phosphate Buffered Saline Tween-20
PCR	Polymerase Chain Reaction
ppi	pores per inch
Pro-K	Proteinase K
r	distance from enter

RCF	Relative Centrifugal Force
RNA	Ribonucleic Acid
RPM	Revolutions per minute
SDS	Sodium Dodecyl Sulfate
SEM	scanning electron microscope
SOS	Sodium Octyl Sulfate
t	time
v	velocity
VZV	Varicella zoster virus
z	number of teeth

**Suffix**

b	bulk
c	centrifugal
D	drag
M	magnetic
rot	rotational

s surface

### **Greek Symbols**

$\beta$  helix angle

$\mu$  dynamic viscosity

$\mu_0$  permeability of space

$\rho$  density

$\sigma$  surface magnetic pole density

$\omega$  rotational speed (rad/s)

*Dedicated to my Late father,  
who made me what I'm today*

# Chapter 1

## Introduction

### 1.1 Motivation

Many biological samples are collected using swabs and complete elution of the sample from the swab fibres is a desired and crucial step in clinical diagnostics. Swabs are made of cotton, rayon, polyurethane foam or polyester and come in a spun or flocked tipped format. They are used to extract biological samples from a patient, which includes mucous, saliva, blood and semen, among other body fluids. Apart from biological agents, swabbing techniques are also used for collecting touched evidence samples for DNA analysis [1], recovery of spores from environmental surfaces [2-4], or removal of dried blood stains from surfaces [5]. These samples are then eluted from the swab fibres for further analysis. “Elution” is defined as a technique of separation of one material from another using a solvent.

The most common samples collected by swabs are human body fluids. These samples are eluted from the swab fibres and the number of eluted particles is affected by the density, viscosity and concentration of cells in the respective samples. The concentration of pathogens in the body fluids for various disease conditions can range from  $10^4$  CFU/ml [6] in the case of respiratory-tract infections and  $10^5$  CFU/ml for urinary-tract infections [7] up to  $2 \times 10^8$  CFU/ml (*Staphylococcus aureus* and *Escherichia coli*) in the case of infected peritoneal fluid [8] and  $10^9$  CFU/ml in dental cases [9]. Higher elution efficiency is desired

for all these collected samples for accurate clinical diagnostics. The necessity of higher elution efficiency becomes more prominent in forensics when the concentration of available micro-organisms is very low. One such example is rape kit analysis. Recovery efficiency of spermatozoa collected from a victim's body which is typically as low as 10%, could potentially affect the diagnostic accuracy of any assay, leading to incorrect characterization of the sample as negative to presence of sperms. [10]

Several methods of elution have been adopted for recovering maximum amount of sample analyte from the swab tip. Conventional techniques for elution include chemical digestion of fibres to remove intact cells and application of mechanical forces encompassing vortexing [11], piezoelectric vibration [12] or pressurized fluid flow [13] (~60% recovery). For instance, chemical techniques involving cellulase digestion of cotton have been used for recovering sperm cells by *Aspergillus niger* enzymes and have shown ~18% efficiency [10]. Similarly, cellular recovery of norovirus and rotavirus from environmental and food surfaces by simple centrifuging have been shown to produce in recovery efficiency of 52 and 58% respectively [11]. Some mechanical impingement techniques comprise of swab analysers with actuator and flexible wall [12] and compressible chambers with a blister containing conditioning fluid [13]. These two elution techniques offer a maximum of ~68% of recovery, which is insufficient for cases where there is low concentration of the microorganism of interest. They also have higher elution volumes, ranging from 0.7 to 5ml. The recovery efficiency of the pathogenic cells from the fibre matrix of the swab has a significant influence on diagnostic sensitivity of any assay. Hence, higher recovery of cells from the swabs is desirable with a lower elution time and elution volumes.

This thesis focuses on developing a robust technique for elution of cotton-tipped applicator swabs for an improvement in recovery efficiency. Several techniques of elution have been previously adopted by inducing convective flow against the swab tip that could enhance the elution process. However, fluid mechanical forces are quite gentle and have not produced high elution efficiencies. For better elution results, higher eluting forces are necessary on the swab fibres. A simple, low-cost technique is needed for elution of samples that will increase the recovery efficiency using lower volume and lower elution time. Mechanical techniques that operate by direct physical impact on swabs can generate higher forces and is one promising avenue. Hence, this thesis investigates the use of magnetically actuated mechanical impingement of particles on to the swab as a method of elution and characterizes the elution efficiencies to demonstrate its effectiveness.

## **1.2 Organization**

This thesis is organized into the following chapters:

**Chapter 2** offers a full literature survey and comprehensive study on the conventional and currently available techniques of elution. Brief introduction is offered on the different types of commercially available swabs, the types of body fluids and methods of elution. The mechanical and chemical techniques of elution of swabs are described. The use of impact as a way of mechanically eluting swabs is emphasized, which forms a strong background for the development of the device described in this thesis.

**Chapter 3** starts with a description of the design criteria that provides the framework for the device design. The working principle of the magnetically actuated physical

impingement method is explained, providing details of the nature of impact forces on the swab fibres. The advantages of the device over existing methodologies are demonstrated.

This chapter also describes the device fabrication and its assembly. A modified device is designed in order to have a compact form factor and its design and construction are detailed. Experimental procedures used in performing characterization experiments by changing the rotational speed, time for elution and the concentration of particles are elaborately explained. Characterization of the swab before and after elution are performed and the microscopic images are presented.

**Chapter 4** offers a comprehensive database of the materials used in the experimental setup and procedures. The type of swab fibres and magnetic particles used in these experiments are discussed. A recipe for preparing artificial mucus is added along with the detailed description of fluorescent-tagged polystyrene beads and *E. coli* that are mixed with it. Furthermore, it describes different techniques for detection of polystyrene and *E. coli* cells in the samples for enumeration both before and after elution. The concept of recovery efficiency is introduced to explain the performance of the experiments.

**Chapter 5** provides detailed analysis of the results obtained for different  $c$ , compared over three different parameters: rotational speed, elution time and concentration. Separate experiments were made with artificial sputum samples mixed with polystyrene beads and *E. coli*. The trends in the plots are compared for both. Physical significances of these parameters on the swab fibres and nature of sample are explained.

**Chapter 6** concludes the report with contributions of the device and possible future works on the elution processes.

### 1.3 Contributions

The main contributions of this research are as follows:

- A mechanical process of elution is proposed that applies strong forces to the swab fibres by direct contact in order to achieve high elution efficiency.
- The reported method of elution provides impact forces on the swab fibres by smaller magnetic particles, imposed by an external rotating magnetic field. A simple low-cost device was designed, capable of generating the rotating magnetic field around a vial and fabricated using laser micromachining and 3D printing. This device uniquely allows simultaneous rotation and revolution of the particles around the swab to ensure complete coverage over the entire surface area of the swab. This allows the device to use lower elution volume (~620  $\mu$ l) and lower elution time (~2 min) to yield maximum recovery. Using this novel approach, the highest recovery efficiency among the available elution methods was achieved.
- Three different detection techniques have been identified for cell counting for accurate enumeration at different concentration ranges. Post elution measurements, as low as  $\sim 10^4$  CFU/ml, has been made with plating techniques.

## Chapter 2

### Literature Review

#### 2.1 Introduction

The Biology-Online dictionary defines elution [14] as:

*“The process of extracting a substance adsorbed to another by means of a suitable solvent or buffering agent”.*

Elution plays an important role in several bio-chemical assays and is a critical factor in the accuracy of these assays.

Biochemical assays are analytical processes that are used to detect and quantify the presence, or activity of a biological molecule. There are various kinds of biochemical assays such as cell-based, protein-based and nucleic acid based assays. Cell-based assays use proliferation of cells in a culture media to identify presence, viability [15], cytotoxicity [16-18] and other growth related parameters associated with cells [19-20]. Protein or enzyme based assays also known as “immunoassays” use the binding of the target antigens with its antibody that is fixed onto a substrate as the mechanism of detection and identification [21-22]. Usually, another protein that carries a label and binds with another end of the target protein is used to amplify the signal from the binding event for higher sensitivity [23-25]. Finally, nucleic acid based assays use the unique property of DNA, which consists of two complementary strands, to provide recognition. Various methods such as hybridization [26-28] and amplification [29-32] are used to detect and amplify the

target nucleic acid from the sample. These biochemical assays are used in several applications including disease diagnostics, environmental monitoring, food quality analysis, cytotoxicology, drug discovery, as well as fundamental biological studies. In all these analyses, proper, accurate and complete extraction and preparation of the biomolecule of interest from the other contaminating/interfering species that may be present in the sample is critically important.

Sampling is the very first step in the preparation of biochemical assays used for pathology testing and analysis of environmental samples. Sampling is defined as the process of collection of biological or environmental samples containing the target analyte for further extraction and analysis. The collection process of specimens and samples from a human body or any environmental surfaces contribute to the accuracy and reliability of those tests. [33] Various biological matrices such as saliva, sputum, urine, faeces and semen are often collected for bio-chemical assays in research or clinical settings. Saliva, sputum, vaginal samples, semen, forensic samples and blood spots are collected using a swab. Saliva and sputum can also be collected by expectorating (cough up or spit) into a container. Urine, stool and semen are generally collected in a container or receptacle directly and often undergoes a filtering process. Blood is taken either by a fine needle in syringes or specialized absorbent collection cards for immunoassays [34]. Samples of body tissues can only be obtained by more invasive procedures. Cerebrospinal fluids are obtained by lumbar puncture whereas bone marrow aspiration is required for examining blood cells present in the marrow.

Swabs are one of the most widely used sample collection devices when sample volumes are low. They are low cost, easy to use, have high absorptivity and are ideal for sample

transportation. Cotton tipped swabs and applicators are most common due to their low cost and, in some cases, can yield better analytical sensitivity than other materials such as nylon. For instance, they yield significantly better results in salivary immunoassays for testosterone and estradiol [35].

Other materials used for swabbing purposes include macrofoam, nylon, filters, rayon or dacron. For example, absorbent materials like saline-wetted dacron swabs, cytobrush, and emery paper were used to collect exfoliated cells from external male genitalia. These were later analysed for HPV (humanpapillomavirus) using a PCR based assay. [36]. Rayon or dacron-tipped collection devices are used mostly as transport swabs and for rapid diagnostics in PCR assays. They are used as transport swabs because the open-weave rayon bud is non-toxic and contains Amies medium with inorganic buffer which preserves microorganisms without overgrowth. They have inferior absorbent characteristics than cotton but superior release properties. [37].

Apart from biological samples, swab based collection is also critical for environmental samples and samples collected from food surfaces as they allow a large area to be sampled. The bacterial spores collected from food or metal surfaces are collected using swabs and eluted to determine the extent and source of contamination [2].

Sampling process is followed by elution, where the collected materials are transferred from the collection device to a separate elution volume. Elution is an integral part of major biological testing processes. The success of all the downstream process like lysis, PCR and detection is a function of the number of organisms collected from sampling devices. Hence, there is a need for proper specimen collection and elution for all assays. The most common method of elution is dipping the swab in an elution buffer and application of mild agitation

to the fluid. Mild agitation results in a small number of cells being recovered from the fibre matrix. Lower recovery of organisms can potentially influence the downstream analysis of the assay and the sample and can result in false negatives or inaccurate quantification [38]. For instance, elution has critical significance in cases of extraction of genetic materials from bloodstains obtained from victim's clothing [39] where the biomaterial of interest may be at low concentration or amount.

Elution is closely associated with the complexity and nature of samples that undergoes processing. Two important parameters are viscosity and concentration of cells in the sample. Samples with saliva, nasal sputum and sperm requires elution steps prior to processing because of their higher viscosities and densities. These samples have a greater tendency to remain attached to the sampling device and require significant driving force for its removal. Another important parameter is the concentration of the samples. In forensics, elution has a greater importance where the available concentration is very low. For instance, removal of dried blood stain samples from fabrics requires higher elution efficiency prior to subsequent DNA analysis steps [5]. Some of these samples are exposed to environment for a prolonged period of time and hence there is a significant loss of sample. Because of its low availability, maximum recovery of cells is desired from these samples.

## **2.2 Importance of elution in DNA analysis**

Nucleic acid based assays are increasingly used for molecular diagnostics of human diseases [40] which includes identification of disease-causing pathogens, genetic or protein markers that are liable for various human diseases. One of the common use is the

identification of bacterial infection of patients presenting with cold and fever. Usually, a nasal swab is taken to collect mucous or sputum samples from these patients and the infectious agents is then analysed using culture or molecular methods. Elution of samples collected from these swabs is an important pre-processing step prior to DNA analysis of a specimen. Complete elution of body fluids from swab is essential for clinical and forensic diagnostics where the sample concentration or amount may be low. Higher recovery from the elution ensures sufficient number of cells are available for proper lysis and amplification. Lower concentration of pathogens offers lower sensitivity during diagnostic tests and care is taken to maximize the yield by maximising the number of pathogens recovered after elution. The eluted cells then undergo lysis and DNA amplification before it can be detected through electrochemical or optical sensing. The success rate of all these downstream processes of elution depend on the recovery of pathogenic cells from swab tips.

### **2.3 Swabs**

Swabs are the most commonly used sampling devices for collection of specimens for further analysis. It is a type of applicator device, which consists of a fibrous head and a shank. Among different collection devices (e.g. absorbent pads, porous heads, filters, wipes, brushes etc.), swabs are the most popular collection device owing to their low cost and ease of use. Swabbing procedures are quick, relatively painless, comfortable and have no adverse side-effects. Swabs use passive capillary flow of liquid into their absorbent porous tips to collect sample from a location. The ability of the swabs to hold a large amount of liquid in their pores is also used for storage and transport of biological or clinical

samples, that are collected in a remote settings. These swabs should be able to maintain the viability of the organisms for a certain period, before it is processed. These transport swabs are made up of non-toxic open-weave rayon bud and contains Amies medium with inorganic buffer which preserves microorganisms without overgrowth. Transport swabs are used for transfer of anaerobic and fastidious aerobic organism, [41] and were compared to swabs using other mediums (Stuart's medium) that yield better recovery [42].

Swabs are used for collection of a varied range of body fluids especially those that are located in body cavities. For instance, secretions from throat, nose and buccal cavity are mostly collected using swabs. Samples of vaginal secretion and endometrial tissues are also collected using swabs. Swabs are also used for collection of samples from a wound or sore present on the epidermal layer of skin especially where localized extraction of sample is needed. Apart from these, blood in small volumes is often collected using cotton-tipped swab applicators [33].

Apart from biological samples, swabbing techniques are also used for collection of samples from touched evidence [1], recovery of spores from environmental surfaces [2, 4], or removal of dried blood stains from fabrics [5]. Depending on the field of application, the nature of the collection device can be varied to double-swab for touched evidence samples [1], dry and pre-moistened swabs, or macrofoam swabs (environmental surfaces) [2]. After collection, these samples undergo elution, where the analytes are transferred to an elution volume for further analysis.

A complete range of dry or pre-moistened swabs are used for clinical purposes to suit most applications. Swabs basically consists of two parts, namely: the swab shaft and the tip

- The swab **shaft**, which is 10-23 cm long [43] and are made of wood or plastic. They are usually cylindrical, straight wire (urethral) or fine twisted wire (paediatric and nasopharyngeal) [44].

- The swab **tip**, which is usually made of cotton, rayon, foam, polyester, or polyurethane. In some cases, calcium alginate or albumin coated swab head tips are also used. Calcium alginate swabs are used for sample isolation from areas such as the eyes, ears, nasopharynx, urethra and paediatric ENT (Ear nose throat) or recovery of spores from environmental surfaces [45]. Albumin coated swabs are used primarily for nasal, wound site or skin lesion samples for MRSA (methicillin resistant *Staphylococcus aureus*) screening [46]. Examples of various swabs types are shown in Figure 1. Detailed characteristics and application of all these swabs (based on the type of swab tip) are given in Table 1. Most of these swabs are used for collecting samples of human body fluids. These body fluids include saliva, nasal mucus, semen, vaginal fluid, blood and urine. Apart from body fluid samples, swabs are also used for collecting samples from food and metal surfaces. Foam and cotton swabs have high absorbency and are used for collecting surface samples. Special pre-moistened swabs [47] are also used for swabbing food surfaces in food processing and beverage industries.

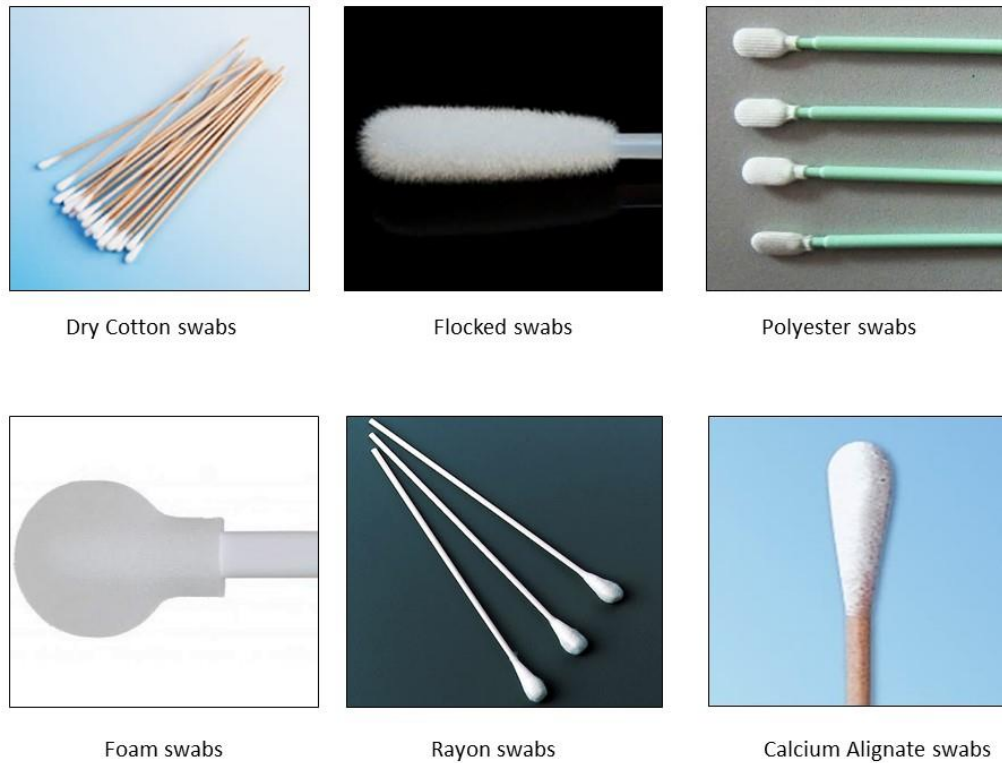


*Fig. 1 Types of swab tip: Cotton, Flocked, Polyester, Foam, Rayon and Calcium Alginate swabs. [Source: Puritan Swabs]*

<b>Types of swabs</b>	<b>Characteristics</b>	<b>Application</b>
Cotton	Pharmaceutical-grade spun cotton fibres	Most commonly used swab: from basic patient care to crime scene investigation
Foam	Medical-grade polyurethane foam, produced in sheet form in a range of ~100 ppi (pores per inch) porosity	Chemical-resistant swabs

Knitted Polyester	Woven polyester fabric, commonly made without soluble adhesives	Used as cleaning tools, introduces the least number of contaminants to swabbing process
Polyester/Dacron	Synthetic spun fiber made from a polymer, good in collection and release properties	Specimen collection in microbiology, rapid test diagnostics, and PCR analysis
Rayon	Spun fiber made from wood pulp, soft and absorbent, can substitute cotton	Transport swabs
Calcium Alginate	Organic material, derived from seaweed, alginate fibers are slowly dissolved by body fluids and tissues	Contains no fatty acids and hence can be used for many strains of Gonorrhoea
Flock	Unique microstructure and multi-length fibers of flocked swabs, enhance rapid absorption and complete elution of biological specimens	Sampling of small or elusive specimens

*Table 1. Types, characteristics and usage of various swab heads [44, 47]*

Copan Inc. has recently developed a patented technology to make highly absorbent swabs. Copan's patented flocked swabs [48] use electrostatic field to spray short Nylon fibres onto the swab tips. Flocking is a process where the fibres are sprayed perpendicularly onto the tip of the swab, while it is held in an electrostatic field. The process creates a

highly absorbent thin layer of fibrous matrix with an open structure. Capillary action between swab fibres enable better holding capacity and easy elution.

Swabs can be made of different types of head (Figure 2), designed specifically for the sampling location and the type of sample matrix to be absorbed. These include flat top cylindrical head and round top tapered head swabs. Round and cylindrical tops are generally used for nasal and blood sampling. Cotton and rayon tipped swabs of cylindrical heads have a tip length of 17-18 mm and 5-6 mm diameter. Round top heads with larger surface area has tip length of 56-58mm and diameter of 15-16 mm. Swabs with higher surface areas are used predominantly for swabbing environmental and food surfaces [37, 49]. Conical head swabs are preferred for vaginal cases and funnel shaped ones with lower cross sections are used for buccal cavity. Smaller conical shaped swabs for cleaning small slotted areas have head width of 4mm and thickness of 3.5mm. Funnel top and conical head swabs of smaller length of swab head is used for ear infections.

It is also important to understand the choice of collection device based on the compatibility of the organism. Some swab fibres have adverse effects on the organisms or even some foreign particulates collected with them. For a long time, this was not taken into consideration. Perry et al. [50] pointed out the necessity of using the correct type of swabs by citing an example about a failed experiment concerning the toxic effects of sponge swabs on *Neisseria gonorrhoeae*, which then highlighted the need for careful study and comparative evaluation of swab types and tip materials used for each purpose. Subsequently, standardized protocols for swabbing and elution methods were developed for quality control of microbiological recovery [51]. To maintain the viability of micro-

organism long after they are collected, it is necessary that the swab tip material be non-toxic or non-inhibitory to the organisms.

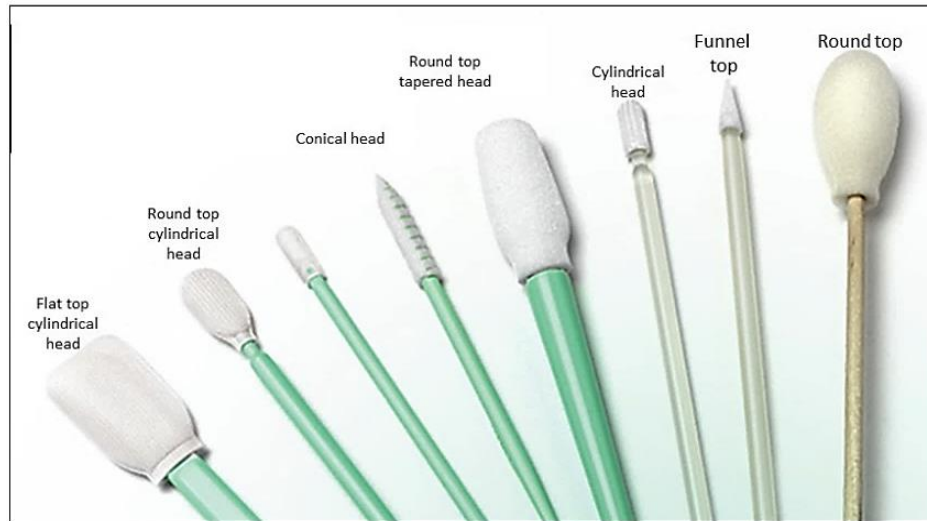


*Fig. 2 Different types of swab heads: Flat top cylindrical, round top cylindrical, conical head, funnel. [Source: Cleanroom swabs Inc.]*

Most body fluids are collected by swabs, prior to their respective elution. The selection of swabs is based on the ease of application and nature of the sample to be collected. Saliva, nasal mucus, semen, vaginal fluid, blood and urine are the principle body fluid samples collected by swabs. These samples are characterized by their key properties – viscosity, density and concentration. These parameters constitute the key criteria that determines the elution efficiency. Hence, detailed analyses of body fluids are required.

## **2.4 Body fluids**

Body fluids constitute the different secretions obtained from various parts of the human body. Swabs are used to collect most of these body fluids such as saliva, mucus, blood,

vaginal fluid, urinary tract or semen. Certain properties like the concentration of cells, viscosity and density of these body fluids affect the rate of recovery from swab fibres. Most of the samples such as mucus from the nose used to determine respiratory infection contain a single type of body fluid. Others such as forensic samples collected at a crime scene can contain a mixture of two or more body fluid types [52].

Saliva is the prime body fluid that is collected by swabs and is important for the diagnosis of endocrine, infectious and immunological conditions. Saliva comprises of a mixture of secretions from the major and minor salivary glands and traces from the gingival crevicular fluid. It functions as a cleansing solution for the buccal cavity, a buffer and an ion reservoir of calcium and phosphate. Saliva has an average pH of  $7 \pm 0.3$ , buffering capacity (moles of acid/base required to change the pH by 1) of  $5.2 \pm 0.5$  and relative viscosity levels of  $1.1 \pm 0.15$  compared to water [53]. Salivary assays are made with 2-12ml of samples extracted from the buccal cavities with buccal cytobrush or buccal foam swab. A range of pathogen concentrations has been reported depending on the type of disease that was dealt with. For example, Sahin et al. [9] found salivary HCMV (Human cytomegalovirus) of  $\sim 4.2 \times 10^4$  CFU/ml and salivary EBV (Epstein-Barr virus) of range  $3.6 \times 10^2 - 1.6 \times 10^9$  /ml in major periodontitis patients. Higher proportions ( $4.5 \pm 2.2 \times 10^5$  /ml) of *P. gingivalis* was found in patients with EBV [54] while  $1.2 \times 10^4 - 2.1 \times 10^5$  /ml concentrations of HSV-1 (Herpes simplex virus) were found in patients with Herpetic lesions [55]. Salivary samples from patients with Ramsay Hunt Syndrome showed higher concentrations of VZV (Varicella zoster virus  $2.6 \times 10^4$  CFU/ $\mu$ l) [56].

Nasal mucus is the second most common body fluid for swabbing purposes and is categorized based on the viscosity of the samples. Sputum, a mixture of mucus and saliva

coughed up from the respiratory tract, is categorized into: Mucoïd, Mucopurulent and Purulent. Their respective viscosities for samples, collected from chronic bronchitis patients and calculated at a shear rate of  $90 \text{ s}^{-1}$ , was found to be around 0.42, 0.46 and 0.7 Pa-s [57]. Elasticity of mucoïd or mucopurulent nasal discharge samples were found to be around  $31.8 \pm 3.1 \text{ Pa}$  [58]. Small volumes (100 - 1200  $\mu\text{L}$ ) of mucus samples are usually collected with cylindrical nasopharyngeal cotton or flocked swabs. A wide range of bacterial concentrations have been found in mucus of infected patients. For instance, Gwaltney [59] reported a combined concentration of *Streptococcus pneumoniae* and *Haemophilus influenza* to be  $\geq 10^7 \text{ CFU/ml}$  in nasal mucous samples from acute community-acquired sinusitis patients (ACAS). However, lower concentrations of pathogenic *P. aeruginosa* bacteria ( $665 \pm 75 \text{ CFU/ml}$ ), a clinical isolate of *S. aureus* ( $58 \pm 9 \text{ CFU/ml}$ ) and *E. coli* HB101 ( $351 \pm 115 \text{ CFU/ml}$ ), were found in airway surface fluid of trachea of patients suffering from chronic airway infections [60].

Blood is another major body fluid which is collected by swabs. Physical parameters of the blood depend on its origin, like from vomit, diarrhoea, lung, endocrine or kidney infections. The average pH value is around 7.35-7.45, with a relative viscosity of 4 – 5 over water, that rises with haematocrit percentage [61]. Mostly, syringes or cotton swabs are used to collect small volumes of blood (0.8 – 5ml). In case of blood, the concentration of available pathogen is relatively low. Around 45% of septicemia and meningitis cases involve bacterial loads of less than  $10^5 \text{ CFU/ml}$  [62]. These may include *Haemophilus influenzae*, *Streptococcus pneumoniae*, *S. agalactiae*, *Listeria monocytogenes*, enteric bacteria, and *Mycobacterium tuberculosis*. Still lower concentrations of *Salmonella typhi* (387 CFU/ml) was registered by Wain et al. [63] in the blood of typhoid fever patients.

Apart from the most common body fluids, urine also contains a significant number of pathogenic cells. Urine is slightly acidic with pH 6, but can range from 4.5 – 8 depending on the diet [64]. It has a lower viscosity ( $8.02 \times 10^{-3}$  Pa-s) and higher discharge rate 10 - 21 ml/s. 1 – 10ml of urine samples are usually collected for analysis. Different ranges of bacterial concentration have been detected in urine. For instance, Nakamura et al [65] detected  $10^5$ - $10^6$  viable bacterial cells/ml in urine collected from patients with urinary tract infections. The normal range of *E. coli* in urine is considered to be within the range  $10^2$ - $10^4$  CFU/ml. Similar concentrations ( $10^5$  CFU/ml) was found in patients with urinary-tract infections by Najjar et al. [7]. Higher concentrations ( $10^6$  –  $10^8$  CFU/ml) of *Salmonella enterica* and *Enterococcus faecalis* were found in urine samples collected from sanitation systems [8].

Sperm cell recovery is a critical area in sexual assault samples of forensic cases. Semen samples are collected from the undergarment fabric or from the victim's vagina. Semen samples of healthy males have an average pH level of 7.1 – 8 [66]. Viscosity of semen is measured qualitatively based on its rate of coagulation and greatly affects the motility of sperm cells. Typical sperm count of a healthy male average around  $34 - 157 \times 10^6$  /ml in semen [67]. For experimental purposes, 1.5 – 6.5ml of semen are collected. But in case of rape victims, sometimes dried semen samples are also extracted from undergarment fabrics.

Vaginal fluid secretion is another body fluid that is collected by swabs. Secretions extracted from the vagina of a healthy woman has a pH of 4 – 5, which also depends on the menstrual, cervical and uterine secretion. The viscosity and physical consistency of vaginal mucus changes at different times of the menstrual cycle. Conical vaginal swabs

with higher surface areas are used to extract vaginal secretions for infectious bacterial evaluation. For instance, significant amounts of BVAB3 ( $1.4 \times 10^6$  to  $1.9 \times 10^4$  /swab) and *Lactobacillus crispatus* ( $4.6 \times 10^5$  -  $6.9 \times 10^7$  /swab) were found in the vaginal fluid of women with bacterial vaginosis [68].

The concentration of pathogens varies greatly, depending on the nature of disease and type of body fluid. The primary aim of the swab is to collect a higher amount of body fluid to obtain maximum possible pathogen for further analysis. Several techniques of elution are therefore adopted for this purpose.

## **2.5 Elution techniques**

To enhance the recovery of micro-organisms from swab fibres, various methodologies have been adopted. Current techniques include mechanical forces, chemical digestion of cotton fibres, electrophoretic and magnetophoretic methods of elution of biological agents. LB broth is used for elution in a separate vial that requires post-processing cell culture, whereas PBS buffers are commonly used as elution media for cases where the sample is directly loaded to the PCR chamber. Several chemical techniques also use a range of buffers, detergents and solvents as their eluents. Each of the elution techniques have their own advantages and disadvantages, although some processes are suited for a specific type of bacteria. Various techniques of elution from swabs are discussed and the parameters associated with elution such as the time, efficiency, elution volume, elution time are provided for each of them.

### **2.5.1 Mechanical techniques**

Several methods for removal of samples from swabs have been reported in the literature, and a majority of them involve mechanical forms of elution. These processes typically provide a gentle tangential shear force through associated flow (centrifugation, piezoelectric or pressurized flow) to aid recovery of materials from the swab. Vortexing and convective flows are the most used technique for a significant number of elution devices. Sometimes, convective flow is accompanied with different mechanical methods of agitation of swab fibres for higher recovery of materials. Mechanical elution processes can be applied to a varied range of swabs and is independent of the physical and chemical characteristics of the swab tip. The various mechanical processes of elution include agitation by vortexing, abrasion by physical contact, sonication, compression, piezoelectric vibration, pressurized flow and wringing. Among mechanically induced processes, liquid extraction techniques involving vortexing comprise the most popular approach.

#### **2.5.1.1 Vortexing**

Vortexing is a technique where the swabs are immersed in a vial of elution fluid and the fluid is rotated by external means. The convective nature of the flow around the swab fibres allows the materials adhered to the swab to be separated from the fibres both by diffusion and advection. The rotational speed is an important parameter in vortexing, that determines the rate of elution. The rotational speed is measured in RPM (revolutions per minute) or by a specific parameter called the Relative Centrifugal Force or g-force.

$RCF \text{ or } g\text{-force} = 1.12 \times R \times (\text{RPM}/1000)^2$ , where R is the radius of spinner.

Vortexing can be used on a varied range of samples and swab types, and has low elution times. Cotton, flocked, rayon, foam and polyester swabs are used with vortexing. In some cases, the whole swab is used during elution, but sometimes the swab tips are also removed from the shank and immersed into the vial. Typical elution fluid volume used in vortexing based elution ranges from 0.5-5 ml, while the typical rotational speeds are 8000 – 15000 x g. As an example, vortexing has been used for recovery of bacterial spores in environmental samples from cotton, macrofoam, polyester and rayon swabs with an average recovery of 6.6% and 26.7% for dry and pre-moistened swabs respectively [4]. In another example, samples taken from cutaneous lesions, containing *B. anthracis* ( $10^7$  CFU/ml), were also eluted by vortexing [69]. Three types of swabs, flocked-nylon, rayon, and polyester were used in this process. A swab extraction tube system was used with 500 $\mu$ L of PBS for centrifuging for 1 min at 8,000 x g speed. Low recoveries of 6 – 9% were obtained from this method. Due to this low recovery efficiency, as with this case, vortexing is sometimes repeated for two or more steps or accompanied by another means of elution to enhance the rate of recovery.

Repeated steps of vortexing has been used to elute the *Bacillus anthracis* spores from swabs with environmental samples [2]. Separate experiments were made in these cases to extract BA spores samples (Phase 1) and BA combined with dust and background organisms (Phase 2). In this method, pre-moistened macrofoam swabs were vortexed in 5ml PBST (Phosphate Buffered Saline Tween-20) for 2 min in 10s bursts and the eluted samples were processed to count the number of colonies. These bursts create a periodic convective flow in the swabs that helps in better elution. This procedure can detect between

1 and  $0.2 \times 10^6$  spores/cm<sup>2</sup>, with an ability to recover 27.9 to 55% spores. It allows comparatively higher recoveries (~26 – 31%) than standard vortexing.

Special enzymes to facilitate easy elution have been combined with vortexing in order to increase the efficiency of elution. For instance, Cellmark Labs offers two methods namely, sperm elution and water elution methods for the elution of sperm cells. The “Cellmark’s sperm elution” method [70] combines a special elution buffer consisting of proteinases that can digest the proteinaceous matrix material without lysing the sperm cells. This process use two stages of vortexing at high speeds as method of agitation. This technique facilitates elution of sperm cells from cotton swabs. 750 µl of Mo Lite buffer (pH 7 – 8) is used as an eluent for vortexing at 15,115 x g for 5 minutes. (*Mo Lite buffer (pH 7.0–8.0) was prepared by diluting PBS ten times in Milli Q water*) After the supernatant was removed, 50 µl of cell pellet remained, which was again transferred to a solution of 750 µl Mo Classic buffer (*Mo Classic buffer (pH 8.0–9.0) was prepared using a 20% Sodium Dodecyl Sulphate (SDS), diluted twenty times in 0.01 M Tris buffer (pH 8.5))*) and 30 µl of diluted proteinase K. They are sonicated for 5mins followed by 5mins of vortexing to complete the entire elution. Higher sperm recovery was obtained with Cellmark’s sperm elution techniques over that of water elution. A combination of this enzyme with vortexing was able to increase the elution efficiency from 25% to 71%. Lower recovery was obtained from samples of lower concentrations, with the corresponding values being 26% and 11% respectively.

Swab elution methods for different vortexing techniques were analysed by Allard et al. [71]. Different speed, elution time and elution volumes were compared for these techniques that are based on water-based elution and are shown in Table 2. Most of these

techniques require higher elution times (~5 minutes) and yields low recovery efficiency (max 71%). For vortexing processes associated with chemical techniques, the amount of elution volume is higher (~750 – 1000  $\mu$ l) and requires several steps of pre-soaking before the vortexing period. Hence, although vortexing enhance the recovery to a certain limit, the total process time increase several folds.

<b>Swab/Volume of eluate</b>	<b>Method</b>	<b>Spin speed/ Time</b>
Tip in 50 $\mu$ l	Macerate (soaking) on slide	
Whole in 1000 $\mu$ l	Soak 60 s, agitate, vortex to produce extract. If weak, extract may be pelleted.	13000g for 5 min
Half with 25 $\mu$ l	Leave 60 s, agitate, pipette off 5 $\mu$ l liquid from swab.	
20% with 40 $\mu$ l on slide	Palpate (by touch) on slide, squeeze out and wipe swab on paper for AP (acid phosphatase) test.	
Whole in 200 $\mu$ l	Agitate vigorously for 2–5 min, vortex	11000 rpm for 5 min
Whole in 400 $\mu$ l	Swab placed in Dolphin filter tube with 200 $\mu$ l, pummel (strike), repeat with further 200 $\mu$ l, spin	14000 rpm for 1min
Whole in 300 $\mu$ l	Agitate vigorously for 2–5 min, vortex, spinaroo,	11000 rpm for 5 min
Whole in 50 $\mu$ l then add 100 $\mu$ l	Filter tube, agitate, leave 20 min, spin, remove filter, vortex	8000 rpm for 3 min
	Roll damp swab onto slide	

Whole in 400 µl	Differential extraction in 450 µl with 50 µl ProK (Proteinase K), vortex, incubate, spin, resuspend pellet in 350 µl with ProK, spin	13,000 rpm for 4 min twice
-----------------	--	----------------------------

Table 2. Various vortexing techniques of elution [71]

### 2.5.1.2 Abrasion

Abrasive contact is an effective method of elution. Different techniques have been reported that extract materials from swabs using electrostatic wipes, roller sampler and contact plates. Each of these processes use physical contact to extract the samples from the swab surface by gentle scrubbing. These techniques are used for recovery of samples collected from environmental and metal surfaces by swabs. For example, A comparative performance was made by Lutz et al [72] for extraction of *Staphylococcus aureus* from swabs containing environmental samples using electrostatic wipes, roller sampler and contact plates. The electrostatic wipes were wiped on the rayon swab surface three times and then processed with a membrane filter for concentrating the bacteria. Roller samplers were made using a custom autoclavable mould filled with molten mannitol salt agar (MSA), which also serves as a growth medium for the bacteria. They were then dried for 10 minutes at room temperature before using it on the swabs. These cylindrical samplers were rolled on the swab head to squeeze out materials from the surface. Contact plates utilize the downward pressure of its weight on the swab surfaces. MSA were also utilised to prepare 60mm contact plates with a convex meniscus. The convex side is kept downwards while pressing it against the swab head. Subsequently, recovery efficiencies of

bacterial cells were calculated from these techniques. These techniques of elution showed recovery efficiencies of 18% for electrostatic wipes, 10% for roller sampler and 0.04% for contact plates. These abrasive processes have lower recoveries compared to vortexing or convective flows. The tools that produce the scrubbing effect are also responsible for removal of swab fibres and contaminating the elution fluid.

### **2.5.1.3 Sonication**

Sonication is another method of agitation for elution of materials from swabs. Sonication uses fluid vibration to elute the samples from the swabs. The to and fro movement of the fluid particles offered by the periodic vibration of the bath allows dissociation of materials from swab fibres by shearing forces caused from high frequency sound waves. In this process, an ultrasonic bath is used to provide necessary agitation to the swabs. Swabs containing samples are hydrated in 2ml screw cap tubes and then ultrasonicated at 50-60 kHz for 15mins in a bath. Nylon, rayon and polyester swabs are the most popular types of swabs used in this technique. This technique can be used for both environmental and clinical samples. For example, ultrasonication has been used for recovery of skin lesion samples with *B. anthracis* from clinical swabs for diagnosis of cutaneous anthrax [69]. A relatively low recovery (0.07%) has been observed in these samples. Sonication has also been used for recovery of *Francisella tularensis* in environmental samples from cotton, polyester, rayon or foam swabs [73]. Significantly higher recoveries (~32.1%) were obtained with a cellular concentration of  $10^5$  CFU/ml in the samples. Another important area of application is the recovery of *Bacillus anthracis* spores from nonporous surfaces. Dry rayon swabs were used for collecting spores from 10-

25 cm<sup>2</sup> steel stainless surface areas to yield lower recovery efficiencies of 7.6% by sonication [74]. When premoistened swabs are used, there is an increase in the recoveries (17.75 and 13.6% respectively), but is still lower than the corresponding values obtained from vortexing (43.7 and 41% respectively) [4]. Sonication is an expensive process for elution, that can recover very low amounts of analyte from swabs. Also, the periodic vibration is not sufficient for effective elution, resulting in low recovery [73-74] and can also remove some fibres from the tip. Hence, it is the least used method among all the mechanical processes of elution.

#### **2.5.1.4 Thermal elution**

Thermal energy has also been utilised for elution of certain bacterial cells [75]. Thermal elution is used primarily in cases where there is also a need to lyse the cells, since the proteins that are present either on the surface or inside them are the analytes of interest in subsequent diagnostics [76]. Heat is utilized to release antibodies from the samples by disrupting the antigen-antibody bonds. This process can be used with cotton, foam, polyester and rayon swabs. Often thermal elution of swabs is combined with vortexing to enhance the recovery efficiency. In this method, the swab tips are rehydrated in 300µl PBS aliquots after sample collection and kept in 2-ml screw-cap tubes. The swab and its samples are incubated at moderate temperature (such as 65°C) for high durations of time (~10 mins). After heating, the swabs are vortexed at 8000 x g for 30s to remove residual liquids. Some gram negative aerobic bacteria have been eluted at high temperature from rayon swabs. For instance, Swabs spiked with *F. tularensis* were thermally eluted to yield an average of 31.1% recovery efficiency [73]. Another example of thermal elution is the Landsteiner heat

elution technique [77-78] which involves providing heat at 56°C for 10 minutes and shows a 47% recovery efficiency. Thermal processes have a significant advantage in DNA analysis techniques, since appropriate amount of heat can elute and lyse the cell walls simultaneously, thereby combining two steps together in one device. When associated with vortexing, the thermal processes of elution can elute significantly higher cells than vortexing, but it is still significantly less than that obtained from chemical techniques. Moreover, it denatures the cell membrane and causes dissociation by change in membrane structural configuration [79].

#### **2.5.1.5 Pressurized flow**

Some devices also use pressurized flow to elute samples from the swab tip. These devices [80] contain eluent fluid in a hollow shank that can be pressurized out of the swab tip using a blister bulb at the other end. (Figure 3). The forward end of the unit has a short stem of a brush with bristles that acts as a swab for collection of analytes. During use, the rear end of the swab is pressed to break the capsule containing reagents, which forces the fluid through the porous plug and hollow shank to the bristles. This pre-moistened swab acts as a better absorbent of biological samples. Due to the pressurized flow, the excess fluid from the swab head drips in droplets along with the eluted materials, and hence we have a small elution volume. This unit also shows enhanced performance in direct antigen testing (e.g. Strep A), minimizing the exposure of personnel to the pathogen. The main disadvantage of this device is that a significant volume of the fluid is retained by the swab tip and only the excess is eluted. Therefore, the elution efficiency is expected to be small.

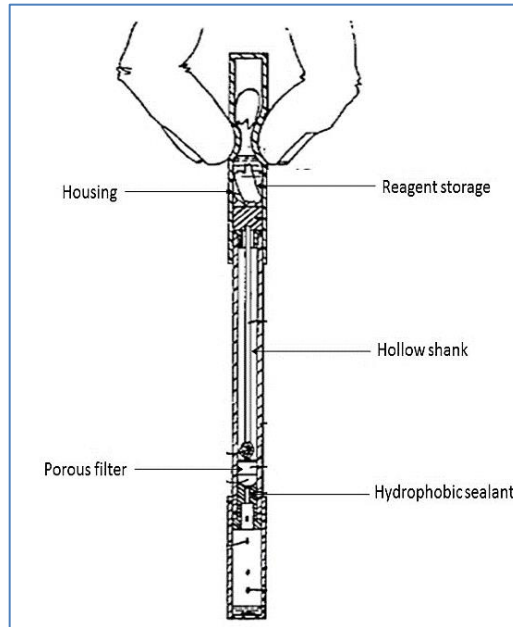


*Fig. 3 Specimen test unit with a blister end [80].*

### **2.5.1.6 Indirect contact-based elution**

Apart from the widely-used techniques such as vortexing, sonication, abrasion and pressurized flow there are a number of mechanical elution methods that are described in the patent literature for which detailed publications are not available. These methods provide indirect contact to the swab fibres by specific tools such as porous swabbing pens, compressible walls, piezoelectric actuator, and wringing units. Some of the interesting methods are described below.

#### **2.5.1.6.1 Piezoelectric vibrations**

Another example of a contact-based elution method is the use of repeated mechanical vibrations imparted to the swab through a compressible wall. Certain piezoelectric methods

[12] allow an actuator to strike a flexible film (Figure 4) at low frequency ranges between 10 to 100 Hz. The device incorporates a flexible-walled chamber to house a swab, a fluidic channel for eluent flow, an actuator striking the outer flexible wall and collection zone at the end. The fluidic channel is connected to the elution chamber to allow flow of conditioning fluid, while being eluted by the synchronised impact of the actuator. This allows automation of the molecular and immunoassay testing, that include rapid elution and sample homogenization. This entire setting is incorporated within a cartridge housing that includes a plurality of storage chambers, reaction chambers, ports and interconnected fluidic network. This device offers a faster elution technique, but the requirement of continuous flow of conditioning fluid across the swab limits its use to certain environmental samples only.

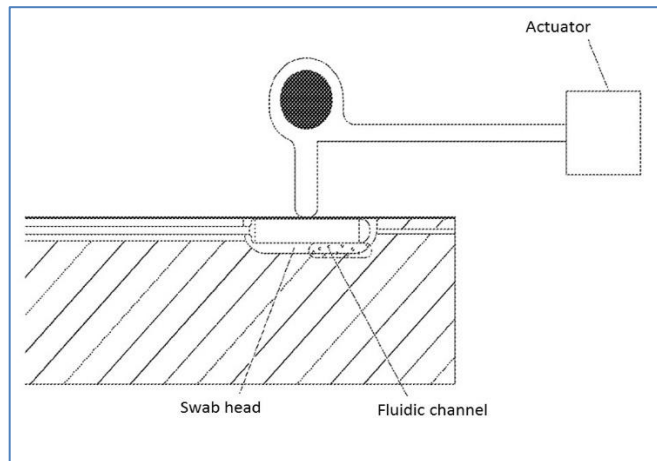


*Fig. 4 Swab Elution Chamber in a Test Cartridge by actuated impact [12].*

#### **2.5.1.6.2 Compression and squeezing**

In some cases, deformation of the device walls and compression of the swabs has been used for elution. These processes [13] provide a compressible device (Figure 5) for elution

of the receiving end of swabs, which allows a conditioning fluid to be flown in from a blister along a transfer path. The device includes a compressible region for the swab head intake, a blister for storing conditional fluid, a transfer path for eluate and sensors for detecting the analyte. For detection of Amphetamine Sulphate from human saliva, the swab head was directly rubbed on the tongue and taken inside the deformable region of the device. This method use 5 ml of elution fluid, that was applied for 30 seconds. This device offers a faster elution method, accompanied by a convective flow, but also utilises a higher elution volume. It is ideal for point-of-care applications, with disposable absorption pad at the collection area and a relatively small number of handling steps. One important disadvantage of this system is that the mixing time of the conditioning fluid inside the receiving region of the swab is very low. Also, the convective flow generated around the swab head is not sufficient to recover all absorbed samples from inside of the fibre matrix. Hence, the overall recovery of materials from the swab is low.

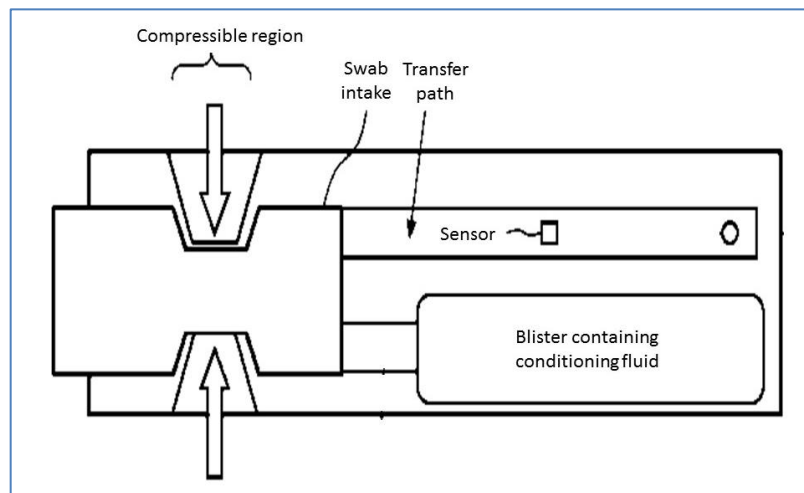


*Fig. 5 Sampling deice with conditioning fluid [13]*

Another method that uses mechanical squeezing of the soft swab tip to elute has been developed by Fleming [81]. This sample recovery device includes a receptacle with a wringing unit (Figure 6) that allows the swab to transfer the sample into the corresponding fluid. The device has a receptacle, a cap and a shaft to transfer the sample through the hole in a vial. The receptacle had an open upper end, covered by a cap with a hole and a flat rubber plug as means of wringing to compress the fibres for elution of the sample.

Before using, the receptacle is filled with the elution fluid, which generally ranges from 5 to 1000  $\mu\text{l}$ . The swab, containing the sample, is first immersed in the fluid inside the container prior to wringing. During compression of the fibres in the wringing unit, the samples are extracted from the swabs and transferred to the receptacle. This unit provides a better recovery of dilute samples of low viscosities for various immunoassays, with advanced sensitivity. It offers a higher recovery of 66%, but also has a disadvantage of removal of fibres from the swab during wringing, some of which eventually gets contaminated with the final eluate.

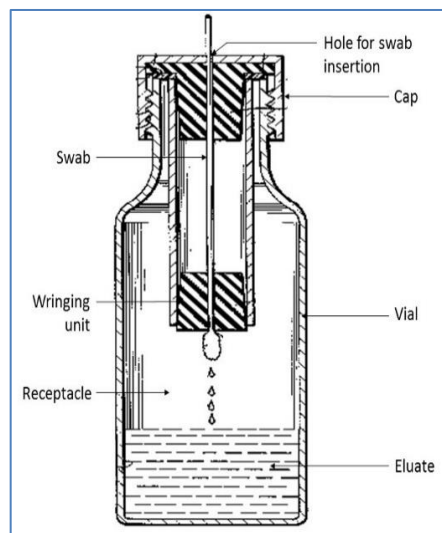


*Fig. 6 Liquid recovery device by wringing [81]*

Squeezable centrifuge tubes (Figure 7) have also been used as elution devices. These devices [82] have an open proximal end and closed distal end. Two compressible (flexural modulus of 690 MPa) bulges are created at opposite ends of the inner wall (5mm) of the tube to extract maximum amount of material from the swab for further centrifuging process. Another similar configuration of a sample collection and recovery device [83] has a cap and swab system as one single composite unit. The swab goes into the vial with compressible walls with indentation and gets eluted when squeezed through them. These modified centrifuge tubes are fit to be used in collection of forensic evidences, sample collection at bioterrorism sites, surface swabbing for contaminated industrial accident sites. It removes the use of elution fluid, but is unable to provide efficiencies higher than regular vortexing.

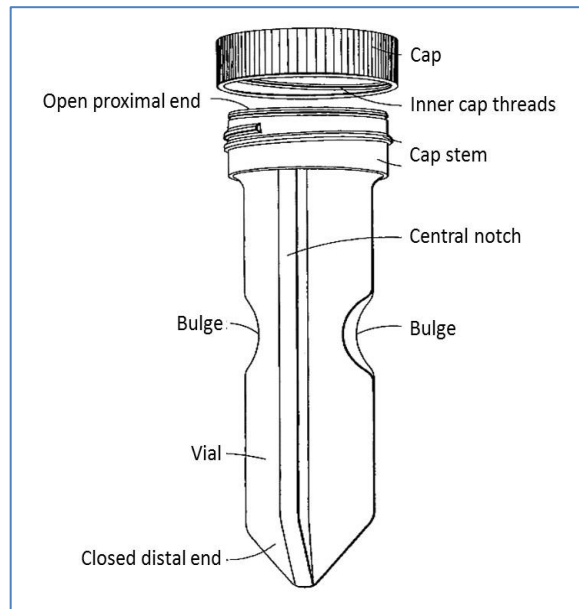


*Fig. 7 Centrifuge tubes with squeezable bulges [82]*

The above mentioned mechanical techniques are the most common approaches to elution. Lower recovery efficiencies are obtained with simple vortexing. To enhance the efficiencies, vortexing are sometimes accompanied with chemical techniques or some other methods of agitation like convective flows. These methods can yield up to 56% recovery efficiency [70]. Other processes that provide tangential shear forces with associated flow (piezoelectric, pressurized flow etc) can yield a maximum of 60% recovery [80]. Higher recoveries can be obtained with compressible and wringing units (~66%) [81]. Elution by vortexing, squeezing, pummelling, maceration, rolling and differential extraction of semen from swabs showed higher average elution times (~5 minutes), with 8000-13000 RPM rotational speeds and ~400 to 1000 $\mu$ L of eluate. Most mechanical techniques of elution are generic, works with a wide range of sample types and have lower elution times (~30s – 10 mins). But they require higher volumes (~5ml) or continuous flow of eluent and highly intricate systems for detecting the target analyte. Although these techniques offer impact as a method of elution, none of them inflict direct physical contact to the swab fibres. Mechanical techniques that produce direct impact forces on the swab fibres can extract higher number of particulates as they can penetrate deep into the fibre matrix than impact or agitation by convective flows or non-physical impact. Hence, elution by direct physical impact can be an important area for elution.

### **2.5.2 Chemical techniques**

Many chemical methods have been used to increase the recovery of the sample constituents from the swab. These techniques aim at digesting the swab fibres and remove the intact cells. Some techniques are also employed to simultaneously elute and lyse the

cells. Differential extraction techniques are used in some cases such as in vaginal samples to separate the sperm cells from female epithelial cells by sequential enzymatic dissolution. The chemical combinations used in these processes usually constitute of an enzyme, detergent, surfactants and a suitable solvent. Enzymatic digestion and chemically enhanced recovery are the most common techniques for chemical elution and recovery of cells. They are mostly used in cases of elution of sperm cells from cotton swabs for forensic DNA analysis [84]. Isolation of DNA from bloodstains recovered from cotton swabs is also an important field of application for forensic use [85].

Each of the chemical techniques use a combination of enzyme, surfactant, detergent and sometimes a redox agent. Different enzymes are used for different applications. For digesting cotton fibres, *Aspergillus niger* cellulase is used. Proteinase K is used to digest protein and remove contamination during preparations of nucleic acid. Along with the enzymes, detergents are used to enhance the enzyme activity by making its substrate cleavage sites more accessible. For example, detergents like 0.5-1% sodium dodecyl sulphate (SDS), or 4M urea are used with Proteinase K. Similarly, several anionic, non-ionic or Zwitterionic detergents are also used with cellulase enzymes. EDTA (Ethylenediaminetetraacetic acid) is used with these enzymes as a chelating agent to bind with calcium ions. Redox reagents like DTT (Dithiothreitol) are used with sperm samples to break down the protein sulphide bridges that make up the sperm nuclear membranes. The differential extraction technique uses DTT to digest female epithelial cells exclusively and retain only sperm cells which are robust and cannot be digested. Specific solvents are used to prepare the final solutions and buffers are used to maintain its pH.

Chemical methods of elution are important in some clinical and forensic applications. Some of these techniques offer combined elution and lysis of cells from the body fluid samples. They are utilised for elution and DNA extraction from samples of blood, semen, vaginal fluid and hair roots by incubating in a mixture of SDS, Proteinase K and DTT mixtures [85]. Small volumes of clinical samples are sufficient for these procedures (~5-40 $\mu$ L of semen, ~60-100  $\mu$ L blood). Chemical techniques are important in cases where trace amounts of samples are available or when the samples are 4-5 years old. These may include dried semen or bloodstains. Apart from these, use of chemical enzymes are also popular in differential extraction of semen and epithelial cells. But the combination of chemicals used for elution is specific to the nature of the sample and hence, cannot be generalized for all kinds of biological, environmental or surface samples.

#### **2.5.2.1 Effect of enzymes**

Chemical techniques have been used to elute sperm and epithelial cells by enzymatic digestion. The most common approach to the separation of DNA from perpetrator and victim is the differential extraction method. The samples, collected by vaginal swabs, contains a mixture of epithelial cells and semen. The differential extraction method uses two steps to separate the epithelial cells from sperm cells. The epithelial cells are dissolved in Proteinase K and SDS, removed by centrifugation and then resuspended in 5ml buffer containing dithiothreitol (DTT) to digest the sperm cells. [85] Modifications have been made to DE (Differential extraction) process to incorporate both centrifugal extraction and phase separation to separate the epithelial from sperm cells [86]. These techniques yield

only about ~53% recovery and the separation of two different cells of the opposite sexes are not exact in most cases.

Another popular enzyme for digestion of cells is cellulase. Effects of cellulase on the recovery of sperm cells from vaginal swabs comprise an established forensic technique for genetic analysis of the perpetrator. Cellulase refers to a group of enzymes produced by fungi, bacteria and protozoans that hydrolyse cellulose. Cellulase from *A. niger*, *T. reesei*, or *T. viride* were mixed with citrate buffers to prepare a solution. Swab samples were vortexed in cellulase solutions and incubated for 1-4 hours at 37°C. For instance, Voorhees et al. [10] explored the use of enzymatic dissolution of cotton fibres with *Aspergillus niger* cellulase to recover sperm cells. This yielded a 18% recovery, as opposed to 23% obtained from conventional Differential extraction. The concentration of the enzymes affects the rate of recoveries. An optimal concentration of 50µg/ml was found to show recovery efficiencies (21%) more than twice over samples eluted in citrate buffer only (9.4%). Lower concentrations of *A. niger* cellulase show that the fibres were not properly digested by the enzymatic solution. *A. niger* cellulase produce an enzymatic hydrolysis of cellulose. But, sufficient volume of enzyme (at least 100µL) is required in order to maximise the hydrolysis of the entire fibre matrix and break its attachment to the cells. Hence, the concentration of cellulase affects the recovery to a greater extent.

#### **2.5.2.2 Effect of detergents**

The effects of detergents on different enzymatic solutions for elution has been studied. Detergents are used to enhance the enzyme activity by making its substrate cleavage sites more accessible. Higher sperm cell recovery has been obtained when sodium

octyl sulfate (SOS), Sarkosyl (54.4 %) and sodium dodecyl sulfate (SDS) (78.50%) detergents were used [87], showing the prevalence of anionic detergents over other cationic (1% w/v CTAB), non-ionic (1% w/v Triton- X) or zwitterionic (1% w/v CHAPS) detergents. Detergent solutions were prepared from a mixture of Nanopure water, sodium dodecyl sulfate (SDS), sodium lauroyl sarcosinate (Sarkosyl) 3-[(3-cholamidopropyl)dimethylammonio]-1-propanesulfonate(CHAPS), cetyltrimethylammonium bromide (CTAB), or Triton-X. Swab fibres are vortexed in the reagent briefly, and incubated for 2 hours. Average recovery of sperm cells was higher when cellulase was used with 1% Sarkosyl detergent (53%) as compared to just conventional DE buffer. The respective recovery efficiencies of sperm cells in different detergents have been shown in Figure 8.

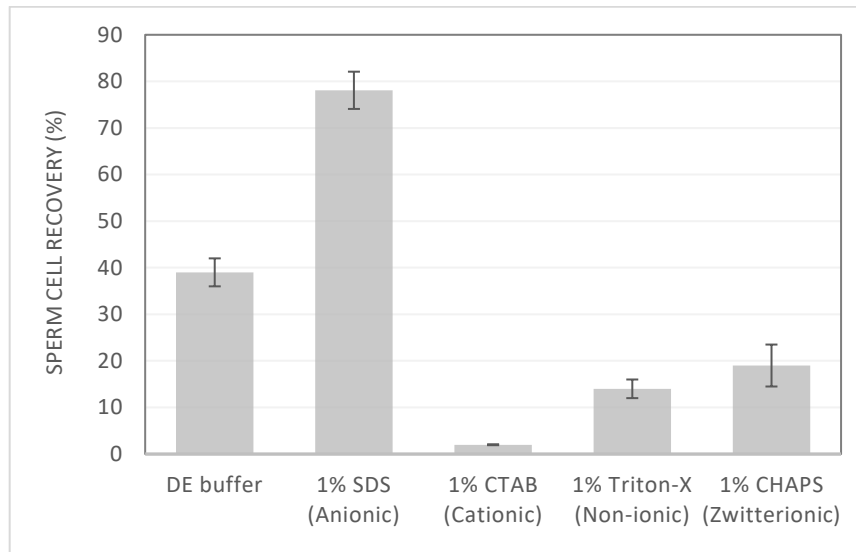


*Fig. 8 Comparison of sperm cell recoveries for different detergents [87]*

### 2.5.2.3 Effect of buffers

The pH of buffer also has a pronounced effect on the recovery of cells. Cellmark's [70] improved two-phase cellular recovery technique allows higher release of nucleated epithelial cells (NEC) in the first step and spermatozoa in the second. Traditionally, DE buffer containing 10 mM Tris-HCl, 10 mM ethylenediaminetetraacetic acid (EDTA) and 0.1 M NaCl, mixed with 2% SDS and 20  $\mu\text{g}/\text{mL}$  ProK are used for separating sperm cells from epithelial cells [88]. Swab samples were soaked in 1% SDS, dried and mixed with 0.2  $\mu\text{L}$  of 10 mg/mL ProK, added for a final volume of 100  $\mu\text{L}$ . An optimal buffer pH of 8.5 showed upto ~82 % recovery of sperm cells, which also increased with incubation period (Figure 9) and plateaued after 30min. By increasing the pH of the buffer, the recovery increases to ~200% of that of a conventional DE buffer, but the sperm cell yield drops significantly when the buffer components are separated. This is due to the fact that the epithelial cells are not completely lysed and hence were not separated during the second stage of elution, where the sperm cells were being eluted. These buffers are used in two-step elution system, where all cells are eluted followed by a lysis of epithelial cells.

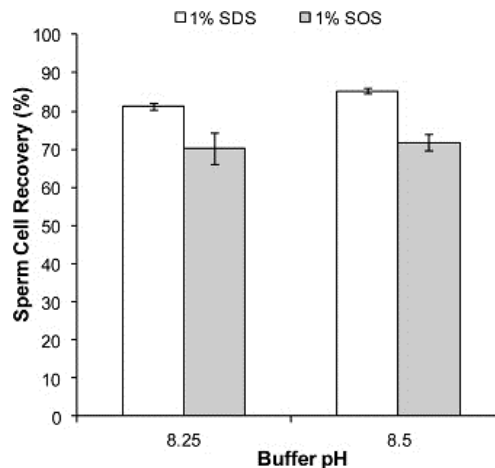


Fig. 9 Effect of DE buffer pH on recovery efficiency [89]

A novel buffer introduced by Lounsbury et al. [89] showed increased efficiency in sperm elution. These experiments showed that replacing the previously mentioned conventional buffers by SDS or SOS and ProK enhances the recovery efficiency to upto 80%. Buffers containing 10 mM Tris(hydroxymethyl)aminomethane (TRIS), 10 mM 2-(Nmorpholino)ethanesulfonic acid (MES), and 1% sodium dodecyl sulfate were brought to pH of 8.00, 8.25, 8.50, 8.75, or 9.00 using 0.1 M HCl or 0.1 M NaOH. 1% SDS solution in water showed higher recoveries (~81%) than both MES or TRIS buffers alone. Additionally, the recoveries of each individual buffers increased when their respective pH was increased from 6 to 8. This shows a higher affinity of sperm cells towards slightly alkaline buffers. When the buffers components are separated, the elution efficiency reduces considerably.

Although chemically induced techniques allow for differential extraction of male and female DNA separately, they use a series of steps, involving overnight incubation and high cost. Moreover, they are not suitable for cases where trace amounts of samples are available. Enzymatic digestion can provide a higher elution efficiency (~78%), but it requires a complex combination of citrate buffer, cellulose or detergent solutions and upto 2 hours of incubation period for elution. Hence, the use of chemical methods of elution are limited only for forensic experiments dealing with sperm cells. Also, unlike mechanical methods, the choice of chemicals for each sample type is unique and cannot be generalized for all swab types and body fluid samples. Hence, mechanical methods of elution are better than chemically induced techniques.

## 2.6 Effect of nature of swabs on recovery

The type of swab fibres also determine the recovery efficiency of the elution process. These might include dry and pre-moistened swabs of cotton, macrofoam, polyester and rayon fibres. Elution from different swab fibres were compared using mechanical agitation methods for recovery of spores from stainless steel coupons by Rose et al. [4]. *B. anthracis* spore samples of  $1 \times 10^6$  CFU/ml suspension were spread on 2" x 2" stainless steel coupons. Different types of swab fibres, such as cotton, macrofoam, polyester and rayon were used for collecting samples. Spore-laden coupon surfaces were swabbed using dry and pre-moistened swabs and eluted in 5ml of PBST (Phosphate Buffered Saline Tween-20). Post sampling, the swabs were either simply dipped in the solution, vortexed for 2 mins or ultrasonicated for 12 mins.

The recovery efficiencies were calculated after each experiment and categorized based on the nature of swab fibres. Effects of efficiency on dry and pre-moistened swabs were evaluated. Hucker et al. [90] showed that the recovery of microorganism is proportional to the ease of wetting the surface of collection. Hence, a majority of the environmental samples are collected by cotton swabs, premoistened with surfactants (e.g. Tween 80) that reduce the adherence of microorganisms to the surface when swabbed. Premoistened swabs showed significantly higher recovery of spores for cotton (20%) and macrofoam (22.5%) swab tips due to better absorbing properties, as compared to dry swabs (5.1 and 8.4% respectively). Comparison were also made depending on the nature of fibre materials. When the swabs were directly inoculated with spores, similar recovery efficiencies were obtained (93.9% for cotton, 93.4% for macrofoam, 91.7% for rayon and 83.8% for polyester). But macrofoam (average 30.7%) and cotton (average 27.7%) swabs were the

most efficient ones when the spores are swabbed from steel surfaces and the recovery efficiencies were calculated. This showed that absorbing properties was predominant in macrofoam and cotton swabs, which led to higher recovery than polyester (10.6%) and rayon (10.0%). Hence, absorbing properties of swabs are critical during selection. Efficiencies of various swab type and extraction procedure are given in Table 3.

Recovery method, type of swab	Recovery efficiency (%)			
	Cotton	Macrofoam	Polyester	Rayon
Extraction, dry	5.1	8.4	1.2	3.0
Extraction, pre-moistened	20.0	22.5	7.7	7.0
No extraction, dry	0.	0.7	0.1	0.1
No extraction, pre-moistened	4.7	6.3	2.0	1.0
Vortexing, dry	8.0	11.9	2.1	4.4
Vortexing, pre-moistened	41.7	43.6	9.9	11.5
Sonication, dry	6.9	12.7	1.4	4.5
Sonication, pre-moistened	13.6	17.7	11.2	8.5

*Table. 3 Effect of different swab tip materials on Recovery [90]*

## 2.7 Summary

Elution of swabs is an important step for most diagnostic analysis. Different approaches to elution have been made, chemical and mechanical techniques being the most prominent ones. A range of efficiencies have been obtained with these techniques. Each of the process have their own advantages and disadvantages. Lower recovery can lead to incorrect

characterization of samples, and hence ways for enhancing the efficiency has been under scrutiny.

In this thesis, we focus on developing a mechanical technique for elution of cotton-tipped applicator swabs for an improvement in recovery efficiency. Most of the abovementioned techniques use higher elution volumes and intricate systems to yield a maximum of only ~76% recovery. Thus, a simple, low-cost technique is needed for portable elution of samples that will increase the recovery efficiency using lower volume and lower elution time. Mechanical techniques, with application of forces by direct impact on swabs, is one promising area. Hence, the primary aim of this thesis is to demonstrate the highest elution recovery procedure by inflicting physical impingement on the swab fibres by magnetic particles.

## Chapter 3

### Device design and experimental setup

#### 3.1 Introduction

In this thesis, a technique is developed to improve the recovery efficiency of elution of samples from cotton-tipped applicator swabs. Cotton swabs are the most widely used sample collection devices with salivary or sputum-based biochemical assays because of its easy availability, low cost and high absorbance. Several processes for elution of swabs have been discussed in the previous chapter. Although, chemical techniques offer upto ~76% recovery, they involve a series of complex steps and require reagents for effective elution that comprise of a combination of various buffers and enzymes. Mechanical techniques of elution of swabs has simpler handling steps, but they can't match the higher recovery efficiencies obtained from the chemical methods. Hence, the primary aim of this thesis is to establish a process for mechanically eluting a swab that can result in higher recovery.

Fluid agitation is the primary method that has been used in mechanically eluting swabs. Vortexing is the most common approach, followed by convective flows, compressive forces, piezoelectric vibrations, pressurized flow and sonication. These techniques have a wide range of recovery efficiency and eluent requirements. They provide mild impact or tangential shear across the swab fibres to remove materials off the swab fibres. These processes only produce a low-to-moderate recovery efficiency. A modified technique with

higher agitation and forceful impact on the fibres can potentially lead to an increased recovery.

In this chapter, a device has been designed to impart direct mechanical impingement onto the swab tip for effective elution from the swab. The criteria for device design and its working principle is discussed first along with the operation procedure. A detailed description of the device is provided. Based on the understanding obtained through the design and construction, a second iteration was designed that has a more compact form factor and special grooves in the vial to uniformly distribute the impact. The fabrication and assembly of both the devices and their advantages over the existing techniques are also demonstrated.

### **3.2 Design criteria**

The proposed device should be able to meet certain operational considerations for elution of swabs. The goal of an optimum elution technique would be to completely elute the entire sample content from the swab and into the elution fluid. Practically, this goal can be accomplished by mechanical elution methods if the following criteria are met:

- Mechanical forces of impact should be imparted directly to the swab fibres. This would result in better recovery of samples as compared to mild agitations or tangential shear forces through convective flows.
- The device should produce multiple physical impingement to reduce the retention of cells within swab fibres, especially the ones trapped deep inside the fibre matrix.

- The effect of parameters like viscosity of samples, nature of pathogens and type of swab fibres on recovery efficiency should be mitigated, thereby introducing a generalized process of elution.
- The device should increase the recovery efficiency compared to passive dissolution and centrifuging.
- The device should reduce the elution time and volume as compared with the existing methods and devices so that it can be integrated easily with downstream processes.
- The device should be cost-effective and suitable for a wide range of forensic, research and clinical environments.

### **3.3 Working principle**

Higher impact forces are desired on the swab fibres to improve elution efficiencies. This can be obtained either by piezoelectric vibrations, abrasion, sonication or by periodic impact of particles onto the swab. Piezoelectric vibrations offer periodic vibrations on the outer walls, but has no direct contact with the swab fibres. Abrasive methods allow scraping of samples from the surface of the swab only. Sonication uses fluid vibration to elute the samples from the swabs. But this periodic motion is not sufficient for effective elution, resulting in low recovery efficiency [73-74] and carries the potential to remove some fibres from the tip. Ultrasonication, with large particles inside the bath, can be an effective option to produce higher impact forces as they have higher inertia. This will allow the particles to strike on the swab fibres along with the periodic vibration of the fluid. However, larger

particles are also heavy and will quickly deposit on to the bottom of the elution vessel, as soon as they are immersed in the fluid. Hence, their impact will be felt at the very tip of the swab and the rest of the swab surface remains unaffected.

Periodic impact on the swab is an effective way to elute the samples because it allows physical contact between the particles and the swab, which provides better release of the samples. Repeated impingements are desired along with turbulent motions of the fluid, which allows fresh fluid to enter the fibre matrix after each impact. A rotary motion of the particles is required to create a scrubbing action on the swabs due to the subsequent impingements. To cover the entire surface area of the swab, another circulatory motion is required for the particles around the swab head. A rotating magnetic field can be used to generate circulatory motion of small magnetic particles in order to cause distributed impact and effective elution from the swab. A magnet can, therefore, be used with a sun and planetary gear mechanism to create this rotating magnetic field for both rotation of the magnetic particles and their curvilinear translation around the centre axis inside the vial as shown in Figure 10.

Impact forces on the swab by smaller particles are considered as a mechanism to produce higher impact forces on the fibres. When a diametrically magnetized ring magnet was placed on the device, they attracted the smaller magnetic particles in the vial towards it. When the motor was rotated, the poles of the ring magnet also rotate and were periodically reversed. This allowed the magnetic particles inside the vial to flip around its own axis. Hence, the magnetic unit underwent a rotational motion around its own axis. This rotational motion created a scrubbing action when it came into contact with the swab fibres and removed materials from the swab fibres. Additionally, it also produced a

turbulent motion of the elution fluid. The ring magnet also underwent a revolution around the central axis of the device due to the rotation of the motor axle and carried the smaller magnetic particles inside the vial along with it. This induced a circulatory translational motion to the magnetic particles around the swab, and thereby covering most of the surface area of the swab.

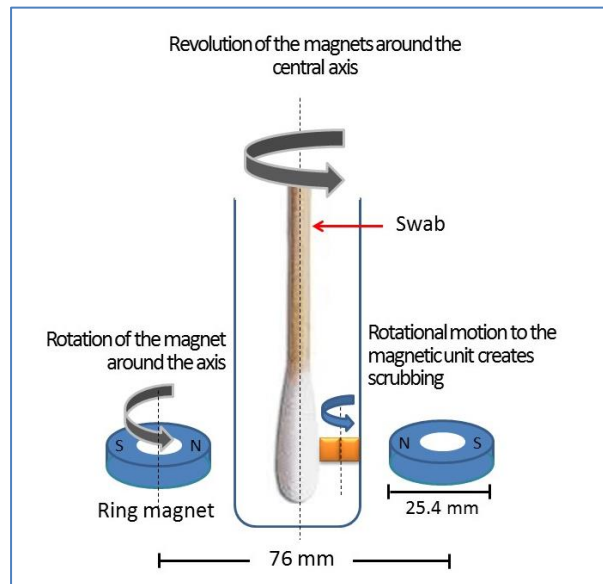


*Fig. 10 Working principle: rotational motions induced by the diametrically magnetized magnet*

The strong magnetic force of attraction between the ring magnet and the magnetic particles inside the vial is responsible for the magnetic levitation. At time  $t=0$ , the magnetic particles were inserted into the vial and they dropped down to the base under their own weight. As soon as the ring magnet was placed on the planetary gear, a magnetic force starts acting on the smaller particles. The magnetic particles remain attached to each other during the period. The horizontal component of the force pushes the particles to the side

wall and the vertical component balances the weight of the magnets and pushes it further up. The magnetic particles move up, gets aligned to the horizontal plane of the ring magnets and remain positioned there in a stable configuration. Any small movement from this position in the vertical direction would cause the vertical component of the magnetic force to act as the restoring force.

### 3.4 Acting forces and the motion of the magnetic particles

The forces acting on the magnetic particles are a combination of the three forces:

1. Magnetic forces acting on the particles, imparted to the fibres.

The radial magnetic field strength (A/m) created by the ring magnet on the horizontal plane is given as [91],

$$H_r(r, z) = \frac{\sigma}{2\pi\mu_0} \left( \tan^{-1} \left[ \frac{z}{r-r_1} \right] - \tan^{-1} \left[ \frac{z-h}{r-r_1} \right] \right) \quad (1)$$

where, h height, r is the radius from center,  $r_1$  is the inner radius,  $\mu_0$  is the permeability of space ( $4\pi \times 10^{-7}$  T-m/A) and  $\sigma$  is the surface magnetic pole density.

The force exerted on the smaller magnetic particles by the influence of this field can be given as:

$$F_M = \frac{B^2 A}{2\mu_0} = \frac{\mu_0 H^2 A}{2} \quad (2)$$

where, A is the total surface area of the magnetic particles and B (Tesla) is the magnetizing field.

2. The centrifugal force due to rotation around its own axis.

$$F_c = m\omega^2 r = m \left( \frac{2\pi N}{60} \right)^2 r \quad (3)$$

where m is the mass of the particles, N is the speed of rotation.

3. The viscous drag force opposite to the movement of the particles in the elution fluid.

$$F_D = \frac{1}{2} C_D \rho v^2 A \quad (4)$$

where,  $C_D$  is the drag coefficient,  $\rho$  is the fluid density  $v$  is the speed of the object (=  $\omega r$ ) and  $A$  is the cross-sectional area. The drag coefficient is both a function of shape of the object and Reynold's number.

The rate of change of momentum of the particle can be given as:

$$m \frac{d\bar{u}}{dt} = \bar{F}_M + \bar{F}_c - \bar{F}_D \quad (5)$$

Where, m is the mass of the particles, u is the velocity,  $F_M$  is the force due to the magnetic field,  $F_c$  is the centrifugal force and  $F_D$  is the drag force.

A rotational kinetic energy imparted to the swab is responsible for the elution. The total kinetic energy offered by the magnetic particle can be calculated as:

$$KE_{rot} = \frac{1}{2} I \omega^2 = \frac{1}{2} \times \left( \frac{1}{12} m (b^2 + h^2) \right) \times \left( \frac{2\pi N}{60} \right)^2 \quad (6)$$

The total measured forces (described in Appendix A) on the swab and respective kinetic energy offered by the particles are given in Table 4. A part of this kinetic energy is given to the swab and the rest is dissipated in the fluid as convective forces.

RPM	KE <sub>rot</sub> (x 10 <sup>-7</sup> J)	Force (g-f)	Force (N)
100	1.078	330.85	3.24
200	4.312	389.79	3.82
300	9.702	423.71	4.15
400	17.248	461.12	4.52
500	26.95	484.81	4.75

*Table 4. Forces imparted to the swab by the particles and the total kinetic energy*

The variation of kinetic energy imparted to the swab by magnetic particles and the measured forces acting on the swab tip with the change of rotational speed is shown in Figure 11. With the increase in the rotational speed, the kinetic energy increases. A part of this kinetic energy is imparted to the swab and the rest is dissipated into the wall and the fluid to create a convective motion around the swab. As given by the Equation 6, the kinetic energy shows a parabolic relation with the rotational speed and is reflected in the graph. The measured forces acting on the swab increases almost linearly with rotational speed. Hence, increasing the rotational speed should result in higher forces acting on the fibres, thereby increasing elution efficiency. Higher rotational speed also increases the total number of impacts per minute. The necessary impingement produced on the swab as a result of this produces higher magnitude of force per contact or higher energy imparted to the swab. These forces are essential for scrubbing the materials out of the swab and improves the recovery of samples.

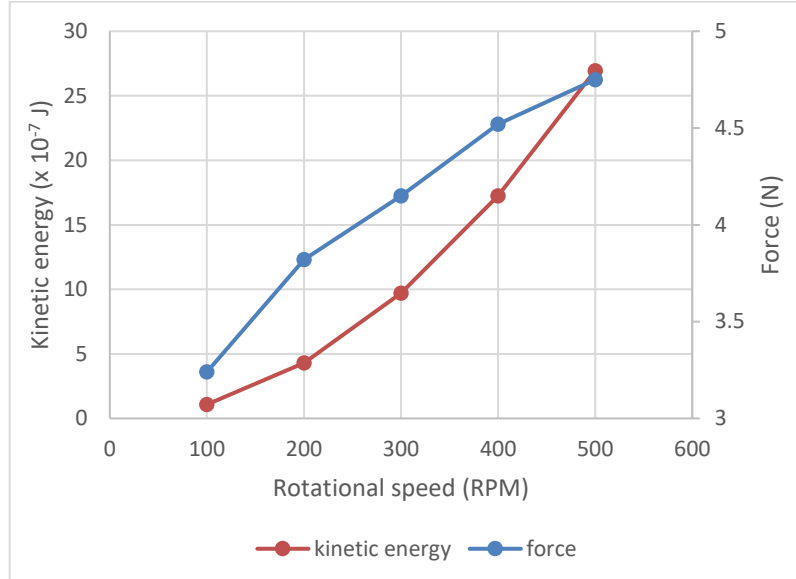


*Fig. 11 Variation of kinetic energy imparted to the swab by the magnetic particles and forces acting on the swab with RPM*

The variation of the measured forces on the swab with the corresponding number of impacts/min is shown in Figure 12. This plot shows that the total forces on the swab increases almost linearly with the increase in the number of impacts. For each complete rotation of the motor, the planetary gear rotates  $i$  times ( $i$  is the gear ratio = 2.9 for the proposed design). So, if the motor rotates at  $N_m$  RPM, the planetary gear rotates at  $i \times N_m$  RPM. Now, for each rotation of the planetary gear, the ring magnet undergoes reversal of the magnetic pole twice. This forces the magnetic particles inside the vial to complete two successive rotations. Hence, the magnetic particles rotate at  $2 \times i \times N_m$ . For each rotation, there are two impacts on the swab head. Hence, the total number of impacts per minute is  $4 \times i \times N_m$ . The force applied on the swab due to the impact is responsible for elution and hence it increases along with the increase in number of impacts.

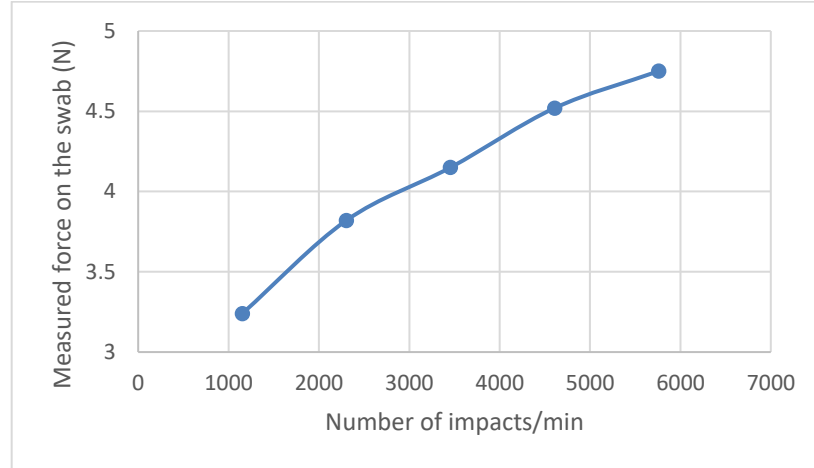


*Fig. 12 Variation of measured forces on the swab vs the number of impacts per minute by the particles*

Rotational motion of the smaller magnetic particles is necessary for elution. Rotating the vial alone will not produce any subsequent impact of particles to the swab, as it will only generate a convective flow of the fluid. Hence a magnetic stimulus should be provided to the particles which creates the necessary impact. The planetary motion of the magnet was designed to introduce both rotational motion of the magnetic particles around their own axis as well as their circular trajectory around the swab, inside the vial. The rotation of the magnetic particles not only introduces a turbulent motion in the elution fluid, but is also useful in generating a scrubbing like motion on the fibres of the swab when they make contact. When the particles are rotated around their own axis, it can create the necessary scrubbing at one particular point. But these rotations are also necessary at different points around the swab to create multiple impingements. The circular translation of the particles around the swab can then cause multiple such impacts at various locations around the swab

leading to a uniform and thorough extraction of the contents of the swab into the elution fluid.

Under the influence of the magnetic force of the ring magnet, the magnetic particles inside the vial rise from the base and gets levitated to the same horizontal plane of the magnet. The two magnetic particles remain attached together under the influence of the magnetic force and create a unit. The rotation of the motor cause the magnetic unit to rotate around its own axis and produces a scrubbing action to dislodge sample materials from the swab fibres. The rotation of this magnetic unit generates a rotational kinetic energy, a part of which is also dissipated in the fluid to create a convectonal motion. The motion of the fluid is also essential in dissolution of the sputum samples and hence have been studied in detail.

### **3.5 Nature of fluid motion**

The study of the fluid motion and the generation of turbulent flow around the swabs is critical for elution and creating a homogenized mixture of eluted samples. The kinetic energy of the rotating particles is dissipated into impact on the swab, the wall and then in creating convective motion of the fluid through drag forces. There are two types of motion applied to the magnetic particles: rotation around its own axis and the revolution around the central axis of the device. These are shown in Figure 13. The magnetic unit gets stuck to one end of the vial and undergoes a circular translation to drag the fluid layers adjacent to it in a spiral motion around the central axis of vial. When a particle is dragged in one plane, a streamlined motion is expected, following the trajectory of the particle. The

maximum velocity of the fluid is expected at the outermost surface of the particle and zero at the centre.

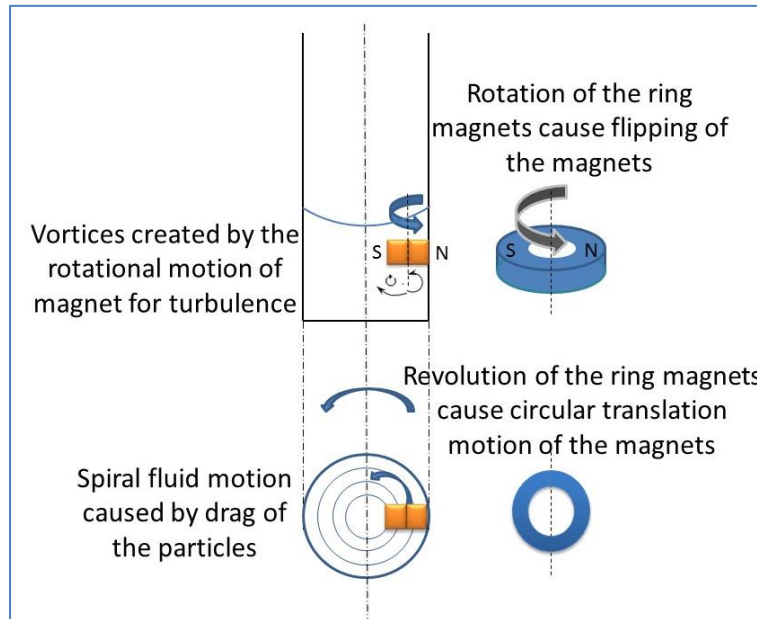


*Fig. 13 Fluid motion generated by different trajectories of the magnetic particles*

The rotation of the diametrically opposite ring magnet unit around its own axis enables alternating north and south poles to appear on the side facing the vial. This allows the particles inside the vial to rotate by being attracted to the changing polarity of the ring magnet (as described in section 3.3). This motion creates a rotary motion of the fluid particles adjacent to it. Smaller eddies and vortices are formed in fluid body adjacent to the particles. This influences the fluid body to undergo a chaotic motion that disrupts the streamlined motion of the fluid, resulting in turbulent flow. The turbulence helps in mixing of the fluid with the samples eluted from the swabs. Thus, a homogenized eluate is obtained. The uniform mixing of the fluid is necessary while counting the number of eluted particles and thus aids in the calculation of recovery efficiency.

The nature of the rotating fluid flow can also be determined from the Reynold's number.

$$\text{Re} = \frac{\rho v D}{\mu} \quad (7)$$

where  $\rho$  is the fluid density,  $v$  is the maximum velocity of the object relative to the fluid,  $D$  is the characteristic dimension and  $\mu$  is the dynamic viscosity. To determine the velocity, the RPM of the particles is required.

For each complete rotation of the motor, the planetary gear rotates  $i$  times ( $i$  is the gear ratio = 2.9 for the proposed design). So, if the motor rotates at  $N_m$  RPM, the planetary gear rotates at  $i \times N_m$  RPM. Now, for each rotation of the planetary gear, the ring magnet undergoes reversal of the magnetic pole twice. This forces the magnetic particles inside the vial to complete two successive rotations. Hence, the magnetic particles rotate at  $2 \times i \times N_m$ . The velocity of the magnetic particles can be given by:

$$v = \omega r = \frac{\pi(2iN_m)D}{60} \quad (8)$$

The Reynold's number of the fluid flow due to the rotating particles at 500 RPM of the motor is 33,840. The corresponding value for lower RPM (100) is 6768. Hence, the fluid motion is expected to be turbulent at all RPMs from 100-500 and can be used in this range for better mixing of sample with the elution fluid.

### 3.6 Device layouts

The proposed device (Figure 14) consists of several parts:

- A vial that holds the swab and the elution fluid

- A planetary rotation system for rotating the magnet around the vial
- Diametrically opposite ring magnets to create rotational magnetic field
- A motor for creating a circular motion
- Magnetic particles to cause impingement and enhance elution forces

One of the prime criteria for the device design is to reduce the elution volume. The vial sits at the centre of the device and is supported by a pair of clamps. When a typical cotton swab with a tip length of  $1.5 \pm 0.1$  cm and 3.5 mm diameter is inserted into the vial, it should submerge in the elution fluid completely and leave a gap of  $\sim 5$  mm all around it. Hence, the selected vial was chosen to have a diameter of 15mm and height 45mm. The diameter of the vial was chosen to accommodate the swab and the magnetic particles and optimized so that it requires a minimum volume of elution fluid to completely immerse the swab. The volume of the vial was, therefore, designed to hold only 600 $\mu$ L elution fluid to completely immerse the swab head.

In order to introduce mechanical impingement and fluid circulation, a diametrically magnetized ring magnet was used and mechanically moved around the vial in a planetary fashion. The planetary rotation periodically changed the polarity of the magnet which caused rotation of the magnetic particles in the fluid. The rotation of the magnet itself caused curvilinear translation of the magnetic particles around the swab.

The choice of the eluting magnetic particles inside the vial is also an important factor. Smaller particles (in micron range) can migrate through the pores and get attached inside the inner fibre matrix. Hence, sufficiently larger particles are required, that will produce

distributed forces onto the swab. Particles with higher dimensions, immersed in the eluent, will require higher elution volume for the swab tip to get completely immersed in the fluid. Therefore, the optimum size of particles is chosen which has a dimension of a cube with side of 1/8" or 3.175mm.

### **3.6.1 First Design**

Two different designs of the device have been made, with similar constructional features. The first design (Figure 14) consists of a sun and planetary gear configuration, with the external ring gear being fixed and the internal planetary gear rotating around its own axis and also around the centre axis. The ring gear was fixed to the base by 8 pillar supports with epoxy glues. The pillars were fitted to several slots on the base to uniformly distribute the load. The motor was placed at the centre of the device and supported by two vertical walls by means of two screws on either side to prevent any horizontal movements. The motor shaft was connected to a horizontal bar by a tightening screw. One end of the bar was attached to a cylindrical element, to be connected to the inside of the rotating gear by press fit. To allow free rotation of the gears, a bearing was attached to the base of the gear and supported by a snap ring to prevent its fallout from position. A hole was made on top of the planetary gear to place the ring magnet. The cylindrical vial was placed at the centre of the device by means of clamps. This vial was responsible for housing the magnetic particles, eluent and swab in position for the elution process. Detailed constructional features are described in the Appendix B.

A dynamic imbalance is set up in the system due to the uneven distribution of mass around the axis of rotation.

The unbalance can be determined by:

$$F=I_m\omega^2r,$$

where  $I_m$  is the mass imbalance,  $r$  is the distance from the centre, and  $\omega$  is the angular frequency. To overcome this anomaly, the horizontal bar was extended and an equal and opposite weight was attached to the other end to prevent the vibration.

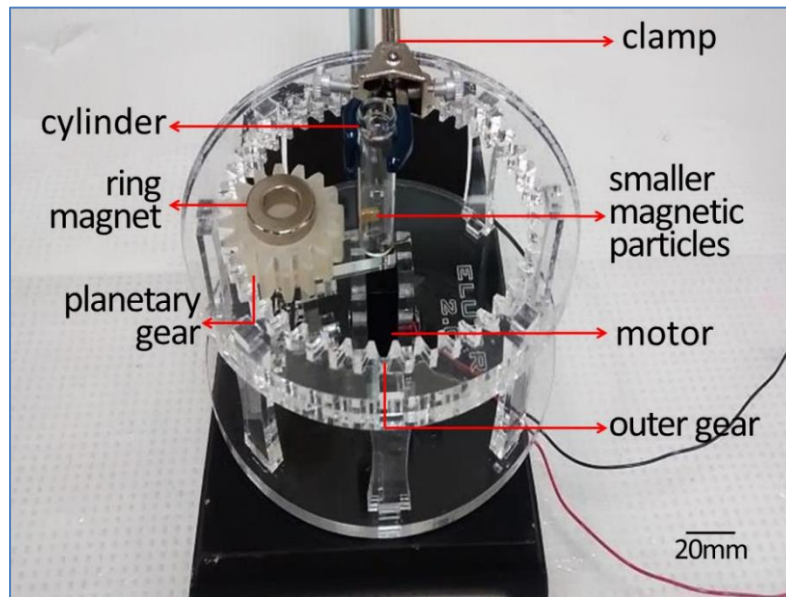


*Fig. 14 Device layout*

The vial sits on the centre of the device, being supported by a pair of clamps. The motor, generating the rotational motion, was positioned at the centre below it and a horizontal arm attached to its axle transferred a circular motion to the centre of the planetary gear. The circular motion of the planetary gear also introduced a rotation about its own centre as it was meshed with the stationary ring gear on the outside. The diametrically opposite ring magnet was placed at the centre of the planetary gear. The rotation of the magnet by the motor produced a magnetic force on the particles under confinement (gap

spacing ~5.08mm) between the swab and the walls. This rotating magnetic field was responsible for the circular motions of the particles that produced repeated impingement on the swab at various angles and locations. The ring magnet is also strong enough to cause levitation of the magnetic particles when the vial was placed in its position.

### **3.6.2 Modifications of the device**

A new compact design was developed in order to reduce the form factor of the device. In addition, the trajectory of the small magnetic particles was also spread out in this design to cover a large surface area of the swab as compared to the previous design by introducing internal grooves on the vials. A new device was thus designed with the same principle, but slightly different structures.

In this new modification (Figure 15), the central sun gear was fixed on an aluminium stand, while the two planetary gears rotate and translate around it due to a coupling mechanism circulating around it. The stand was fixed to the base with a fastener to prevent any movement around the axis. A hinge was made closer to the base to allow a gear to sit on. This gear was meshed with another gear at 1:1 speed ratio. The second gear was connected to the motor, which was fixed to the base and supported by two vertical walls. Two horizontal bars were connected to the inside lower gear to provide rotation to the bars around the axis. The bars in turn were connected to the gears by means of a bearing to allow free rotations and snap rings to prevent its fallout from position. Two gears were provided on each side in order to neutralize the rotational imbalance that could be caused if only one gear was used. The magnet was placed on the slot on top of the gear. A hole was also provided at the centre of the fixed gear where a 3D printed vial was placed. This

vial has internal helical grooves, and holds the eluent, swab and smaller magnetic particles. The internal grooves force the magnetic particles to travel along a spiral trajectory instead of a circular trajectory and enable impact of these particles on a larger surface area of the swab. All the elements can be disassembled and fixed as per the users' need.

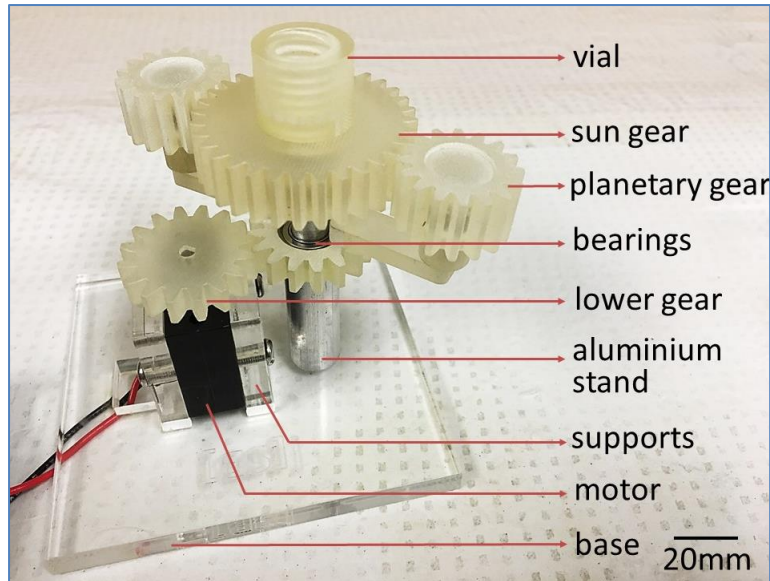


*Fig. 15 Schematic of the modified device*

A diametrically opposite magnet was placed on one of the planetary gears. The other planetary gear was included to balance the weight and to ensure smooth wobble-free rotation. These gears provide a revolution around the central gear and a free rotation to the external gears around its own axis. A bearing at the base of these planetary gears allowed free rotation of the planetary gears and snap rings were provided for holding the bearings in place. A place was provided at the centre of the static sun gear for holding the vial. An extra pair of gears were introduced at the bottom. The horizontal arms were made to rotate

by the help of these gears, that supported and aided the revolution of the top external gears around the static gear. Detailed constructional features are described in Appendix B.

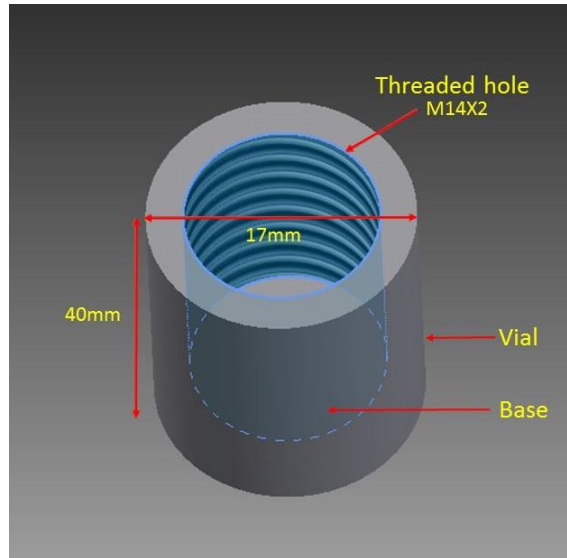


*Fig. 16 Modified vial to with internal helical groove*

The vial, holding the elution fluid and magnetic particles, was placed at the centre of the device (Figure 16). The vial has been designed with a right-handed ANSI Metric M profile internal thread (M14X2) of class 6H to aid a spiral motion of the smaller magnetic particles, when introduced into it. The swabs when placed inside this vial creates an annular confined space of  $\sim 4.2$  mm, that leaves the particles ( $2 \times 3.175$ mm) no alternate way than to follow the spiral and move up along the walls of the container, thereby allowing full contact to the entire length of the swab. This new vial and device arrangement allowed better and complete coverage to the entire surface area of the swab in a compact device.

### **3.7 Device fabrication**

The devices were fabricated using acrylic, which can be easily cut, has higher abrasion and chemical resistance and is a good insulator. It has a Young's modulus of 1.3 GPa and Flexural modulus of 1.2 GPa and a glass transition temperature of 52.5°C. Higher tensile strength of 42.4 MPa and Izod notched impact strength of 2.5 kJ/m<sup>2</sup> makes it suitable for continuous use in gear transmission systems. To prepare the desired shapes and structures two different methods have been used: laser micromachining (Trotec Speedy 300 Laser engraving machine) and 3D printing (ProJet HD 3000 Multi-jet printing). Detailed descriptions are given in Appendix C.

### **3.8 Electrical control**

The first iteration of the device used a DC power source attached to a wall plug. The positive and negative terminals of the motor was connected to the respective terminals of the DC power source. The voltages were regulated (0-12V) to change the speed of the motor shaft within the range of 0-900RPM.

Subsequent iterations were designed (Figure 17) to use power from a laptop using USB connection and an Arduino controller (Arduino Uno - R3). The motor was connected to the Arduino by means of a driver (SparkFun Motor Driver - Dual TB6612FNG), which helped to regulate the speed and directions of motion. A switch was also included in order to switch the motor on/off. The controller was programmed to enable both clockwise and anticlockwise rotation of the motor shaft at any desirable speed between zero and maximum speed of the motor. This setup can be used with any DC motor and is flexible with their respective type and speed variations. The Arduino controller can be powered

directly from the laptop for low-torque and low-speed usages. The motor draws the power from the controller board. For higher voltage requirements, the controller is connected to an external power source.

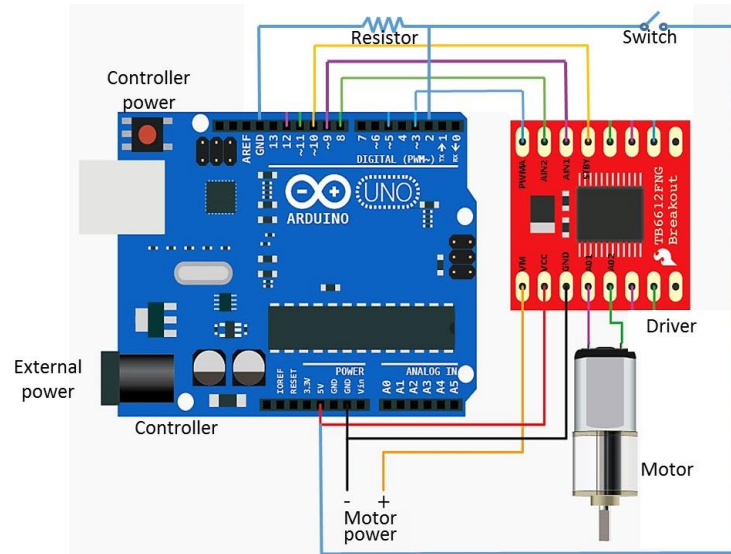


*Fig. 17 Electrical connections of the motor to the controller*

### 3.9 Motor calibrations

A DC reversible gear motor (Sparkfun, ROB-12316) was used in the device configurations. The motor has a 30:1 net gear ratio that operates on 0-12 V supply. The size of the motor is 26 x 12 x 10 mm, with a shaft size of 3mm diameter and 10 mm length. It has a no-load current of 120mA (at 12V) and stall current of 1600mA (at 12V). The maximum speed is 900RPM at 12V DC supply. The motor was placed at the base of the device and solely responsible for providing the torque to the gear and support the mating

loads. The motor calibrations were made after the device was assembled and set up with magnet and motor.

For the calibrations, a Laser Photo Tachometer (Epak Electronics, M005-098 Laser Tachometer) was used to calculate the RPM at various applied voltages (0-12V). An optical paper (white paper with a black mark) was attached onto the facewidth of the gear and the laser was pointed to it. When the motor was turned on, the gear started rotating and the tachometer read the number of rotations made by the mark on the optical paper per minute and displayed the value. Various voltages (0-12V) were applied to the motor using a DC power source and the rotations of the gear was recorded using the laser tachometer. The results are shown in Figure 18.

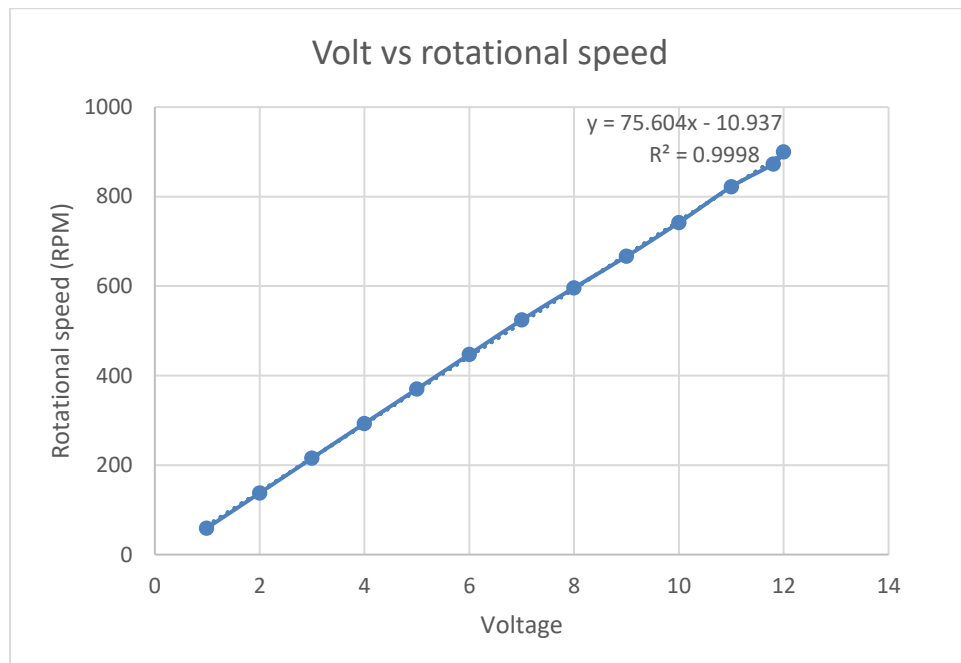


*Fig. 18 Rotational speed (RPM) vs Voltage calibration curve*

### **3.10 Advantages of the technique**

The device has certain advantages over other mechanically-induced elution processes. It elutes the swab by imposing multiple impingement on the swab head to scrub the samples out of the fibre matrix. The spiral chamber allows the magnetic particles to impose the necessary forces throughout the length of the swab in the vertical direction. The rotating magnetic field is responsible for two simultaneous effects:

- Magnetic levitation of the smaller particles from the base, inside the vial, to an optimum height, depending on the length of swab tip.
- Simultaneous rotation and revolution of the smaller particles. The rotation of the particles around its own axis generate the necessary impact forces for scrubbing the samples from swab fibres. The revolution of these particles around the central axis allows complete coverage of the swab surface area and helps to produce multiple impingement on the swab. It also produces a vorticity in the fluid, which enables fluid mixing and enriches the homogeneity of the eluate with the micro-organisms.

Most of the previous techniques of mechanical elution used vortexing or mild agitation by convective fluid flow, ultrasonication or piezoelectric vibrations. They elute the samples by gentle tangential shear forces across the surface of the swab. This device use mechanical impact as the method of elution. Here, the samples are eluted by direct physical contact to the swab fibres. The magnetic particles produce multiple impingement throughout the entire surface area of the swab, thereby allowing complete elution of the swabs. Apart from

impact, the convective forces generated in the fluid helps to elute the sample and prepare a homogeneous mixture of sample and elution fluid. The design of the vial also helps to reduce the elution volume to  $\sim 600\mu\text{L}$ , from 2 – 10ml used in the previous devices.

## Chapter 4

### Materials and Methods

The elution process consists of several steps post collection of samples from the swabs. For experimental purposes, the swabs were dipped in the artificial sputum solution loaded with polystyrene beads or bacterial cells. These swabs were then transferred to a vial with an elution fluid and magnetic particles are used for impingement. These are all the essential materials required for the experiments.

In this chapter, all the materials used for the experimental procedures are described. The specifications of the swabs and magnets used in the device are described. Preparation techniques for artificial sputum samples are detailed. The different beads and bacterial cells mixed with the sputum samples are described. Different techniques for enumeration and calculation of recovery efficiency are also explained. Finally, the detailed experimental setup for both devices and elution procedures are discussed.

#### 4.1 Swabs

Swabs are used as collection devices for most biological and environmental surfaces. Among them, cotton swabs are the most widely used sample collection devices with salivary or sputum based bio-chemical assays because of its easy availability, low cost and high absorbance. For experimental purposes, non-sterile cotton-tipped applicators, manufactured by Medline Industries, Inc., Mundelein, IL, were used. Each cotton tipped applicators were  $15.2 \pm 0.6$  cm in length with a swab tip length of  $1.5 \pm 0.1$  cm and

diameter of 3-3.5mm. The shank of the swab was wooden, while the fibrous tip was latex-free cotton. The swab fibres constitute only a fraction (1/6<sup>th</sup>) of the total weight of the swab. The water retentive property of the swab is, therefore, determined by the absorptivity or water holding capacity of the fibres.

#### 4.2 Absorptivity

Absorptivity is defined as the fluid (water) retaining capacity of the swab fibres. Water holding capacity of the swab fibres is an important parameter that determines the effectiveness of swab based sample collection techniques [92]. In order to measure this parameter, each swab was individually pre-weighed and immersed in 1 ml of DI water for 30 sec. The tube was then mildly agitated at ambient temperature for 1 min to facilitate water absorption. The weight of swab infused with water was then determined for each swab. This process was done with 9 different swabs and their percent water absorption was computed. Each trial represents a single experiment using a single cotton-tipped swab. Water holding capacity is calculated as:

$$\% \text{ Water Absorption} = \frac{\text{mass of hydrated swab} - \text{mass of dry swab}}{\text{mass of dry swab}} \times 100 \quad (9)$$

Sample	Water absorbed (µl)	% Water absorption	Average
Expt 1	216	36.2	35.81 ± 3.12
Expt 2	193	33.6	
Expt 3	221	37.5	

Expt 4	208	35.2	
Expt 5	211	35.2	
Expt 6	224	37.6	
Expt 7	185	32.6	
Expt 8	238	38.5	
Expt 9	206	34.37	

*Table. 5 Water absorptivity of the swab fibres*

### **4.3 Actuating Magnet**

As described in section 3.3, a diametrically magnetized ring magnet has been used to create a rotational motion and circular translation of magnetic particles inside the vial for elution. The ring magnet has a distinct magnetic distribution, where the north and south poles lie on the opposite curved surfaces. The polarity is maximum at two opposite poles and decreases smoothly to a low value at the equator before reversal of polarity. A ring magnet was chosen as compared to the more commonly available bar magnet in order to minimize the duration of time per rotation cycle when the magnetic field imposed by it is tangential to the surface of the swab (Appendix D). Furthermore, because of the wide, flat surface, disc magnets have a large pole area making them stronger magnets than any other configurations [93].

The selected ring magnet is a N42 grade of diametrically magnetized NdFeB magnet (K&J Magnetics Inc.), with dimensions of 1/2"(12.7 mm) OD x 3/16" (4.76 mm) ID x 1/4"(6.35 mm) thick ( $\pm 0.004"$  x  $\pm 0.004"$  x  $\pm 0.004"$  (0.1mm) tolerances). The diametrically

magnetized ring magnets are magnetized perpendicular to the central axis through the centre of the magnet. The north and south poles are on the opposite sides of the curvature and will have attraction or repulsion forces from the sides. These magnets have a pull force (Pull force is defined as the normal force required to detach a magnet from a steel bar) of 4.11 lbs (1.86 kgf), with a surface field of 6282 Gauss and  $B_{r,max}$  (maximum residual induction) of 13,200 Gauss. The “N42 grade” indicates that the maximum energy product at the highest point on the B/H Curve is 42 MGOe (MegaGaussOersteds).

The particles that are used inside the vials to cause physical impingement of the swab were also chosen to be magnetic. Magnetic particles, coated with biologically inert materials, were chosen to provide higher pull forces as compared to ferromagnetic materials. The phenomena of action are depicted in Figures 19a and 19b. Figure 19a shows the action of the ring magnet on magnetic particles as used in the device. The magnetic particles initially get attracted to the opposing pole of the ring magnet and is attached together to remain as one unit. When the motor is rotated, the poles of the ring magnet are reversed. This allows the magnetic unit inside the vial to flip around its own axis. Figure 19b shows the nature of attraction if ferromagnetic particles are used. In case of ferromagnetic particles, with the change in magnetic poles of the ring magnet, alternating north and south poles will be induced on the face closer to the ring magnet. Hence, the rotational motion of the particles, due to flipping of poles, will not be achieved.

Moreover, the self-assembling of the magnetic particles under the influence of magnetic field increases the effective area of contact during flip than a single magnetic particle, thereby producing higher impact forces on the swab. Any higher number of magnetic particles will occupy more space in the vial for free motion and will require

containers of higher diameter. This will increase the total elution volume to immerse the swab head completely. Hence, the number of magnetic particles were confined to two.

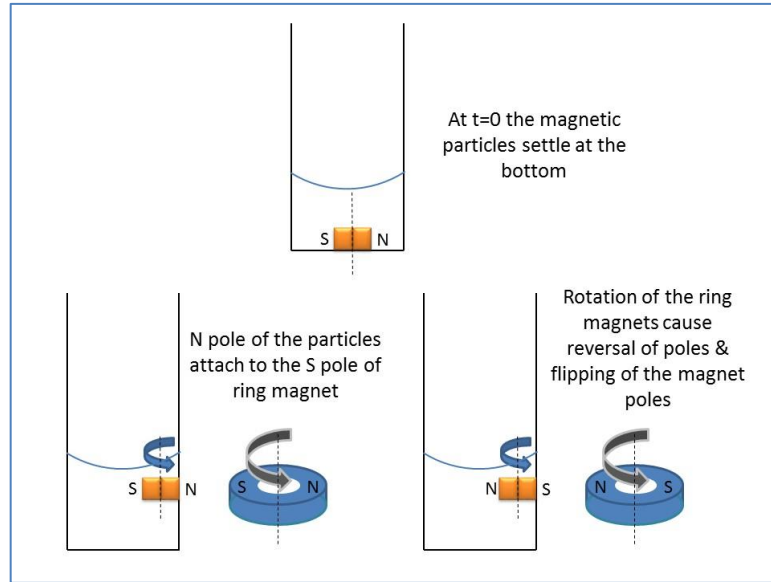


*Fig. 19a Magnetic effect on the particle motion when magnetic particles are used*

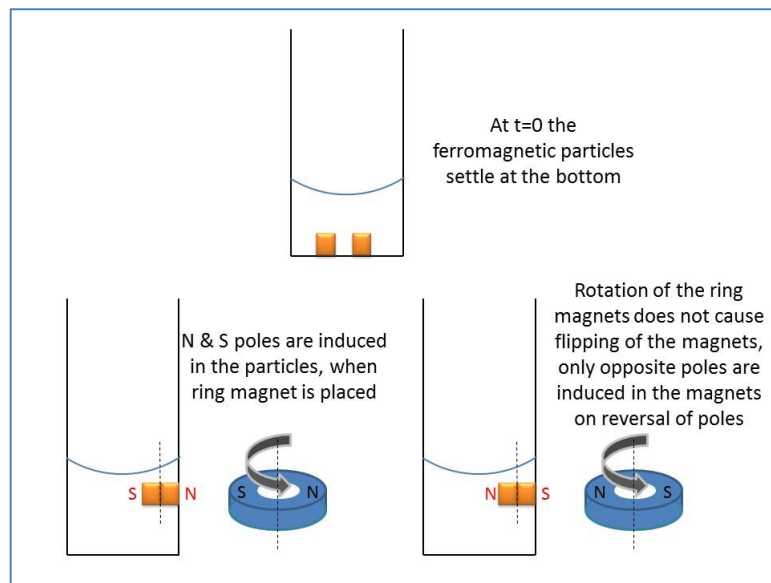


*Fig. 19b Magnetic effect on the particle motion when ferromagnetic particles are used*

The magnetic particles used were N42 grade of NdFeB block magnets with Ni-Au-Ni (Gold) plating and magnetized through its thickness. These particles had a pull force of 0.86lbs (0.39 kg-f), with a surface field of 5754 Gauss and a maximum Residual Induction of 13,200 Gauss. Two small magnetic particles were used in each device and each has a dimension of a cube with side of 1/8" or 3.175mm. The rotation of the diametrically polarized magnet by the motor produces a magnetic force on the particles under confinement (gap spacing ~5.08mm) between the swab and the walls, repeatedly impinging on the swab at various angles and locations.

#### **4.4 Polystyrene beads**

Live bacterial samples are not ideal for characterizing the performance of the elution method as they are constantly multiplying. Therefore, a suitable model was required that will resemble its physical characteristics, is easy to quantify and can be easily handled. Polystyrene beads have used in several applications such as cell tracking, cell sorting, and particle image velocimetry as substitutes for cells. Polystyrene beads of 1µm has similar size as *E. coli* bacterial cells and therefore can be used as easily quantifiable substitutes in this thesis.

Negatively charge stabilized colloidal polystyrene particles (Invitrogen FluoSpheres Carboxylate-Modified Microspheres) were used to replicate the presence of microbes in sputum. These polystyrene particles have a nominal bead diameter of 1.0 µm and are labelled with orange fluorophore (proprietary dye) with an excitation/emission wavelength of 540/560 nm [94]. The microbeads are in an aqueous suspension of  $10^{10}$  particles/ml

concentration. They were mixed with the artificial sputum in varying ratios to mimic the bacteria-loaded sputum of a patient.

#### **4.5 Bacterial Samples**

Sputum samples, spiked with *E coli*, were also prepared for use in characterization of swabbing and elution. *Escherichia coli* is a gram-negative, anaerobic, rod-shaped bacterium, found in stool or urinary tract infections of humans or animals. Most strains are harmless, but some serotypes can cause food-poisoning and diarrhoea. Green Fluorescence Protein (GFP) tagged (Excitation/emission wavelength: 487/509 nm) *E coli* K12 MG1655 (Purchased from ATCC 27325) were used for the elution experiments, to count the number of cells by fluorescent imaging.

*E coli* were cultured in Luria-Bertani (LB) broth by picking individual colonies from infested agar plates. They were kept overnight (16 hours) in a shaking incubator at 37°C and 250 RPM, after being mixed with Ampicillin (1:1000 ratio by volume). The resultant bacterial solutions were then serially diluted in LB broth before mixing them with artificial sputum samples at desired concentrations.

#### **4.6 Artificial Sputum**

The artificial sputum used in the set of experiments was formulated to mimic the properties of macroscopic mucoid type of sputum with a viscosity of  $4.20 \pm 0.4$ poise [25] at shear rate of  $90\text{s}^{-1}$ . To obtain the desired properties, a 2% (w/w) solution of methyl cellulose in water was used. Dry methyl cellulose (approximate molecular weight 41,000), with an appearance resembling white powder, was obtained from Sigma Aldrich (product

# M0262). It was first mixed with 1/3<sup>rd</sup> of the required volume of water preheated to 80°C, while being continuously stirred by a magnetic stirrer. The solution was continuously agitated until the methyl cellulose particles get evenly dispersed. The remainder of the water was then added and the temperature of the water was lowered to increase solubility. This procedure obtained a more homogenous solution as compared to mixing the cellulose with water at low temperatures. The solution was stirred for another 30 minutes. The final solution obtained had a viscosity of ~4.1 poise at 20°C as measured using a rheometer, which is close to the targeted value.

#### **4.7 Sample preparation**

Initial experiments were done with artificial sputum mixed with polystyrene beads (Invitrogen FluoSpheres Carboxylate-Modified Microspheres) of 1µm size. The polystyrene bead stock suspension had a concentration of 10<sup>10</sup> particles/ml. This stock suspension was mixed with artificial sputum samples at different ratios to obtain the desired concentrations for the sample. Serial dilutions of the mixed samples were made directly with artificial sputum samples at 1:10 ratios to obtain sample with a range of concentration of beads from 10<sup>9</sup> to 10<sup>5</sup> particles/ml.

Green Fluorescence Protein (GFP) tagged *E coli* K12 were used for the elution experiments. *E. coli* were cultured in Luria-Bertani (LB) broth by picking individual colonies from cultured agar plates. They were kept overnight (16 hours) in a shaking incubator at 37°C and 250 RPM, after being mixed with Ampicillin (1:1000 ratio by volume). The resultant bacterial solutions were then serially diluted in LB broth before mixing them with artificial sputum samples at desired concentrations.

Luria-Bertani (LB) media was used as growing media for bacteria. In order to prepare the media, 25 g/L of LB-Miller's powder (L3522 SIGMA – LB Miller's) was mixed with DI water and its pH was adjusted to 6.8. the solution was then autoclaved for 15 minutes at 120°C to sterilize. This nutrient solution contains peptides, amino acids, water-soluble vitamins, and carbohydrates.

#### 4.8 Experimental setup

The experimental setup (Figure 20) consists of the device, connected to the DC power supply through a switch. A vial containing the elution fluid, magnetic particles and the swab was placed at the centre of the device. The vial is a cylindrical, glass container of diameter 15mm and height 45mm. A pair of clamps were used to support the vial at the centre. The height of the vial was designed in such a way that the magnet holder was aligned with the centre of the swab head. A ring magnet was placed on the gear in the slot. The motor was connected to the DC power supply (BK Precision DC regulated power supply, 1670A).

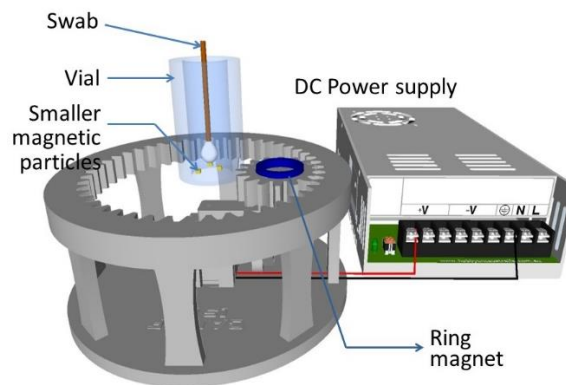


*Fig. 20: Schematic of the experimental setup to characterize the elution of particles and cells from the swab.*

A modified and more compact device design was also developed and the experimental setup for testing it was similar but with a few modifications as shown in Figure 21. In the modified design, the magnet was placed in one of the external gears, while the other gear provided for the rotating imbalance only. A modified vial was created which had internal grooves placed in the slot at the centre of the fixed central gear. The eluent and magnetic particles were loaded to the vial and the swabs were placed inside. The magnetic particles were placed in confinement at the base and started to move up the groove when the motor was turned on. The motor provides rotary motion to the base gears at 1:1 gear ratio, which rotates the top external gears around the fixed central gear, producing both rotation and revolution. An Arduino controller was connected to the computer so that the rotational speed of the motor can be controlled. A switch has been provided to start and stop the motor as per the users' need.

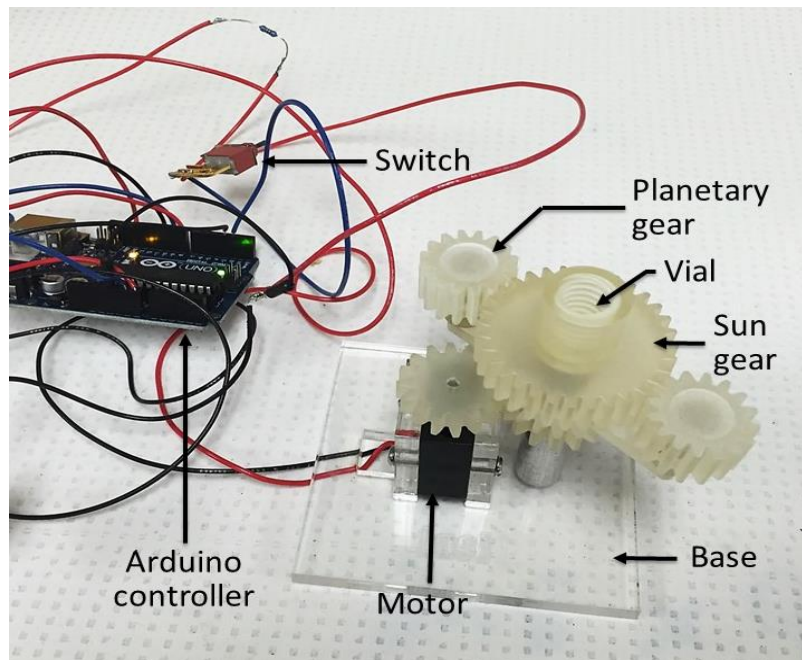


*Fig. 21: Experimental Setup: Second device*

#### 4.9 Experimental procedure

The experimental procedure includes the preparation of artificial sputum samples with polystyrene, the swabbing procedure and its subsequent elution. The sputum samples were made prior to the start of the experiment. The cotton swabs were immersed in a solution of polystyrene in methyl cellulose with varying concentrations ( $10^9$ - $10^5$  particles/ml) for 30 seconds. The immersion time was chosen to be 30 seconds, as it is typical in clinical procedures [95]. The swabs were then air dried for 1 minute and dipped in the vial containing 700  $\mu$ l of DI water solution containing magnetic particles for elution. The motor was turned on at desired speed and the swabs were eluted for the desired amount of time.

Similar procedures were adopted for *E. coli* samples. Freshly cultured *E. coli* K12 was mixed with artificial sputum samples to avoid the multiplication of *E. coli* (*E. coli* grows to twice its count in 20-30 minutes). *E. coli* solutions were serially diluted in LB media in ratios of 1:10 or 1:2 and then mixed with methyl cellulose solutions. DI water was chosen as elution fluid instead of a growth medium to prevent the growth of cells, that might hinder the subsequent enumeration.

The pipetting efficiency was calculated to ensure uniform collection of volumes for each experimental batch. Equal amounts (10 & 100  $\mu$ L) of polystyrene samples were taken by pipettes (Eppendorf, 2-20  $\mu$ L and 20-200  $\mu$ L respectively) and spread on a glass slide and covered by slide covers, before being pictured by a fluorescent microscope. The number of beads were calculated and the error was found to be  $\sim\pm 3\%$

#### **4.10 Quantification of beads and cells**

The number of beads or cells retained by the swab and removed from the fibres after elution is instrumental in the determination of recovery efficiency. Hence, the quantification of beads/cells both before and after elution, is important. The processes of quantification can be categorized based on the concentration range of the initial artificial sputum samples. Fluorescent imaging was used for samples at higher initial concentrations ( $10^{10}$ - $10^7$  particles/ml) and a plate reader for low concentrations ( $10^7$ - $10^5$  particles/ml). In case of *E. coli*, at very low concentrations ( $<10^5$  CFU/ml), plating techniques were found to be suitable. All the experiments were based on the assumption that the samples were mixed homogeneously with either polystyrene or *E. coli*.

Three different techniques were needed for different concentration ranges to increase the accuracy in counting the number of beads/cells. The number of beads/cells was counted for smaller volumes of eluate and then the number was back-calculated for the entire solution. In each enumeration, several small amounts of samples were taken from different zones of the sample and averaged to arrive at the concentration value.

#### **4.11 Quantification techniques**

The number of beads eluted from the swab fibres are calculated post elution to determine the recovery efficiency. After elution experiments were done and the swabs were taken out, the eluate volumes were analysed for the number of beads/cells left over in the samples. For higher concentration of post-elution samples, the eluate was further diluted through two steps of  $10^{-1}$  /ml dilution each, before the concentration of the sample were calculated. But no such steps were deemed necessary for eluate samples lower than about

$10^6$  particles/ml concentration. Depending on the nature and concentration of the samples, one of the following three detection techniques were employed.

#### **4.11.1 High concentration ( $10^9$ - $10^7$ /ml): Particle counting**

High concentration range is defined as bead concentration range of  $10^9$ - $10^7$  particles/ml in artificial sputum. 10  $\mu$ L of the post-elution solution was taken on a microscope slide by means of a pipette. A microscope coverslip (22mm x 22mm) was placed on top of that droplet to ensure the uniform spreading of the elution volume throughout the square cover. Images were taken at 6 different locations distributed over the entire coverslip. An Upright Bright Field & Fluorescence Microscope (Olympus; BX53) was used to take images of the polystyrene beads tagged with fluorophore with a 20X magnification.

These images were then assessed in ImageJ software to automatically count the number of beads at each location. They were then averaged over the entire area to find the number of beads in the region covered by the slide cover. This value represents the number of beads in 10 $\mu$ L. Then, the number of beads in the entire elution volume was back-calculated from the calculated particulate number in 10  $\mu$ l. With known values of the number of the number of beads in the samples pre- and post- elution, the recovery efficiency was calculated using equation 10 described below. Similar method was also used to enumerate the number of GFP tagged *E. coli* cells.

#### **4.11.2 Low concentration ( $10^7$ - $10^5$ /ml): Fluorescent Intensity measurements**

Low concentration range can be defined as bead concentration ranges of  $10^7$ - $10^5$  particles/ml in artificial sputum. With lower concentration, direct particle counting approach as described above was found to be not suitable. Sampling at a number of different locations that were randomly selected led to a wide distribution in the number of particles in the samples collected from those locations. This was due to the low number of particles present in the solution and the entire 10  $\mu$ L needed to be imaged to produce an accurate result. To overcome this issue, the total fluorescence intensity of 300  $\mu$ L of the eluate volume was measured using a plate reader (Tecan Infinite M1000 Pro). Separate calibration curves were obtained for *E coli* and polystyrene beads to work with final eluate volumes in  $10^6$ - $10^4$  particles/ml concentration range. While working with initial sample concentration of  $10^7$ - $10^5$  particles/ml, the total number of eluted particles was found to be in  $10^6$ - $10^4$  particles/ml concentration range. The calibration curves were developed by measuring the fluorescent intensity (in relative fluorescent units or RFUs) in microwells loaded with 300 $\mu$ L of sample solutions containing known concentrations. Opaque 96-well microwell plates with black side walls were used for this purpose as transparent plates caused significant cross talk and noise between the adjacent wells that affected measurements. The different calibration curves for polystyrene and *E. coli* for different concentration ranges are given below [Figures 22-25].

In order to perform measurements from samples, multiple readings were taken per well (each with a volume of 360  $\mu$ L) at 12 different sections with an excitation and emission wavelengths of 488 nm and 507 nm (10 nm bandwidth). Fluorescent intensities were measured using a gain of 158, with 50 flashes, 400 Hz frequency, 20 $\mu$ s integration time

and 10ms of settle time with 10 kinetic cycles (the number of runs taken for each well). Fluorescence intensities were measured for all the post-elution solutions and compared with the calibration curve to know the exact concentrations. Once the elution volume has been measured, recovery efficiency can then be calculated by using the calibrated equation.

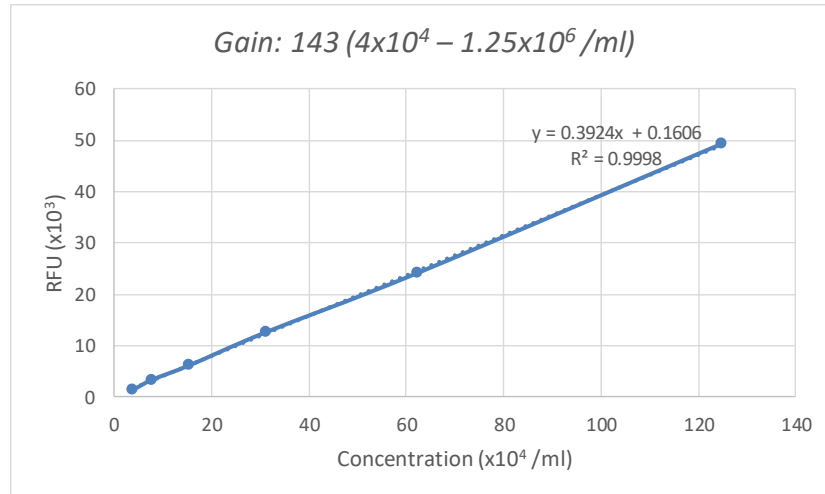


Fig. 22 RFU vs concentration for polystyrene samples,  $5 \times 10^4 - 1.25 \times 10^6$  particles/ml range (Gain: 143)

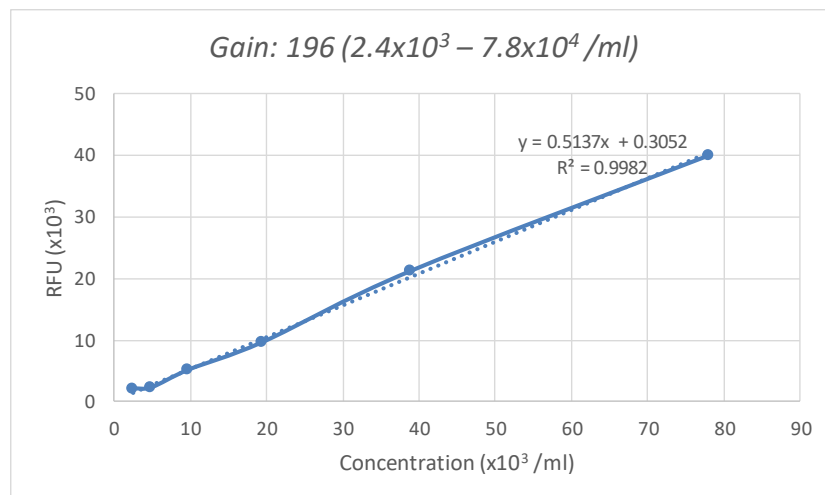


Fig. 23 RFU vs concentration for polystyrene samples,  $2.4 \times 10^3 - 7.8 \times 10^4$  particles/ml range (Gain: 196)

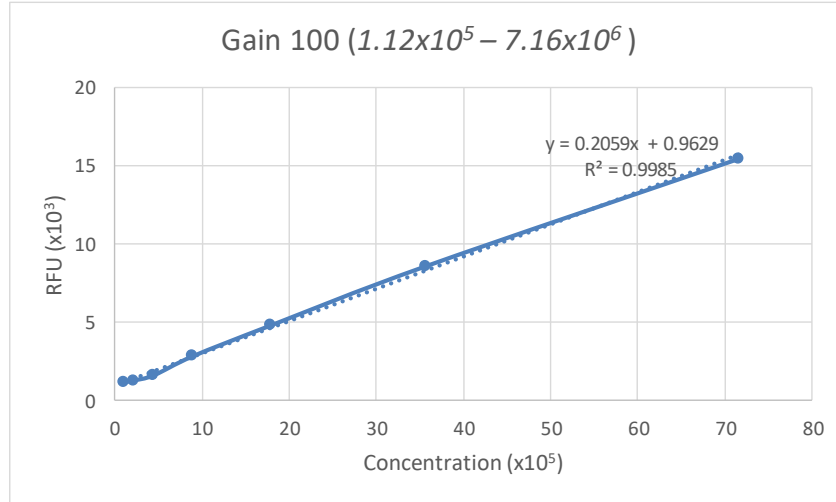


Fig. 24 RFU vs concentration for *E. coli* samples,  $1.12 \times 10^5 - 7.16 \times 10^6$  CFU/ml range  
(Gain: 100)

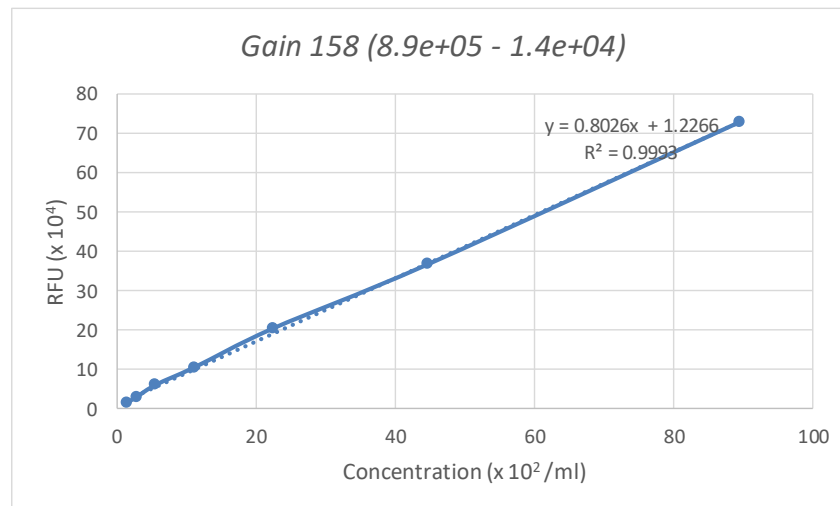


Fig. 25 RFU vs concentration for *E. coli* samples,  $1.4 \times 10^4 - 8.9 \times 10^5$  CFU/ml range  
(Gain: 158)

#### 4.11.3 Very Low concentration ( $<10^5$ CFU/ml): Plating technique

Very low concentration range can be defined as bead/cellular concentration ranges of less than  $10^5$  CFU/ml in artificial sputum. Working with lower concentrations, below  $10^5$

CFU/ml ranges are difficult using particle counting and fluorescent intensity measurements. The swabs absorb around 120  $\mu\text{L}$  of artificial mucous and post elution the number of cells remaining in the eluate is in the order of  $10^4 - 10^3$  CFU/ml. With such a low concentration, the fluorescence intensity values are no larger than the blank/background signal, even with a high gain. Taking fluorescent picture with 10  $\mu\text{L}$  samples is equally challenging, where we might not get any cells in the frame while using a 40x lens on the camera. Hence, plating technique is the only viable option.

The eluate, which comprises of *E. coli* cells and DI water, was first serially diluted in LB media through two steps of  $10^{-1}$  dilution each. Ampicilin was added at 1:100 ratios to prevent the growth of any other contaminating species that may be present. The experiments were repeated five times for 5 different samples of 50 $\mu\text{L}$ , taken from solutions at each stage of elution and at different locations in the vial and spread on an Agar plate. The plates were then placed in an incubator upside down (to prevent condensing water to fall back on the agar) at 37°C for 16 hours. The number of colonies grown on the plate represented the number of cells actually present in the initial diluted sample. The total numbers of cells were then back calculated for the known volume and dilution.

#### 4.12 Recovery Efficiency

Recovery efficiency is a parameter used to define the performance of the elution process. It can be defined as:

$$\text{Recovery Efficiency} = \frac{\text{No. of beads/cells in solution after elution}}{\text{No. of beads/cells absorbed by the swab with the sample}} \times 100 \quad (10)$$

Both the number of particles before and after the elution process has to be determined to calculate the recovery efficiency. To determine the number of beads adhered to the swab before elution, weights of individual swabs were taken before and after dipping it into the solution. Once the weight and density of the absorbed solution were measured, the volume was calculated. That determines the number of beads trapped in the swab fibre matrix, under the assumption that they were homogeneously mixed.

The number of particles post elution can be calculated by any one of the abovementioned methods, depending on the range of concentration. When both the values were obtained, the recovery efficiency was calculated. The value of the recovery efficiency determines the percentage of the beads/cells absorbed by the swabs that were finally recovered after elution. Higher value of the recovery efficiency is desired, and the experimental setup described in this thesis aims to do this.

#### **4.13 Summary**

This chapter provides a detailed description of all the materials and methods for the experimental procedure. Cotton swabs were used for absorbing artificial sputum samples because of their high absorbance properties and ease of use. Artificial sputum samples were prepared by dissolving methyl cellulose in DI water and then mixed with flurophore-tagged polystyrene beads or GFP tagged *E. coli* cells. Smaller magnetic particles were placed inside the vial to impart impact forces on the swabs. A ring magnet was used to provide both rotational motion and a circular translation of the magnetic particles. All these materials were appropriately chosen to produce a compact device, provide higher impact forces to maximize recovery and fasten the enumeration technique.

Different techniques of detection and enumeration of eluted particles have also been described in this chapter. The process depends on the initial concentration of the sample before the experiments were made. Each of the techniques involve calculation of the number of eluted particles based on the known data of different 10  $\mu$ L samples. For each of the calibration and experimental values, repeated measurements were performed by taking samples from different zones of the vial and picturing different parts of the microscope slide cover. These techniques also indicate the best estimate of the number of particles under the assumption of homogeneous mixing of the solutions. The calibration curves were drawn on the basis of the blank, which were calculated for each set of data at the desired gain. The actual values at different concentrations were subtracted from the blank values to obtain the actual RFUs. This allows the data to be used for repeated experiments, by subtracting each experimental RFUs from their respective blanks. These techniques allow examination of bulk samples quickly and efficiently.

## Chapter 5

### Results and Discussions

This chapter deals with the characterization of the elution processes and identification of the important control parameters that influence it. Elution time, rotational speed and concentration of initial samples are considered to be the prime parameters. The rotation of the magnet around the swab determines the energy that is imparted to the particles, which then causes mechanical impingement and elution. Similarly, the duration of elution determines the number of impingements that are caused. These two factors are of primary importance in determining the elution from the swab and have been characterized. Next, the concentration of cells or particles on the swab can also determine the elution efficiency and its effect has also been characterized. The characterization of the effect of physical parameters such as rotational speed and the duration have been performed using polystyrene beads as their number remains invariant during the course of the experiments and they are easy to quantify. Final experiments are conducted with *E. coli* cells to demonstrate the elution under optimized conditions but at varying concentrations.

#### 5.1 Effect of magnetic impingement

Several experiments were done, with and without the use of the said device, to understand the effectiveness of the device over elution processes with no or mild agitation. The impact of the repeated impingements offered by the magnetic particles on recovery efficiency has been compared with that obtained from the no-agitation method.

The experiments were performed by immersing dry swabs in the artificial sputum samples, prepared as per the procedures described in section 4.6 of chapter 4. Separate samples containing 5% v/v ( $\sim 5 \times 10^8$  particles/ml) and 10% v/v ( $\sim 10^9$  particles/ml) polystyrene bead concentrations were tested individually. In order to determine the elution efficiency in no agitation case, the swabs were dipped in the artificial sputum solutions, air dried for 30 seconds and dipped into the vial containing DI water. The experiments were repeated for various elution times (30 s - 180 s) of 30 s intervals. Five repeats of experiments were performed for each condition and the average recovery efficiency was obtained. In order to determine the elution efficiency in the magnetically actuated case, the same experiments were performed with the device at 300 RPM and for various elution times (30 s – 180 s). The swabs were dipped in the artificial sputum solutions mixed with polystyrene beads ( $\sim 5 \times 10^8$  particles/ml and  $10^9$  particles/ml concentrations). They were also air dried for 30s and inserted in a vial containing magnetic particles. The motor was set to a fixed rotational speed of 300 RPM and the swabs were eluted by multiple physical impingements. Recovery efficiencies were calculated and averaged to obtain specific points for different elution times.

The recovery efficiencies for elution procedures with magnetic impingement and without any significant agitation process are shown in Figures 26 and 27. Figure 26 shows the recovery efficiencies for both procedures with a sample of  $10^9$  particles/ml bead concentration. The recovery efficiency increases with elution time, but beyond an elution time of 120s there is no significant increase. This happens for both the cases and for elution without agitation, the recovery efficiencies rise from 33.68 to 41.8 % over the time period of 30 - 120 s. The corresponding values for elution with magnetic agitation at 300 RPM

for 30-120 s is 51 – 63.2% The maximum values obtained by no agitation method and magnetic impingement at 300 RPM are 41.8% and 64.9% respectively. The difference in elution efficiency was found to be statistically significant between no agitation elution method and that at 300 RPM (p-value –  $25 \times 10^{-6}$ ).

Figure 27 shows the recovery efficiencies for both procedures with a sample of  $\sim 5 \times 10^8$  particles/ml bead concentration. For elution without any significant agitation, the recovery efficiencies increase from 31.9 to 51.7% within elution times of 30 s to 120 s, and then gradually attains a steady state. The corresponding values with magnetic agitation at 300 RPM are 57.6 – 81.5% within the same time period. The high recovery efficiencies obtained from the physical impact of magnetic particles at a low rotational speed of 300 RPM shows promise of the device to be used for better elution of swabs. Once again, the difference in elution efficiency was found to be statistically significant between no agitation case and that at 300 RPM (p-value -  $1.9 \times 10^{-4}$ ).

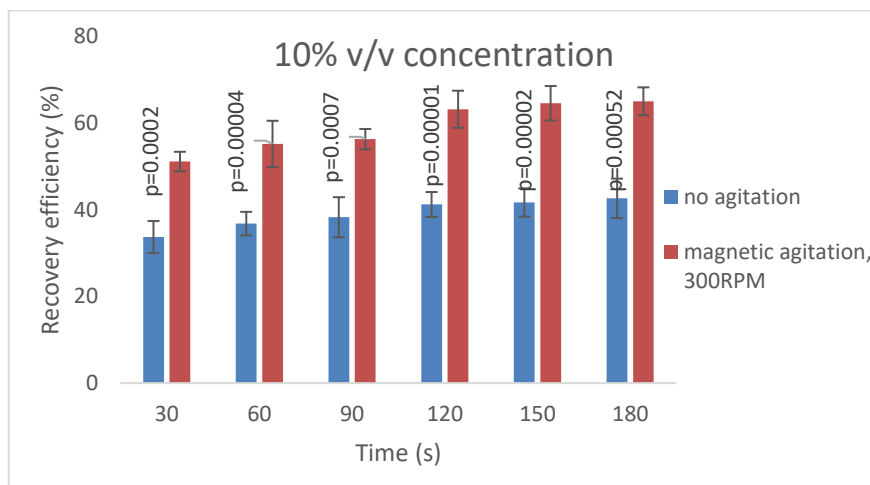


*Fig. 26 Comparison of recovery efficiencies for elution without agitation and with magnetic impingement (300 RPM) of swabs dipped in 10% v/v ( $\sim 10^9$  particles/ml) concentrated samples*

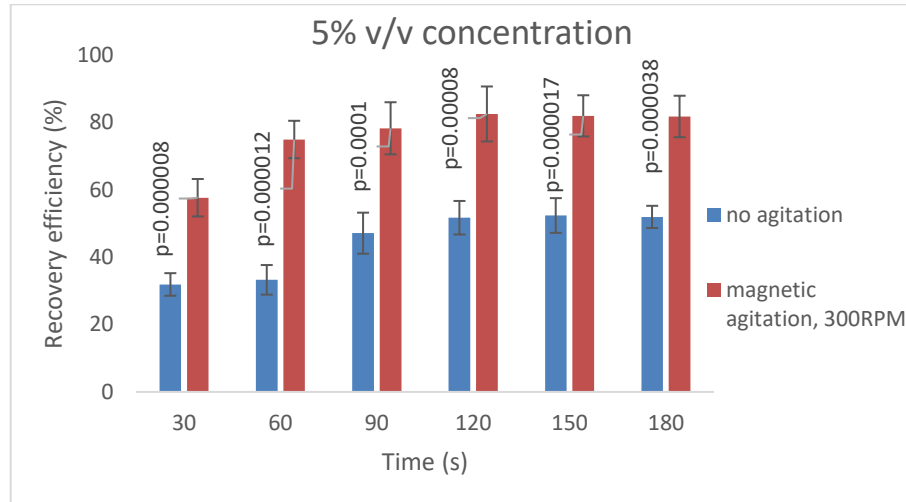


*Fig. 27 Comparison of recovery efficiencies for elution without agitation and with magnetic impingement (300 RPM) of swabs dipped in 5% v/v ( $\sim 5 \times 10^8$  particles/ml) concentrated samples*

In the process with no significant agitation, the elution is primarily guided by dissolution of artificial sputum in elution fluid. The artificial sputum sample entrapped inside the fibre matrix had a higher bead concentration initially. When immersed in an elution fluid, the artificial sputum dissolves in the elution fluid and the beads migrate along with it. This process continues for the first few seconds and finally reaches a steady state when the concentration of the two regions are balanced. The rates of dissolution can be determined from the Noyes-Whitney equation [96]:

$$\frac{dm}{dt} = A \frac{D}{d} (C_s - C_b) \quad (11)$$

where, m is the mass dissolved, t is the time, A is the surface area of the interface between solute and solvent, D is the diffusion coefficient, d is the thickness of the boundary

layer of the solvent,  $C_s$  is the mass concentration of the substance on the surface and  $C_b$  is the mass concentration of the substance in the bulk of the solvent.

Two different mechanisms operate during the processes of elution by magnetic agitation. The magnetic impingement on the swab fibres causes the sample, absorbed in the swab, to be locally squeezed out at the point of impingement. This eluted sample is thoroughly mixed with the elution buffer due to convective motion of the surrounding fluid caused by the motion of the magnets. However, after impingement, the surrounding elution fluid gets absorbed back into the swab locally which dilutes the concentration of the particles at the location. This process repeats itself for every impingement. The elution is the most during the first few seconds as the sample close to the surface of the swab gets eluted. Then, as the elution proceeds deeper into the swab matrix, the physical impact due to the magnets cause mixing inside the swab between surface layers that have a lower bead concentration and deeper layers that have a high bead concentration, as well as higher matrix viscosity. Therefore, the number of beads extracted from the fibre matrix gradually increases with each subsequent impingement. Over the long run, the concentration of the beads in the fluid is nearly the same as that inside the swab and then there is no more elution. Henceforth, the process reaches a steady state.

Higher values of recovery efficiencies are obtained from physical impingement of particles on the swab tip and hence is a better elution process than any technique without any significant agitation. Unlike the no agitation case, where the time constant associated with the dissolution process is long and therefore only the sample at the surface layers of the swab get effectively eluted, under magnetic impingement, not only is the surface elution rapid, but the impingement also imparts forces to actively mix the sputum sample between

the deeper layers of the swab and the surface layers that have absorbed the elution buffer from outside. This effectively brings out the sample that have been absorbed deep inside the swab matrix, which may not be eluted otherwise. The rotation of the magnet around the swab determines the energy that is imparted to the particles, which then causes mechanical impingement and elution. Similarly, the duration of elution determines the number of impingements that are caused. These two are the most important parameters that affects the recovery. The other important parameters which will influence the elution process are – viscosity, concentration and type of cells/particles.

Scanning Electron Microscopy (SEM) images of the swab tips were taken in order to visualize the elution of the microscopic particles from the swab head. Dry swabs were immersed in a solution of artificial sputum with a bead concentration of  $\sim 10^9$  particles/ml for 30 s and air dried for 30 s. Some of these swabs were then introduced in the setup and eluted for 60 s in distilled water at 100 RPM. Others were preserved as is to obtain images of the pre-elution condition of the swab. Both the pre-elution and post-elution swabs were super critically dried using a critical point dryer (Leica EM CPD300). Subsequently, a thin conductive layer of gold (30 nm) was deposited on to it for SEM imaging.

The SEM images of the pre- and post-elution swabs are shown in Figure 28. These images were taken at two different magnifications: 1000x (Figures 28a, b and c) and 5000x (Figures 29a and b). Figure 28a shows the image of the pre-elution swab. It can be clearly seen that the fibres of the swab head are immersed in the artificial sputum solution. Some of the polystyrene beads are also visible. Figure 28b shows the image of the post-elution swab for the control case of no agitation. This figure shows some of the polystyrene beads retained by the swabs on the top matrix. Figure 28c shows the image of swab fibres after

being eluted in the device by agitation with magnetic particles. The fibres of the swab are visible and most of the artificial sputum has been removed (eluted) from the swab. Most of the polystyrene beads are eluted from the top fibres. Some of the polystyrene beads attached to the interior fibers in the swab are also visible. These images illustrate that the active elution mechanism used is capable of removing the bulk of the viscous sample that is trapped in the swab material.

Better understanding of structural details of the fibres and the entrapment of polystyrene beads can be obtained from Figures at 5000x magnifications (Figures 29a and b). Figure 29a shows the polystyrene beads retained in the swab fibres in close detail. The polystyrene beads are absorbed by the swab fibres and some beads also penetrate in the inner matrix, when the swab was dipped in the sample. After elution without agitation, the artificial sputum on the surface layer dissolves and most of the particles on the top matrix are eluted. But some of the fibres in the inner matrices are retained. Figure 29b shows the swab fibres after elution by magnetic actuation. This figure shows that less number of beads are retained in the inner matrix of the swab as compared to the elution without agitation. Beads trapped in the small cracks and crevices are hard to remove, although the ones on the surface of fibres get eluted easily. Hence, these micrographs show the sources of entrapment of beads, which can't be removed even with an active mechanism and higher impact force, therefore the recovery is less than 100%.

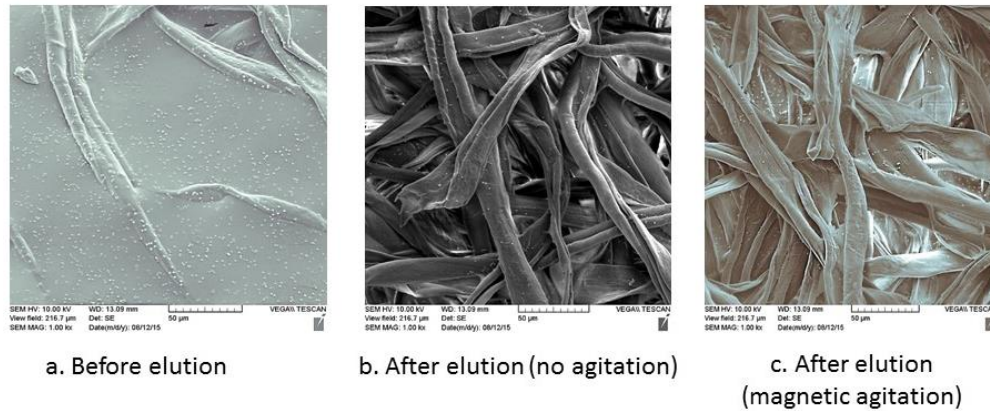


*Fig. 28 a) Distribution of polystyrene beads on swab fibres before elution, b) fibres post elution (no agitation) c) fibres post elution (magnetic beads agitation) – 1000x*

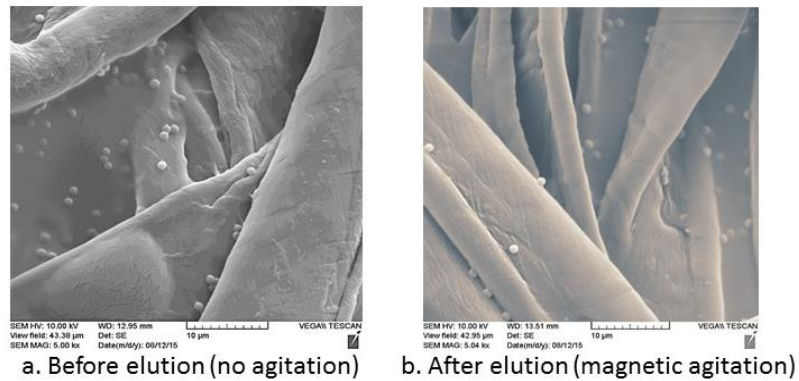


*Fig. 29 Distribution of polystyrene beads on swab fibres after elution with a) no agitation b) magnetic agitation – 5000x*

## 5.2 Effect of Sample Viscosity

Artificial sputum samples, prepared as per the procedures described in chapter 4 section 6, were used in all the experiments. It was intended to mimic the properties of

macroscopic mucoid type of sputum samples as obtained from patients. These samples were prepared by mixing methyl cellulose in DI (Deionised) water and has a high viscosity of ~4.1 poise. In addition, polystyrene beads were also mixed with DI water samples for comparison purposes.

Experiments were performed to compare the recovery of beads from swabs when used with artificial sputum and DI water. Both artificial sputum and DI water were mixed with polystyrene beads at 10% v/v ( $\sim 10^9$  particles/ml) concentrations. Dry swabs were dipped in both the solutions individually, air dried for 30 seconds and placed inside the vial. The device was set to a fixed rotational speed (100 RPM) and magnetic particles were allowed to impinge on the swab tips. The recovery efficiency was calculated from the number of eluted particles and initial absorbed beads, as shown in section 4.12. The experiment was repeated for different elution times (30 s - 150 s). Each experiment with a specific elution time was repeated 5 times and the values were averaged to obtain the bar graph.

The recovery efficiencies for elution procedures with artificial sputum and DI water is shown in Figure 30. The recovery efficiencies increase from 48.2 to 56.9% within 30 to 90 s of elution time when DI water was used, and remains stable henceforth. When artificial sputum was used, the efficiency increased from 39.3 to 48.6% over 30 – 120 s elution time. For artificial sputum, the recovery efficiency increases with elution time, but beyond an elution time of 120 s there is no significant increase. The difference between these two results were found to be statistically different (average p value for population = 0.007), although the 30 s and 120 s elution time were not as significant.

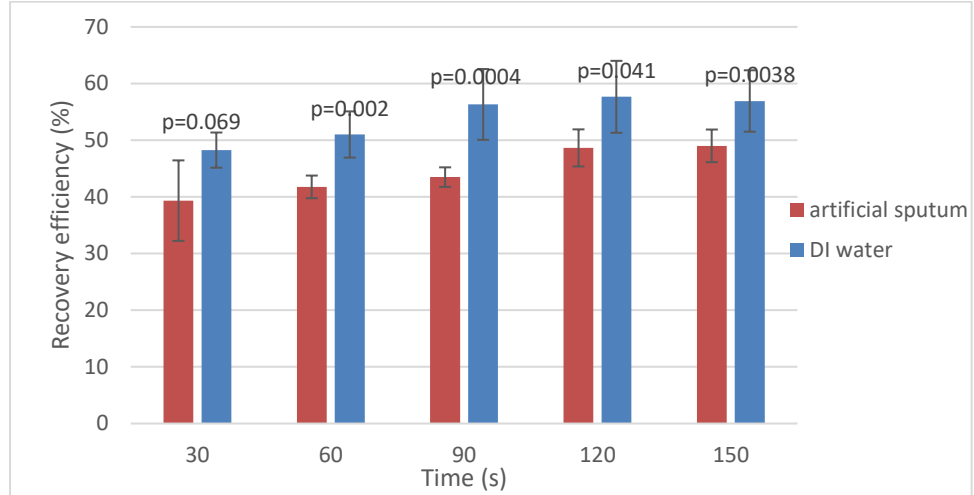


*Fig. 30 Comparison of recovery efficiencies for elution with artificial sputum and with DI water with 10% v/v ( $\sim 10^9$  particles/ml) bead concentration*

Artificial sputum shows lower recovery efficiencies than DI water and reaches a steady value after a longer time. The polystyrene beads take a longer time to migrate into the elution fluid from the swab fibre matrix, when they are present in a highly viscous and dense artificial sputum solution. Also, the value of recovery is significantly less from artificial sputum samples than that obtained from the DI water samples, since less number of beads gets released from a denser and more viscous environment. On the other hand, when dissolved in a less dense and less viscous DI water, the polystyrene beads withstand comparatively lower resistance to migration into the elution fluid. Hence, the number of recovered particles is greater as compared to artificial sputum. Also, the rate of migration of particles from within the trapped swab fibre matrix is faster when DI water is used and the process reaches a steady state comparatively faster. In spite of all the disadvantages,

artificial sputum was used in the subsequent experiments, since it reflects the original nature of macroscopic sputum more accurately than simple DI water.

### **5.3 Characterization**

#### **5.3.1 Effects of rotational speed of magnet**

Rotational speed of the magnetic particles is an important parameter for elution, which determines the number of impacts to the swab fibres and therefore is related to the amount of material scrubbed per minute. This rotation of the magnetic particles is imparted by the rotating ring magnet. In order to understand the variations of recovery efficiency with rotational speed of magnet, experiments were done with constant elution times and bead concentrations, but at different rotational speeds.

Several experiments were done at different rotational speeds to characterize its effect on the number of eluted particles and recovery efficiency. Dry swabs were immersed in artificial sputum solutions of 10% v/v ( $\sim 10^9$  particles/ml) polystyrene bead concentration. They were then air dried for 30s and immersed inside the vial with elution fluid. Several experiments were done by setting the motor at different rotational speeds (0 – 500 RPM), keeping the elution time constant. Both recovery efficiency and the number of eluted particles were recorded for each rotational speed. Five sets of experiments were done for each rotational speed and the recorded values were averaged to obtain each data point. The total number of eluted particles were calculated as per section 4.11 and recorded on the Y axis along with elution times on the X axis. Similar curves were obtained for various elution times (30 s – 120 s). Each curve represents the change of number of eluted particles or recovery efficiencies with rotational speeds at a fixed elution time.

Each dry swab weighing  $0.41 \pm 0.07$  g absorbs an average of  $227 \pm 28$   $\mu$ l of the sample when dipped into a solution of methyl cellulose and polystyrene. Hence, while working with a sample mixed with polystyrene at a concentration of  $10^9$  particles/ml, the number of particles absorbed in the swab was found to be around  $(1.8 \pm 0.3) \times 10^8$  particles. The swabs loaded with the sample were then eluted at different rotational speeds (100-500 RPM). The variation in average number of eluted particles with rotational speed with  $\sim 10^9$  particles/ml concentrated samples is shown in Figure 30. At lower rotational speed (100 RPM), the number of eluted particles were  $\sim 4 \times 10^7$  but it increased rapidly to about  $\sim 7 \times 10^7$  particles at 500 RPM, when eluted for 30 s. When the elution time was increased to 60s, the number of eluted particles increased for each rotational speed. The total number of eluted particles increased to  $\sim 6 \times 10^7$  at 100 RPM and it gradually rose to  $\sim 8 \times 10^7$  at higher speeds (500 RPM). With higher elution times, the number of eluted particles increased further. At 90s elution time, the total number of eluted particles increased from  $\sim 6.5 - 10 \times 10^7$  within 100 – 500 RPM and then remained constant. Similarly, at 120s elution time, the corresponding values are  $\sim 8 \times 10^7 - 10^8$  within the same speed range. The results are not statistically significant at 100 RPM when compared with no-agitation case (p-value = 0.15) or at 200 RPM (p-value = 0.08), but it becomes significant at 300 RPM (p-value = 0.015) and henceforth.

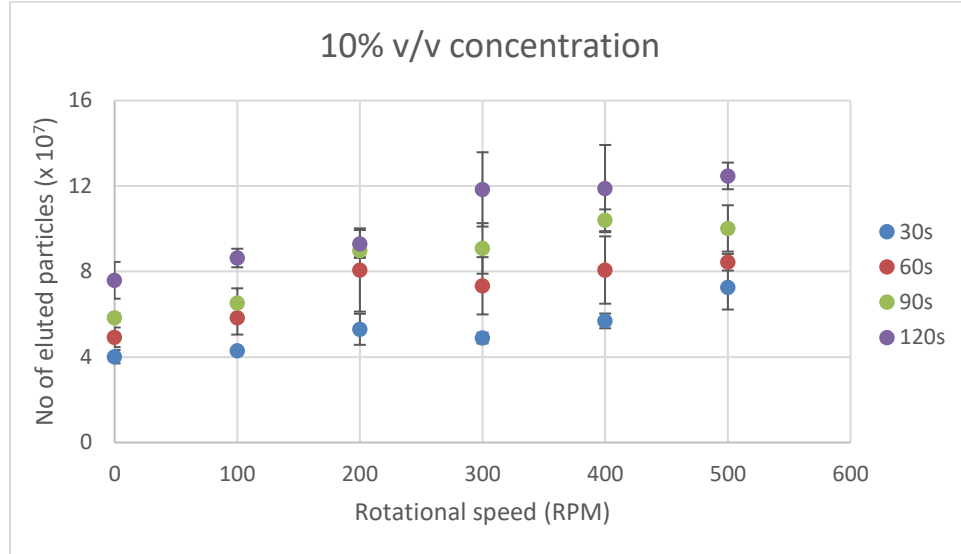


*Fig. 31 Number of eluted particles vs rotational speed for different elution time at 10% v/v (~10<sup>9</sup> particles/ml) concentration*

Multiple impingements on the swab fibres are responsible for higher rates of elution. As shown in section 3.5, the magnetic particles rotate at  $2 \times i \times N_m$ , where  $N_m$  is the rotational speed of the motor and  $i$  is the gear ratio. In one complete rotation, the magnetic particles impart two impacts. Hence, the total number of impacts per minute become  $4 \times i \times N_m$ . As the rotational speed increases, the number of impacts on the swab fibres per minute increase. The number of impacts at 500 RPM is 5 times higher than that offered at a low rotational speed of 100 RPM. Higher forces of impact between the particles and the swab provide better release of the samples due to efficient scrubbing action. Fresh elution fluid enters the fibre matrix after each subsequent impact and allows faster dissolution of artificial sputum. More particles can migrate into the elution volume, facilitating better recovery and hence more beads are eluted from the swab tip.

The forces acting on the swab due to the impingement of the magnetic particles undergoing rotational and circular translational motion around it was measured by using a load cell, as described in the Appendix A. The measured forces at different rotational speeds are shown in Table 6. Higher rotational speed of the motor causes higher impact forces to the swab fibre matrix, resulting in higher recovery of beads.

Rotational speed (RPM)	Force (N)
100	3.24
200	3.82
300	4.15
400	4.52
500	4.75

*Table 6. Impact forces offered by the magnetic particles on the swab tip at different rotational speeds.*

The corresponding change in recovery efficiency with rotational speed at same bead concentration ( $\sim 10^9$  particles/ml) is shown in Figure 32. The recover efficiencies were calculated from the number of eluted particles, as per section 4.12, and recorded on the Y axis along with rotational speeds on the X axis. At lower elution time (30 s) and speed (100 RPM), the recovery efficiency (38.4 %) was slightly better than the no-agitation efficiency (33.7%). But with increase in rotational speed, the recovery efficiency increased to 67.6% at 500 RPM and then remained constant. When the elution times were increased, the recovery efficiency increased for every rotational speed. The highest recovery efficiencies were found at 120 s elution time, where the values increased from 44.6% at 100 RPM to

73.4% at 500 RPM and then remained constant. In this case also, the average results between 100 RPM and the method of no agitation is not significant (p-value =0.14), but becomes significant at 300 RPM (p-value=0.0007).

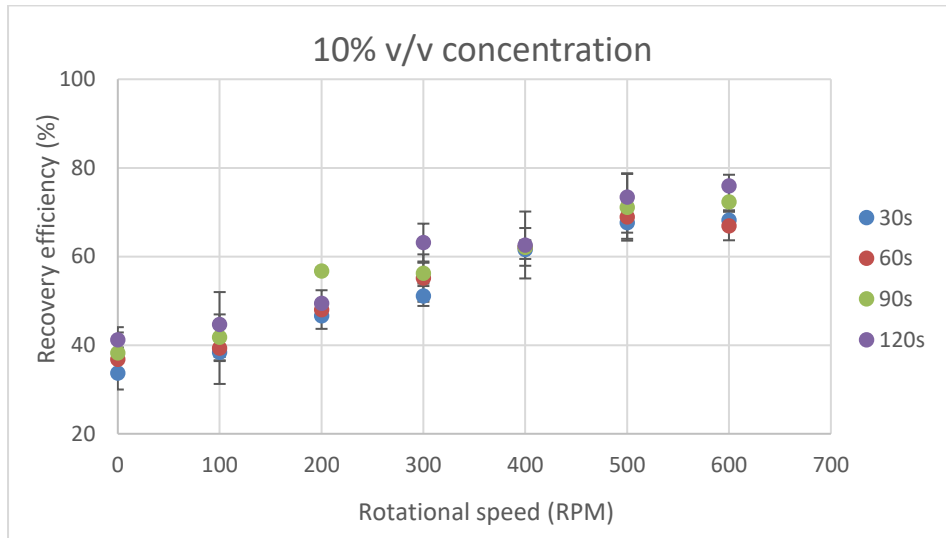


*Fig. 32 Recovery Efficiency vs rotational speed for different elution time at 10% v/v (~10<sup>9</sup> particles/ml) concentration*

The number of eluted particles increases with the increase of rotational speed, owing to the higher forces of impact and increased number of impingements per minute. The recovery efficiencies (calculated as per section 4.12) also increase with higher number of eluted particles. Since, the total number of impacts per minute increases proportionally with rotational speed, the recovery efficiency also increases by an average of 29% between 100 and 500 RPM. The elution is the most during the first few impingement (until 500 RPM) and then the recovery efficiency attains a steady state. This is because initially the bead concentration was higher inside the swab fibres than the elution volume. Multiple impingements on the swab tip cause higher removal of material and simultaneous supply

of fresh elution fluid to the fibre matrix. The rate of dissolution also increases with the increased number of impacts per minute. As a result, more beads migrate into the elution volume. After few impacts, the concentration gradient between the two separate zones decreases and no more recovery of beads are possible. Hence, the recovery efficiency remains constant.

Another important observation was made from the Figures 31 & 32. Figure 31 represent the number of particles eluted from the swab fibres at various rotational speed and elution time. The corresponding changes in recovery efficiency are shown in Figure 32. It is observable that the elution time has a higher effect on the number of eluted particles than the corresponding recovery efficiency. The curves for each constant elution times (30 s, 60 s, 90 s and 120 s) in Figure 31 are much wider apart than the constant elution-time curves of Figure 32. This is because the recovery efficiency is influenced by both the number of particles absorbed by the swab as well as the number of eluted particles. Even though the initial concentration of the beads in the solution was the same, the total absorbed volumes were different for each of the swabs. At a lower elution time (30s), the average absorbed volume over different rotational speed experiments is  $114 \pm 12 \mu\text{L}$ . For experiments at 60 s elution time, this average absorbed volume was  $134 \mu\text{L} \pm 48 \mu\text{L}$ . The corresponding values for 120s elution time was  $126 \pm 21 \mu\text{L}$ . The average change in the absorbed volumes for each of the rotational speed experiments for 30s and 60s constant elution time is ~29% and over 30s and 120s is ~25%. These changes in absorbed volume depends on the swab fibre material and also influence the total number of particles that is absorbed on the swab tip. Since the recovery efficiency parameter takes into account both the pre- and post-elution conditions into account as opposed to the number of eluted

particles, the values between each constant elution time curves for both the figures vary from each other.

Similar observations were made from experiments performed with artificial sputum samples mixed with polystyrene beads at 5% v/v ( $\sim 5 \times 10^8$  particles/ml) concentration. The experiments were performed to record the changes of recovery efficiencies with changes in rotational speeds, while keeping the elution time constant. The change in the number of eluted particles is shown in Figure 33. At lower elution times (30 s), the number of eluted particles range from  $\sim 3 - 5 \times 10^7$  particles/ml over the range of 100 to 500 RPM. A uniform increase in the number of eluted particles is observed with the increase in rotational speed for different elution times. When the elution time is increased, the number of eluted particles increases for each rotational speed. At 120s elution time, the total number of eluted particles range from  $\sim 5$  to  $10 \times 10^7$  particles/ml over 100 to 500 RPM. In this case, also, the average results are statistically insignificant between 100 RPM (p-value = 0.24) and the method of no agitation, but becomes significant after 300 RPM (p-value = 0.018).

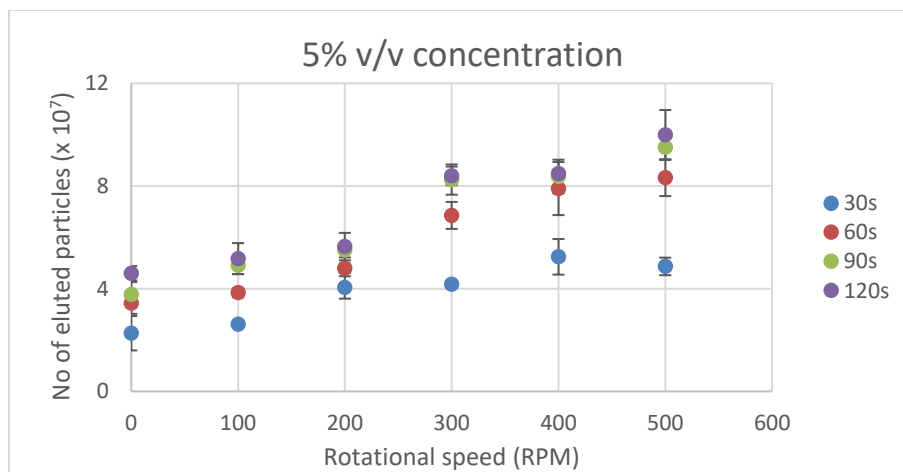


*Fig. 33 No of eluted particles vs rotational speed for different elution time at 5% v/v ( $\sim 5 \times 10^8$  particles/ml) concentration*

The trend in recovery efficiency followed that of the number of eluted particles. The change in recovery efficiency with the change of rotational speed for samples with  $\sim 5 \times 10^8$  particles/ml bead concentration is shown in Figure 34. The recovery efficiency at 30 seconds of elution time increased with the rotational speed from 37.4 to 72% within 100 - 500 RPM, while the no-agitation recovery was only about 31.9% at the same elution time. The recovery efficiency increased uniformly with the increase in rotational speeds for all elution times. Higher elution time also resulted in increased efficiency. The corresponding recovery efficiencies from 100 – 500 RPM increased to 54.7 – 80.4% at 90 s of elution time. At higher elution times, the recovery efficiencies increased up to 400 RPM and plateaued after subsequent speeds. For instance, at 120 s the recovery efficiencies increased to 57% at 100 RPM to 82% at 400 RPM and then remained constant. Following the results of number of eluted particles between the case of no agitation and magnetic impingement at various rotational speeds, the statistical significance is visible after 300 RPM (p-value = 0.0048), but not at 100 RPM (p-value = 0.27).

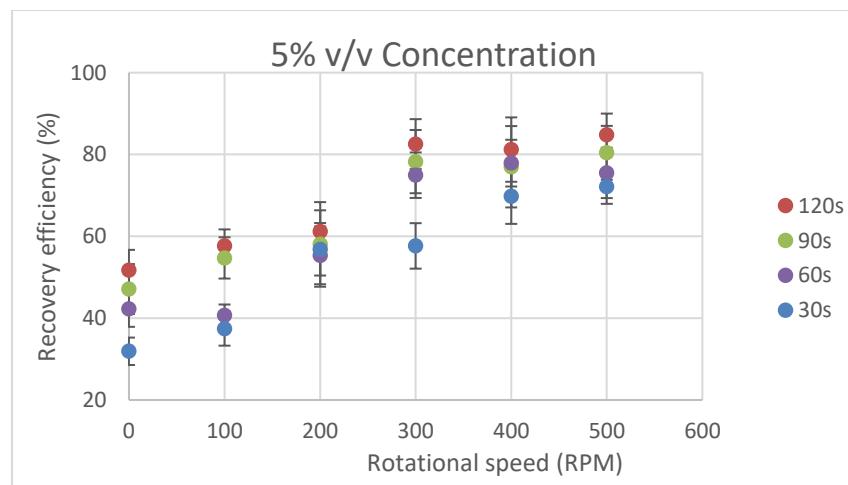


*Fig. 34 Recovery Efficiency vs rotational speed for different elution times at 5% v/v ( $\sim 5 \times 10^8$  particles/ml) concentration*

As described in the previous section, the increased number of impacts at higher rotational speeds is responsible for the increase in the number of eluted particles and the recovery efficiencies. Higher impact forces are inflicted on the swab fibres at higher speeds, which results in a scrubbing action to remove entrapped beads from the swab fibres. Fresh fluid enters the fibre matrix after each subsequent impact, facilitating dissolution of artificial sputum and simultaneous migration of beads into the elution fluid. At low elution time (30 s), there is a 34% increase in recovery efficiency at 500 RPM compared with that at 100 RPM. At higher elution times, there is a lower increase in efficiency within the same speed range. For instance, at 120 s the increase in recovery efficiency is 28%. One of the reasons for this behaviour is that the immersion of the swab by itself for a longer duration of time causes an increase in the elution efficiency. Therefore, the starting point for the data (0 RPM) at higher elution time is at a higher level corresponding to the elution of a larger amount of the surface bound artificial sputum and the particles in it. Due to the higher starting point, the increase after magnetic impingement is not as much as in the case of lower elution time. These results show that elution time also has a significant effect on the recovery efficiency and is a vital parameter to be characterized.

### **5.3.2 Effect of time**

The duration of elution procedure also has a significant effect on the recovery efficiency. As shown in the previous section, the recovery efficiency increases with the rotational speed when the elution times are kept constant. But it also increased at every speed when the elution times are increased. Hence, several experiments were done to observe the change in recovery efficiency with time.

To predict the nature of elution rate with changes in time, experiments were done with 10% polystyrene in artificial sputum samples. Dry swabs were dipped in artificial sputum samples concentrated with 10% v/v ( $\sim 10^9$  particles/ml concentration) polystyrene beads. They were air dried for 30 s and immersed in the vial with elution fluid. The motor was set to a specific rotational speed and the number of eluted particles was noted with the change of time (30 s - 120 s). The recovery efficiencies were calculated as per section 4.12 and recorded on the Y axis along with elution times at X. Five repeats of experiments were performed for each condition and the average values of recovery efficiency were obtained. Similar experiments were repeated for five different rotational speeds (100 - 500 RPM). Each curve represents the change of recovery efficiencies with elution time at a fixed rotational speed.

The changes in recovery efficiency with time for elution with a sample of 10% v/v ( $\sim 10^9$  particles/ml) concentration is shown in Figure 35. The recovery efficiency increased with the elution time. In the control case, without magnetic actuation, there was a small increase in recovery with elution time (33.7 - 41% within 30s - 150s). At low rotational speed (100 RPM), the recovery efficiency increased from 39.3% at 30 s to 48.6% at 120 s and then remained nearly the same. Higher elution time resulted to an increased efficiency, but with a less significant rate of increase than the effects seen with rotational speed. As shown in the previous section, the recovery efficiency increases with the rotational speed. But at higher speeds, the recovery efficiencies also attain a steady value much faster. For example, at 500 RPM the recovery efficiencies increase from 67.9% at 30s to 71.2% at 90 s and became constant afterwards. For 400 RPM, it remains horizontal at around 62%. The effects of elution time on recovery efficiency is significant at lower speeds as compared to

higher speeds. With lower rotational speeds (100 RPM) the recovery efficiency shows an increase of 9% (39% to 48%). But at higher RPMs, the slope of the curve decreases (only about 4% increase in recovery efficiency) and elution efficiency doesn't have a pronounced effect on time. Considering both these parameters, an operating condition of 500 RPM and 120s are found to be suitable for maximum recovery. Even though there is a very low increase in average efficiency, the recovery efficiency values are not significant between 30 s and 60 s (p-value = 0.56) but has a higher significance between 30 s and 120 s (p-value = 0.021) of elution time.

The process of elution is influenced by two factors – impact force and dissolution. The duration of elution determines the number of impingements that are caused. When the rotational speeds are kept constant, the total number of impacts per minute remain the same over the entire time period. At lower elution times, the total number of impacts ( $4 \times i \times N_m \times t$ ) has a significant effect on the number of eluted beads. For 30, 60 and 90 s, the increase in total number of impacts over time results in increased average impact force on the swab fibres, thereby increasing the number of recovered particles and the efficiency. Fresh fluid entering the fibre matrix helps in dissolving the artificial sputum solutions that pushes the beads into the elution fluid. But the dissolution reaches a steady state after a very small amount of time, and after that the impact is the only operating force acting on the swab. The impact force surrounding the swab removes the beads from the swab matrix, but only to a certain extent. After ~90 s, most of the beads that were free to move to the eluate had already migrated. The ones trapped deeper into the fibres does not get eluted and remains inside even at higher elution times.

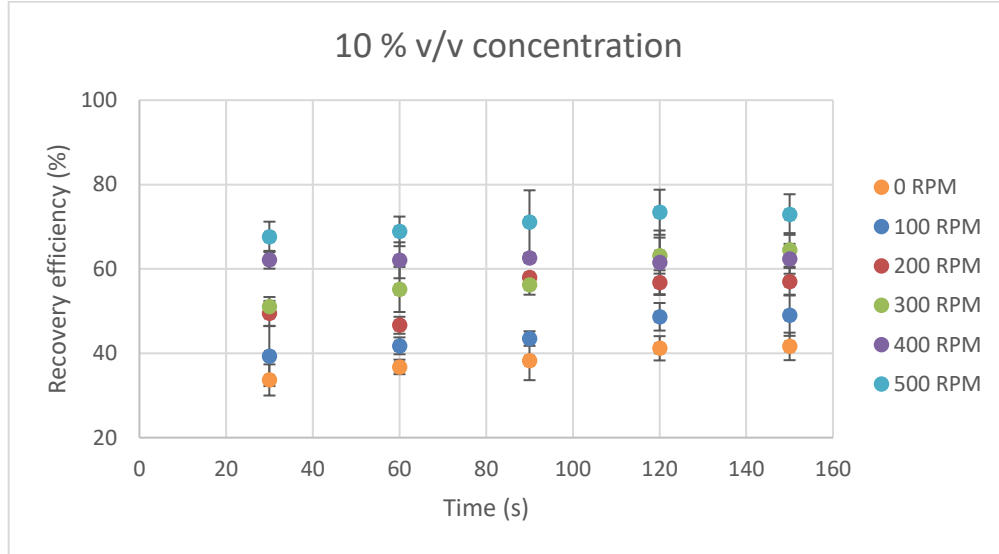


*Fig. 35 Recovery Efficiency vs elution time for different rotational speeds at 10% v/v (~10<sup>9</sup> particles/ml) concentration*

Similar experiments were done with 5% v/v (~5 x 10<sup>8</sup> particles/ml) and changes in recovery efficiencies with elution times were also recorded. For ~5x10<sup>8</sup> particles/ml concentration (Figure 36), the efficiencies ranged from 37.4 to 59% at 100 RPM speed within the range of 30 – 120 s of elution time. The recover efficiencies increased with higher rotational speeds for each elution time. For instance, at the next higher speed (200 RPM), the corresponding recovery efficiencies ranged between 56.8 to 64.5% for elution times of 30 s – 120 s. For higher speeds (500 RPM), the corresponding values translate to 72 – 84.8% within the same range of time. The highest value at 120 s and 500 RPM is ~84.8%. With higher constant speed curves, the change in recovery efficiencies was small over increasing elution time. For example, the values for 500 RPM ranged from 72 – 84.8% for 30 – 120 s. There is no significant increase in average efficiency for 30 s to 60 s of

elution time (p-value = 0.34), but has a statistical significant at around 120 s (p-value = 0.002).

As in the previous case, the magnitude of the slope was smaller at higher speeds than that at lower ones. This is because the elution is predominantly dependent on the impact and dissolution initially. So, maximum elution occurs within the first 30 s. Beyond that, the dissolution gradually reaches a steady state as described before. At higher rotational speeds, with more number of impacts, the rate of migration of fresh fluid is more than that at lower speeds. Hence, the rate of dissolution is faster and the concentration of the beads at two separate zones (elution fluid and artificial sputum) is equilibrated quickly.

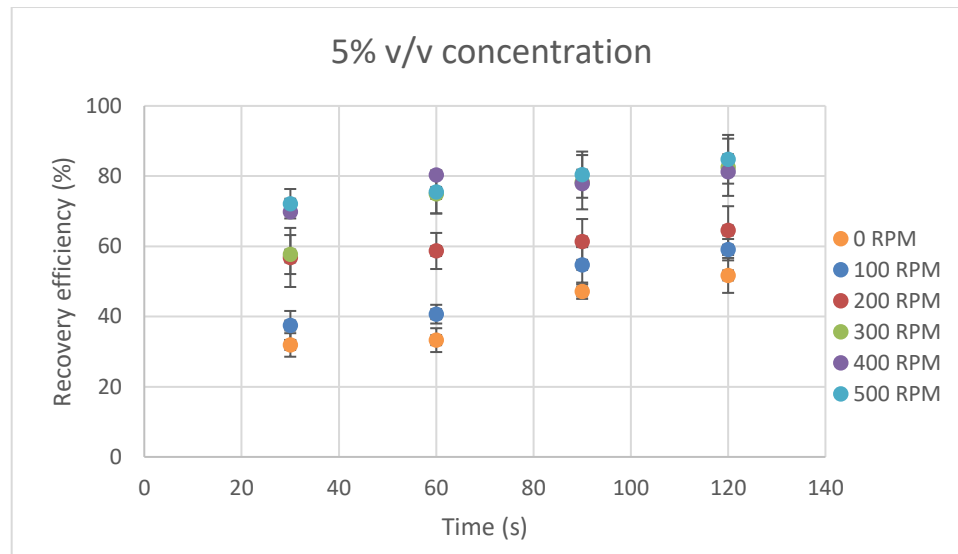


*Fig. 36 Recovery Efficiency vs elution time for different rotational speeds at 5% v/v (~5x10<sup>8</sup> particles/ml) concentration*

### 5.3.3 Effect of concentration

The effects of rotational speed on recovery efficiency were studied in sections 8.3.1 under two different concentrations – 10% v/v (~10<sup>9</sup> particles/ml) and 5% v/v (~5x10<sup>8</sup>

particles/ml). The values of recovery efficiencies were found to change in both the cases and hence further experiments were done to observe the effects of concentration on recovery efficiencies.

Experiments were done with a specific elution time and rotational speed to observe the effects of concentration on recovery efficiency. Since it had already been established that higher rotational speeds (400 - 500 RPM) and elution times (120 s) produce better recovery of beads, experiments were performed only with those specific parameters. Dry swabs were dipped in artificial sputum solutions of different concentrations ( $10^9 - 10^6$  particles/ml), air dried for 30 s and immersed in DI water in a vial for elution. The motor was set at constant speeds of 400 and 500 RPM for each specific set of experiments and magnetic impingement was employed to elute materials from the swab tip. The recovery efficiencies were calculated for experiments with each concentration. Five repeats of experiments were performed for each condition and the average recovery efficiency was obtained. Two different curves were obtained for different rotational speeds (400 and 500 RPM). Each curve represents the change of recovery efficiencies with concentration at a fixed rotational speed.

The variation of recovery efficiency with changes in concentration of polystyrene beads in artificial sputum solution is shown in Figure 37. From this figure, it is evident that higher recovery efficiencies were obtained at lower concentration. The value of the recovery efficiencies decreased with increasing concentrations. For instance, at 500 RPM the recovery efficiencies decrease from 92% at  $\sim 10^6$  particles/ml concentration to 72% at  $\sim 10^9$  particles/ml concentration. As described in section 5.3.1 of the same chapter, the recovery efficiencies increase with RPM with each specific concentration points. At 0.01%

v/v concentration ( $\sim 10^6$  particles /ml) of polystyrene in artificial sputum, the efficiency reaches to 92% for 500 RPM and 89% for 400 RPM. Higher concentrations (10% v/v concentration or  $\sim 10^9$  particles/ml) yield lower recovery (61 and 72 % respectively for 400 and 500 RPMs respectively).

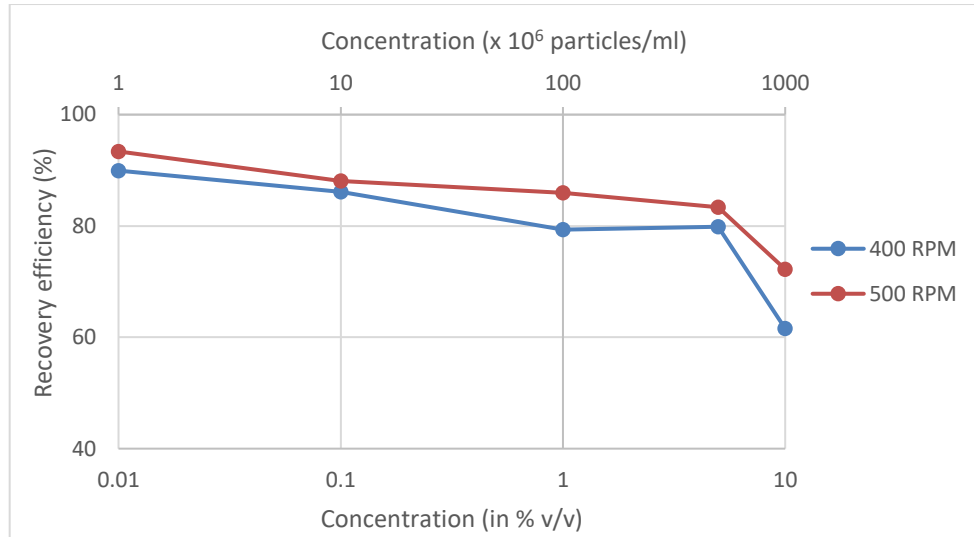


*Fig. 37 Effect of concentration on recovery efficiencies at higher rotational speeds (120 s elution time)*

The increase in recovery efficiency at lower concentration is a surprising result and it could be a result of various effects. When the swabs are dipped in a solution of artificial sputum and polystyrene beads, the sample is absorbed by the cotton tip. Higher concentration of the sample allows more number of particles to get absorbed to the swab fibres. Under the influence of impact forces and dissolution into the elution fluid, the beads migrate from a region of higher concentration inside the swab matrix to a region of lower concentration (the elution fluid). The ability of the artificial sputum sample to dissolve into the eluent fluid could be influenced by the particle loading. High particle loading could

make it more difficult to dissolve sample that are in the deeper layers of the swab and therefore produce a lower elution efficiency. Alternatively, the process of reabsorption of the eluent fluid after local impact into the swab and the particle loading of the surface layers due to the reabsorption can be influenced by the concentration of the particles in solution. In low concentration samples, the number of particles in the eluent solution is comparatively low. The reabsorption could preferentially absorb some of the fluid post elution and therefore retain more of the particles in the eluent fluid as compared to the high concentration case. Finally, after the elution process is complete, some of the fluid is adsorbed on the outer surface of the swab while it is being taken out. The number of particles adsorbed on the surface from the fluid is dependent on the number of available adsorption sites and can also be dependent on the concentration of beads in the elution fluid. This phenomenon can be demonstrated from the Freundlich adsorption [97] isotherm,

$$\frac{x}{m} = KC^{1/n} \quad (12)$$

where, x is the mass of adsorbate, m is the mass of adsorbent and C is the concentration of adsorbate in solution, K and n are temperature-dependent constants. As these processes happen simultaneously during the elution process it is difficult to decouple them separately to identify the specific causative factor. All the three factors are expected to have some role in the behaviour of the elution process and the dependence of elution efficiency on concentration.

The concentrations of polystyrene beads were adjusted in all the cases to demonstrate real-life bacterial samples. Different concentration ranges were defined in section 4.11 – high ( $10^9$  - $10^7$  particles/ml), medium ( $10^7$  - $10^5$  particles/ml) and low ranges ( $<10^5$ ). The

effects of concentration on recovery at different rotational speeds were also studied from the recovery efficiency vs rotational speed curves for different concentration.

Several experiments were done, as described in section 5.3.1, with polystyrene bead concentrations of  $\sim 10^8$  particles/ml,  $\sim 10^6$  particles/ml and  $\sim 10^5$  particles/ml in artificial sputum samples. Dry swabs were immersed in artificial sputum solutions, air dried for 30s and eluted in a vial with DI water by agitating with magnetic particles. The concentrations were kept constant during the entire experiments and recovery efficiencies were obtained for different rotational speeds. Five experiments were done for each rotational speed at a specific elution time and averaged to obtain a single point in the curve. Similar curves were obtained for different elution times (30 - 120 s).

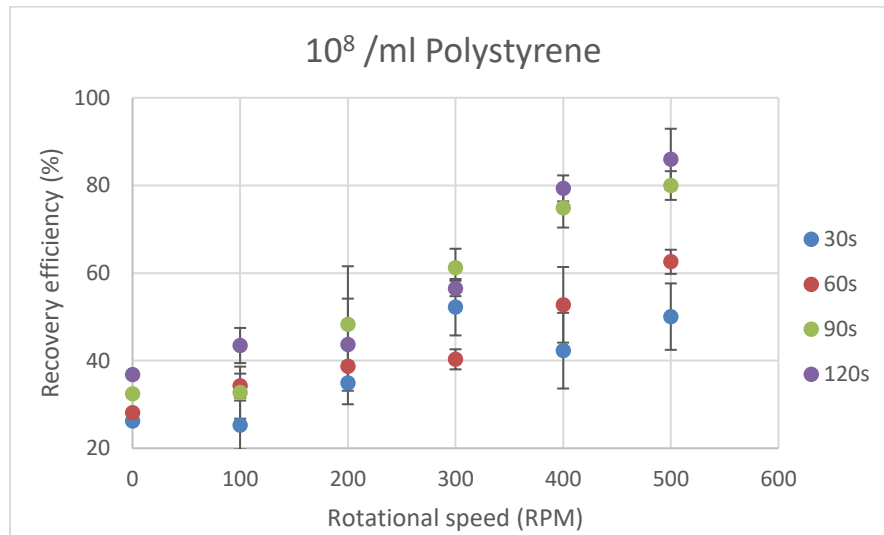


*Fig. 38 Recovery Efficiency vs rotational speed for different elution time at 1% v/v ( $\sim 10^8$  particles/ml) concentration*

The variations in recovery efficiencies with changes in rotational speed with 1% v/v ( $\sim 10^8$  particles/ml) concentrated samples is shown in Figure 38. At low elution time (30 s)

the efficiencies increase from 25.3 to 50% over 100-500 RPM. With higher elution times, there is a corresponding increase recovery efficiencies. For 120s elution time, the corresponding recovery efficiencies range from 43 – 85% with increase in rotational speed (100-500 RPM). Also, the highest value of recovery efficiency (85%) at 120 s elution time and 500 RPM is a significant improvement over the control case of no agitation (36.8%) at the same elution time.

Significant improvements in recovery efficiencies were observed when experiments were done with samples at a lower concentration of  $\sim 10^6$  particles/ml. The effects of recovery efficiency with rotational speed for different constant elution times (30 – 120 s) are shown in Figure 39. At this concentration, recovery efficiencies of 48 - 84% were obtained over the range of 100-500 RPM at low elution time (30 s). With increase in elution times, the recovery efficiencies increased and the highest went up to 90.3% at 500 RPM and 120 s. The average errors in recovery were significantly lower ( $\pm 4.06\%$  average). Hence, working with lower concentrations can be beneficial in terms of both productivity and accuracy.

Artificial sputum samples with 0.001 v/v ( $\sim 10^5$  particles/ml) concentration samples were also eluted from the cotton swabs. The changes in recovery efficiency with rotational speed for different elution times are shown in Figure 40. Higher efficiencies also mark the recoveries of these samples as a significant improvement over highly concentrated samples. At 30 s elution time, the recover efficiency increased from 50-89% over 100-500 RPM range.

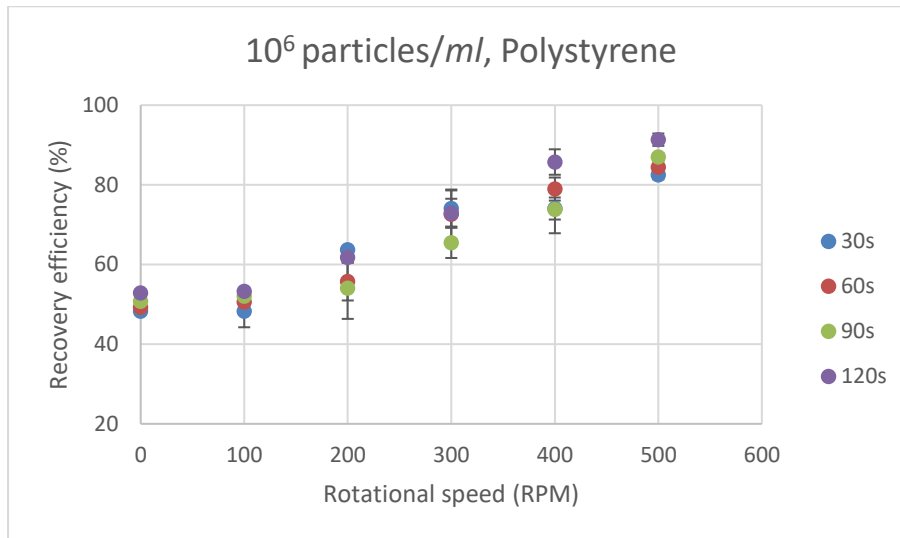


Fig. 39 Recovery Efficiency vs Rotational speed for different elution time at 0.01%  $v/v$  ( $\sim 10^6$  particles/ml) concentration

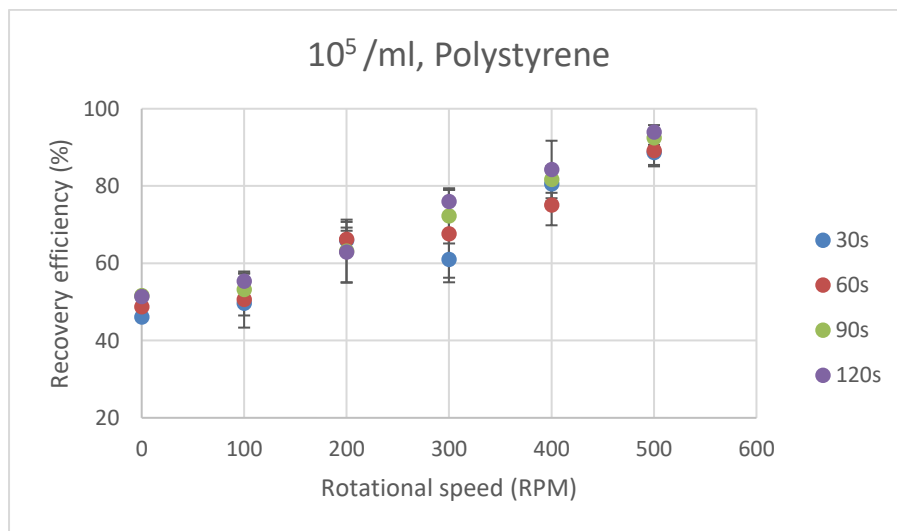


Fig. 40 Recovery Efficiency vs Rotational speed for different elution time at 0.001%  $v/v$  ( $\sim 10^5$  particles/ml) concentration

An important characteristic, obtained from the above three figures (Figures 38 – 40), is that at high concentrations, the effect of time on recover efficiency is more significant as compared to the low concentration. That is why there is a much more difference between different constant-elution time curves in Figure 38 than those in Figures 39 and 40. As mentioned before, for samples with lower bead concentration, a small amount of time is sufficient to dislodge the low numbers of particles absorbed by the swab tip. This happens within the first few seconds of elution. Also, at a constant rotational speed there is no significant increase in efficiency over time. But with samples at higher concentration, more number of particles gets absorbed by the fibres and only the surface layers get eluted first. After subsequent impacts, the beads trapped within the inner fibre matrices get eluted. With higher elution time, the swab fibres are subjected to more number of impacts and hence the recovery efficiency slowly increases. This has already been shown in section 5.3.2 for higher concentration samples.

The characterization of various parameters done with polystyrene beads provides optimum values of operations. Although higher values of both these parameters are desired, after an optimum value of 500 RPM and 120 s of elution time, the recovery efficiency attains a steady value. Polystyrene beads mixed with artificial sputum served as a model for actual bacterial samples in viscous body fluids. Hence, subsequent experiments were done with *E. coli* to validate the results obtained from polystyrene beads.

#### **5.4 *E. coli* samples**

Experiments were done with bacterial samples mixed with artificial sputum at different concentrations to observe the effects of rotational speed, elution time and concentration on the recovery efficiency. The artificial sputum was prepared by dissolving methyl cellulose in DI water, as described in section 4.6. Methyl cellulose have been frequently used for cell culture of colony forming cells and toxicity assays without any adverse effects [98]. Hence, the artificial sputum samples acted as an ideal model for all elution experiments.

##### **5.4.1 Effect of rotational speeds**

Similar experiments were done with cultured *E coli* mixed with the artificial mucous at two different concentrations ( $\sim 6 \times 10^9$  CFU/ml and  $\sim 6 \times 10^8$  CFU/ml). Although the concentration of bacteria could not be kept exactly the same between different experiments due to its growth, care was taken to ensure that the order of magnitude of its concentration was maintained. These experiments were performed to study the effects of rotational speed of the magnets on the recovery efficiency.

Experiments were done with a specific concentration and elution times to observe the effects of rotational speed on recovery efficiency. Dry swabs were dipped in the artificial sputum samples and air dried for 30s before being immersed in the elution fluid inside the vial of the device. Experiments were performed at various rotational speeds (100-500 RPM) of motor while keeping the elution time constant. Five repeats at each experimental condition was performed and the average recovery efficiency was recorded. Four different curves were obtained for different constant elution times (30 s-120 s). Each curve represents the change of recovery efficiencies with rotational speeds at a fixed elution time.

The recovery efficiencies were calculated as per section 4.12 and recorded on the Y axis along with rotational speeds at X axis.

The variation in recovery efficiencies with the change in rotational speeds at a fixed concentration of  $\sim 6 \times 10^9$  CFU/ml is shown in Figure 41. As observed in experiments with polystyrene beads (Figure 31), the recovery efficiencies increase with increase in rotational speeds. The recovery efficiencies increase from 47.6 to 78.4% with increase in rotational speed from 100 to 500 RPM for 30 s of elution time. With higher elution times, the recovery efficiency increases, similar to the experiments with polystyrene (Section 5.3.2). The change in the recovery for 100 RPM across different elution times (30 s-120 s) is minimal (47.6 – 53.9%). At higher elution time (120 s) the recovery efficiencies increase from 53.9 to 81.5% within the same range of rotational speed. Also, the average difference in recovery efficiencies for different elution times, while keeping the RPM same, is only 3.6%. As seen in the experiments with polystyrene, the average recovery efficiency values are not statistically significant for lower rotational speeds, between 100 RPM and the case of no agitation ( $p=0.46$ ), but is statistically significant at 300 RPM ( $p=0.0006$ ).

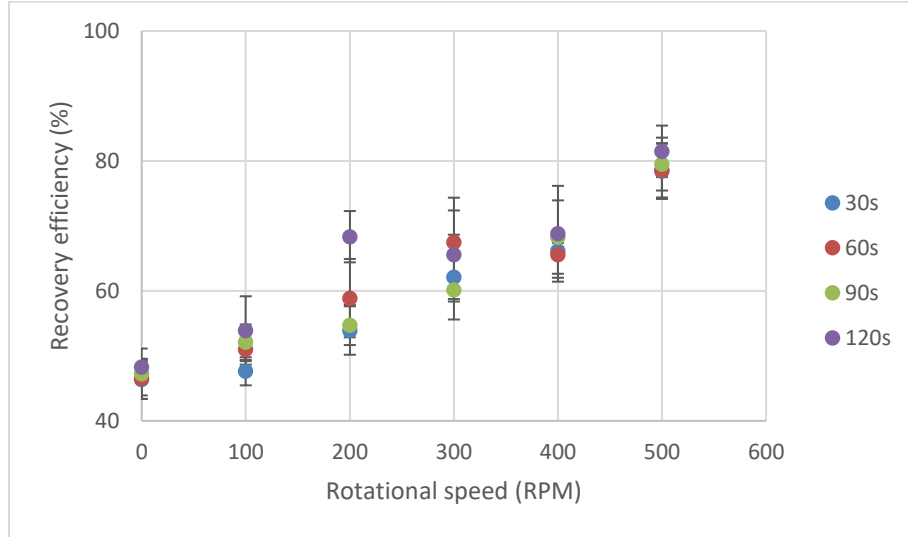


*Fig. 41 Recovery efficiency vs Rotational speed for  $\sim 6 \times 10^9$  concentration samples at different elution times*

Multiple impingement on the swab fibres is responsible for higher recovery of bacterial cells than the control case of no agitation (46.3% at 30 s to 48.2% at 120 s). The number of impacts inflicted on the swab tip per minute by the magnetic particles depend on the rotational speed ( $= 4 \times i \times N_m$ ). With the increase in rotational speed, the total number of impacts increase resulting in higher number of impact forces on the swab fibres of same magnitude. This provides higher number of eluted cells from the swab fibres and hence the recovery efficiency also increases. The rate of elution is also aided by the increased rates of dissolution at higher speeds. With each impingement of the magnetic particles on the swab tip, fresh elution fluid enters the fibre matrix and dissolves the artificial sputum. The *E. coli* cells absorbed in the inner matrices along with the artificial sputum migrates into the elution volume along with the dissolution.

Similar experiments were done with  $\sim 6 \times 10^8$  CFU/ml concentration samples and is shown in Figure 42. At lower elution times (30 s), the recovery efficiency increases from 47 – 82% with increase in rotational speed from 100-500 RPM. With increase in elution times (30 s – 120 s), the recovery efficiency increases, but the change is not in significant. For instance, at 500 RPM, the change in recovery efficiency is only  $\sim 2.7\%$ . This is also similar to the results obtained from the experiments with polystyrene (section 5.3.2). Once again, the recovery efficiency values between the control case of no agitation and low rotational speed (100 RPM) are not statistically significant (p-value = 0.25), but is significant at 300 RPM (p-value = 0.007).

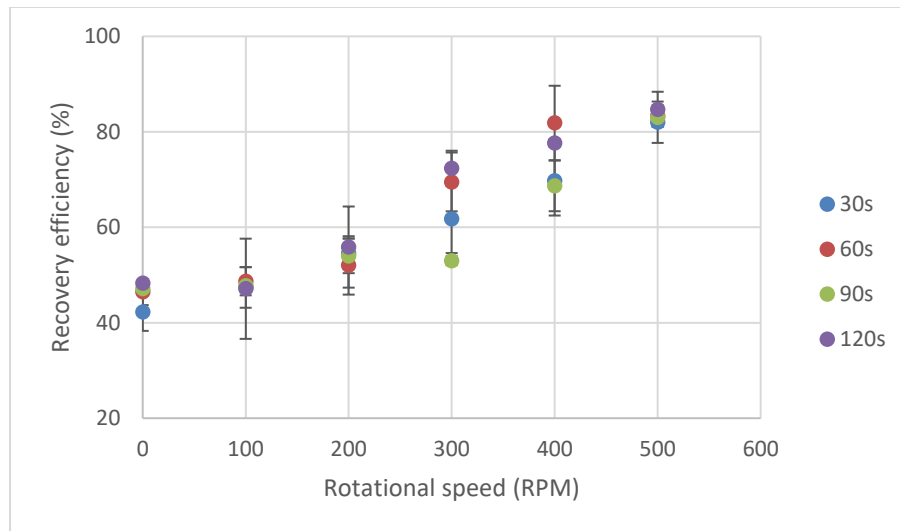


*Fig. 42 Recovery efficiency vs Rotational speed for  $\sim 6 \times 10^8$  concentration samples at different elution times*

The effects of speed, elution time and concentration on the recovery efficiency of bacterial cells are similar in trend to the effects obtained from the experiments with polystyrene beads (section 5.3.1, 5.3.2 and 5.3.3 respectively). The recovery efficiencies

increase with both the rotational speed and time. Higher changes in efficiencies are visible in case of rotational speed, while small changes are visible in case of elution times. This is because, the dissolution attains a steady rate after only ~90 s of elution time. Post dissolution, when majority of the beads have migrated from the fibre matrix to the elution volume, the concentration becomes identical in both the zones. Hence, no further elution is possible. Also, the highest attainable efficiency tends to increase with decreasing concentration, owing to the opposite movement of cells from the eluate to the fibre matrix due to a negative concentration gradient between the higher number of eluted cells in the fluid and that of the region inside fibre matrix. For concentrations in the medium concentration ranges, further experiments were done to establish this concept.

#### **5.4.2 Effect of concentration**

Subsequent experiments were done to study the changes of recovery efficiencies with rotational speeds at lower concentrations. Lower concentration ranges (in the order of  $10^6$  and  $10^5$  CFU/ml) were explored. The dry swabs were immersed in the bacteria-laden artificial sputum samples, air dried for 30 s and eluted in the device. The changes in recovery efficiencies were calculated with the change in rotational speed of the motor, while keeping the elution time constant. Similar curves were obtained for samples with two different concentrations.

For measurements with significantly lower concentration, fluorescent intensity values have been measured for each set of experiments and compared to a calibration curve. Fluorescent intensity values ranged from  $2328.9 \pm 357.7$  RFU to  $3249.77 \pm 418.1$  RFU for 100 to 500 RPM respectively, at  $10^6$  CFU/ml concentration range. These fluorescence

intensity values were compared with the calibration curve to obtain the concentration and the required no of eluted cells from the measured volume:

$$Concentration = \frac{RFU - 944.06}{0.0113} \quad (14)$$

The equivalent values of fluorescence for  $10^5$  CFU/ml concentration at 100 and 500 RPMs are  $1260 \pm 80$  to  $1563.4 \pm 174.9$ .

The recovery efficiencies, changing with rotational at constant (120 s) elution time, are shown in Figure 43. Elution with lower concentrations of *E coli* in the artificial sputum sample show similar increasing trend in recovery efficiency as observed before. At a concentration of  $\sim 2 \times 10^6$  CFU/ml, the recovery efficiencies increase from 52% to 86% over the range of 100-500 RPM, which is a significant improvement over the control case (46.25%) of no agitation at the same concentration. Recovery efficiencies up to  $\sim 90.4\%$  can be obtained at 500RPM with  $\sim 3 \times 10^5$  CFU/ml sample. Hence working with lower concentration of cells can be beneficial at higher rotational speeds. The average recovery efficiency values between the control experiments and various speeds are statistically insignificant at lower rotational speed (p-value = 0.36 at 100 RPM), but is significant at 300 RPM (p-value = 0.0016). But, when compared between two different concentrations, the values are mostly insignificant (p-value = 0.27 at 100 RPM, p-value = 0.39 at 200 RPM), but is closer to statistical significance at higher rotational speed (p-value = 0.078 at 400 RPM).

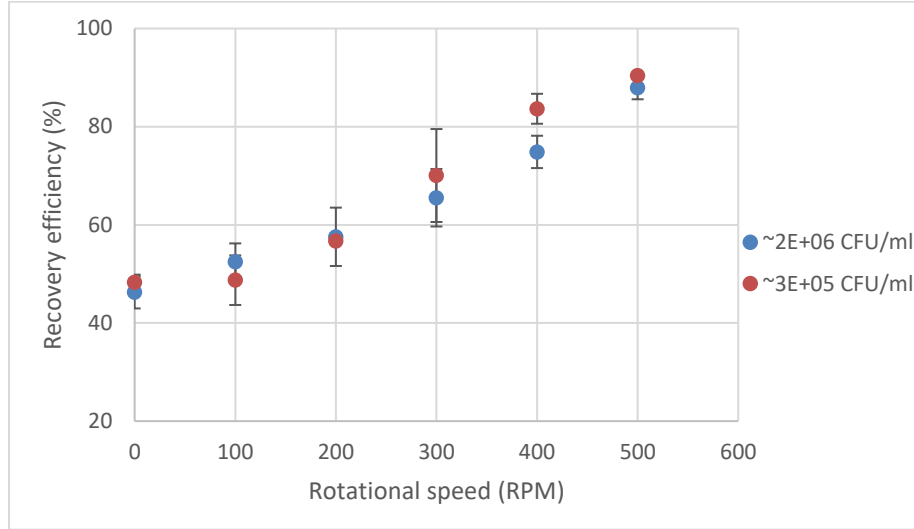


*Fig. 43 Recovery efficiency vs rotational speed for low concentration samples at 2 min elution time*

Similar experiments were done for 1 min elution time to obtain the same nature of curve. The recovery efficiency vs rotational speed curves of the two concentrations ( $\sim 2 \times 10^6$  and  $\sim 4 \times 10^6$  CFU/ml) is shown in Figure 44. For  $\sim 2 \times 10^6$  CFU/ml concentration, the average number of eluted particles range from  $\sim 1 - 1.5 \times 10^6$  CFU/ml over 100-500 RPM. This corresponds to a recovery increase from 49.1 – 86% with an average error of  $\pm 3.4\%$ . For  $\sim 4 \times 10^5$  CFU/ml samples the efficiencies increase from 50.8 – 86.6% over the same range of rotational speed and almost coincides with the values of the previous curve for higher rotational speeds. The recovery efficiency values obtained from experiments with lower cell concentrations were lower at low rotational speeds than higher concentration experiments, but it increases when operated under higher rotational speeds. Also, the values obtained for recovery efficiency at 60 s is lower than those obtained from the previous curve with 120 s. Similar to the previous experiment, the average recovery efficiencies

between the control case and that of different speeds are insignificant at 100 RPM (p-value = 0.3) but is statistically significant at 300 RPM (p-value = 0.006). Also, when compared between two different concentration, the recovery efficiency values between control case of no agitation and lower rotational speeds are insignificant at 100 RPM (p-value = 0.41), but the values are close to statistically significance at higher rotational speeds (p-value = 0.066 at 400 RPM).

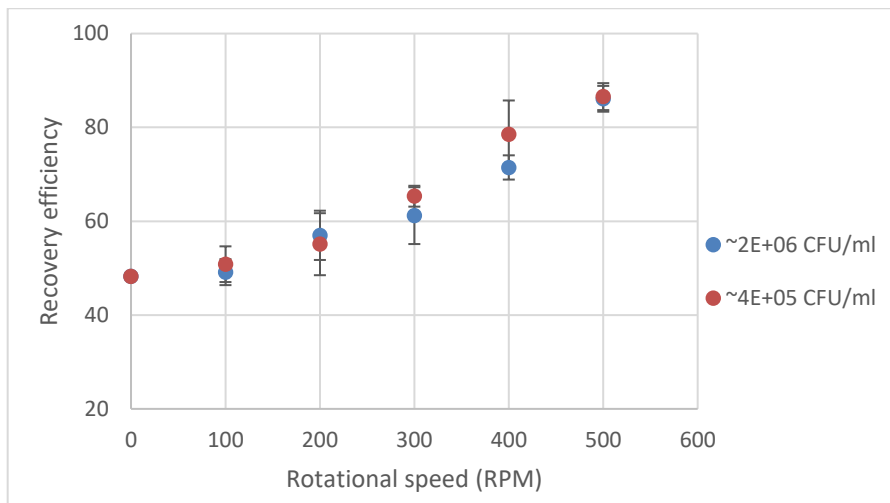


*Fig. 44 Recovery efficiency vs rotational speed for low concentration samples at 1 min elution time*

The trends for  $\sim 10^8$  and  $\sim 10^9$  CFU/ml concentration ranges was also studied at 120 s elution time. The variation of recovery efficiency with rotational speed at higher bacterial concentration for 120s elution time has been shown in Figure 45. This shows a similar trend to the results obtained from polystyrene samples. The recovery efficiencies increase with increase in rotational speed for constant concentration and constant elution time. These curves also become steeper with lower concentration. Lower concentration ( $\sim 6 \times 10^8$

CFU/ml) of *E. coli* shows higher maximum efficiencies at high rotational speeds (81.5% at 500 RPM). But at 100 and 200 RPMs, higher concentration samples show better efficiencies (53.9 and 68.3% respectively) than lower concentration samples (47.1 and 55.8% respectively). While working with samples at higher concentration, it can also be seen that there is no statistical significance between the recovery efficiencies of control case and at low rotational speed of 100 RPM (p-value = 0.08, but has statistical significance with an increase in rotational speed (p-value = 0.003 at 300 RPM). At higher concentration ranges, the curves once again collide with each other and mostly has no statistical significance between two different concentration curves (p-value = 0.15, at 100 RPM, p-value = 0.08 at 300 RPM, p-value = 0.02 at 400 RPM).

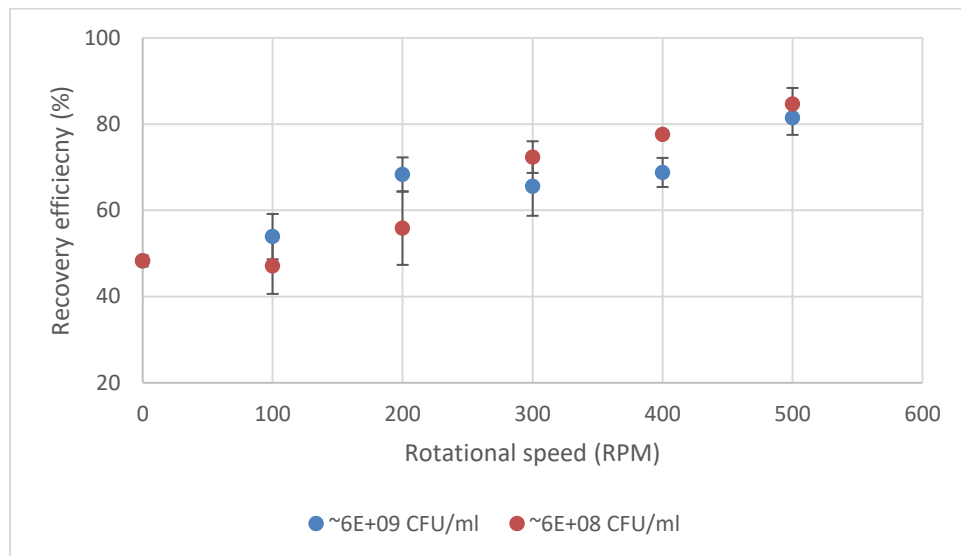


*Fig. 45 Recovery efficiency vs rotational speed for high concentration samples at 2 min elution time*

Higher recovery efficiencies are obtained at lower concentration of samples, as seen in the above figures and also with the polystyrene experiments (in section 5.3.3 of this chapter). Higher concentration of the sample allows increased number of cells to get absorbed to the swab fibres. But, the higher cell loading can produce an impediment to the dissolution of samples from the inner fibre matrices. Also, the process of reabsorption can affect the recovery efficiencies of samples with lower concentration, by retaining more cells onto the swab tip than samples with higher eluate concentration. Finally, some particles are also adsorbed on the surface of the swab fibres. More number of adsorption sites are available on the surface layers of the swab after elution, when samples with lower cellular concentration is used. Hence, more number of bacterial cells can get adsorbed to the surface when the swab is taken out, resulting in a decrease of recovery efficiency.

#### **5.4.2.1 Low concentration**

For samples lower than  $10^5$  CFU/ml, cell counting with both imaging and plate reader is inadequate. Working with lower concentrations are difficult using particle counting and fluorescent intensity measurements. The swabs absorb around 120  $\mu$ l of artificial mucous and post elution, the total number of cells remaining in the eluate is in the order of  $10^3$ . With such a low concentration, the fluorescent intensity values almost coincide with those obtained from the blank/background signal, even with a higher gain. Taking fluorescent picture with 10  $\mu$ L samples is equally challenging, where we might not get any cells in the frame while using a 40x lens on the camera. Hence plating technique is the only viable option.

Experiments were performed to study the effects of rotational speed on recovery efficiency. Cultured *E. coli* bacteria were mixed with artificial solution at  $\sim 4 \times 10^4$  CFU/ml to prepare the samples. The swabs were immersed in the sample, air dried for 30s and immersed in the vial of the device with LB media as elution fluid. Elution was done at a constant speed of 500 RPM with two different elution times – 60 and 120 s. Post elution, the cells were plated on agar plates and grown into colonies inside an incubator. Two separate batches were done for each elution time and the efficiencies were calculated based on the number of eluted cells.

Higher efficiencies of 82.7 and 71.5 % were found at 120 s elution time, while the corresponding recoveries were 63.8 and 60.5% at 60 s. These values represent lower efficiencies than the ones witnessed in previous experiments. The possible reasons behind these lower efficiencies could be due to non-homogeneous mixing of cells in the eluate or rupture of the bacterial cells. Since 5 batches of only 10  $\mu$ L samples were taken for plating, it is possible that due to non-homogeneous mixing there is inadequate number of cells in the sample taken. This results to lower colony formations and hence leads to inappropriate determination of concentration. Also, the death of bacterial cells will reduce the number of colonies formed and thereby undercount the bacterial concentration in the eluate. Despite these issues, the plating technique is the only viable method of counting the number of eluted cells at lower sample concentrations.

## **5.5 Summary**

Elution, aided with impact from magnetic particles, provides a better performance compared to the process without agitation. Rotational speed, elution times and

concentration of polystyrene beads/cells in the sputum samples were considered as important parameters for characterizations. Experiments were done with polystyrene and artificial sputum solution to validate the effects of the device and then repeated for *E. coli* samples. The effects can be summarized as follows:

- Higher rotational speed prompts more impact force to the swab fibres, thereby provoking higher recoveries. With polystyrene, the maximum attainable efficiencies 73% at high concentrations ( $10^9$  particles/ml), while with *E. coli* the corresponding value is 81% at 120 s elution time.
- The recovery efficiencies increase with increase in rotational speed but plateaus after the elution reaches a stability at 120 s.
- Higher elution time promotes better efficiencies as well, although the slope of the curve is lower than that of the Efficiency-rotational speed curve, which proves the quicker stability of dissolution. Hence, most of the elution occurs within the first 60 s due to dissolution, centrifugation and impact and beyond which the concentration between the two separate zones become the same.
- Better efficiencies are recorded at lower concentrations compared to higher ones, effectively implying the use of the setup at lower concentration.

## Chapter 6

### Conclusion and Future Work

#### 6.1 Conclusions

Swabs are used as a collection device for many biological samples and its complete elution is a desired step for clinical and forensic diagnostics. Several efforts have been made to enhance the recovery efficiencies of elution processes. Mechanical and chemical techniques of elution are the most popular approaches to elution and are described in chapter 2. These include the use of chemicals to digest the cotton fibres to remove intact cells, vortexing, piezoelectric vibration or pressurized fluid-flow. Although some of the chemical techniques reach the 70% recovery efficiency mark, they require the addition of a number of reagents specific to the analyte of interest. Most mechanical techniques of elution are generic, work with a wide range of sample types and have lower elution times (~30s – 10 mins). But they also require higher volumes (~5ml) or continuous flow of eluent and highly intricate systems for detecting the target analyte. Although these techniques include some indirect agitation methods for elution, none of them inflict direct (normal) physical contact to the swab fibres. Mechanical techniques that produce direct impact forces on the swab fibres can extract higher number of particulates as they can penetrate deep into the fibre matrix than agitation by convective flows or non-physical impact. Elution by multiple impingement on swab fibres can, therefore, be an important area of elution. Hence a mechanical approach of elution has been introduced in this thesis to improve the recovery efficiency and elution time.

In this thesis, a device has been designed to facilitate better elution by using impact forces on the swab by magnetic particles. These magnetic particles undergo simultaneous rotation around their own axis and a circulatory translation around the central axis to cover maximum surface area of the swab. This process improves the efficiency to ~92% at low concentrations ( $\sim 10^5$  particles/ml) when experimented with polystyrene and ~86% with *E. coli*. The device offers a robust design with reduced cost of parts and manufacturing. Laser micro-machining and 3D printing allows rapid manufacturing and mass production in a short time. Since this is a bench top device, it can be used in any research or clinical environment. The device also has a provision to be controlled by a laptop for an easy plug-and-play operation.

This device solves major issues typical of other elution processes. First, this technique provides higher recovery efficiencies than other mechanical and chemical processes. This device also provides higher recovery efficiencies for samples with lower concentration and hence can be used in forensic labs where the number of available samples are very low. Secondly, unlike some other chemical processes, this technique is generic to any kind of sample and swab fibre types. The device is most suitable for recovering cells from different body fluids like saliva, mucous, semen or blood, absorbed by the swab fibres. Apart from body fluids samples, swabs holding biological agents from environmental surfaces can also be eluted. Thirdly, the robust design and smaller size allows the device to be used in different clinical, forensic and laboratory settings. Also, due to cheaper means of manufacturing and assembly, the vials and smaller magnets can be discarded after every experiment, thereby preventing contamination.

However, several design considerations had to be made. For instance, precise fitting is required to maintain the specific gap between the central vial and planetary gear. The ring and planetary gears were manufactured with microscopic precision to eliminate the possibility of backlash errors and interference. Hence, the assembly of this device is a bit difficult as it contains a lot of smaller parts. Secondly, this device is capable of eluting different types of swab fibres, but swabs with larger tips might require larger elution volumes to get completely immersed into the fluid. Furthermore, a portion of the impact forces applied by the magnetic particles on the swab fibres can also be translated to the cell. Under the influence of compressive forces or mechanical shocks, the different properties of *E. coli* (cell wall & cytoplasm elongation rate, proliferation rate, DNA replication rate) can undergo some reversible change [99]. The cell volume and growth rate (volume/time) are very insignificant and is observable only at high stresses (over ~134 kPa). These effects on the cell wall can be seen only over a very small period of time, after which they retain their normal shape and all properties on the removal of compressive forces [100]. Care has been taken to start the enumeration process after a certain period to provide enough time for the cells to retain its structural properties and avoid any anomalies in counting of the number of eluted cells. Furthermore, the outer surface of the *E. coli* cells consists of lipopolysaccharide molecules, which contains several truncated carbohydrate chains [101], and can interact with the cellulose molecules of the cotton swabs. Addition of cyclodextrines to neutralize the effect of cellulose adhesion, thereby liberating *E. coli* cells more easily.

## 6.2 Future work

Even though the effectiveness of the use of multiple impingements to elute samples from the swabs have been described, other mechanisms of elution by these magnetic particles have not been explored. In this device, the magnetic particles undergo a rotational motion around its own axis and also a circulatory translational motion around the central axis. Further modifications can be made to the device by introducing different trajectories of motion to the impacting particles. This can be done by using multiple magnets at different angles, or by synchronised motion of magnets. Electromagnets are the best options for these cases, although the magnitude of the magnetic force obtained will be significantly lower than those obtained by neodymium magnets.

Moreover, the characterization of different parameters was done only with samples of artificial sputum mixed with polystyrene beads and *E. coli* K12 cells. *E. coli*, being a gram-negative bacterium, has higher rate of elution than gram-positive bacteria as shown by Harry et al [92]. This showed that the values of recovery efficiencies can be slightly different for different kinds of bacteria. Experiments can be done with different other pathogens: a combination of virus, bacteria or mammalian cells, which might act differently by clinging to the fibre matrices differently. Experiments can also be done with real biological samples containing human sputum, blood, urine etc. Moreover, the techniques can be extended to environmental sampling and recovery of bacterial spores from stainless steel surfaces or food surfaces.

Another important area of improvement is the sensitivity of the detection techniques. Experiments were done with the device for different concentration ranges up to  $10^4$  CFU/ml, beyond which the detection techniques fail to provide significant values.

Repeated experiments can be done with the plating technique by taking several small aliquots of elution fluids from different parts of the collection vials to get an average value of the total number of eluted particles from the number of colonies. For samples with *E. coli* concentrations less than  $10^4$  CFU/ml, the cells can be concentrated at the bottom of the vial by spinning it in a laboratory centrifuge at high speeds. Most of the elution fluid can then be collected from the top, leaving the cells and a small volume of residual fluid. Plating technique can be used subsequently to count the number of eluted cells.

Finally, the elution chamber can be modified to incorporate an outlet with a valve to allow the flow of elution fluid to lysis and PCR chambers. Since the purpose of the experiments is to provide increased number of eluted particles for subsequent processes of DNA analysis, it is beneficial to provide the eluted fluid directly to the lysis or PCR zone without loss of samples. This will produce a compact lab-on-a-chip device for the entire chain of process.

## **APPENDIX A**

### **Measurement of forces on the swab**

#### **Load cell**

A load cell was used to measure the forces on the swab head. For this purpose, a load cell (3132\_0 - Micro Load Cell (0-780g) - CZL616C) has been used along with a bridge board (1046\_0 - PhidgetBridge 4-Input). For force measurements, a swab is attached to the surface of the load cell and hanged from the top by clamps in a vertical direction. The load cell and swab setup acts as a cantilever beam and works on the principal of strain gauge. Calibration was done at no weight and 4 known weights with a gain of 128 to create an equation of converted force (gm-force) vs bridge value (mV/V). The calibration curve was found to be:

$$\text{Converted force} = -2961.95 \times \text{bridge value} + 21651 \quad (15)$$

Experiments were then performed, replicating the actual cell elution process at different RPMs, and the corresponding bridge values were compared with the calibration curve to obtain the force values. The load cell is sensitive to the 100th decimal places and has a range of 0-780 g-force.

#### **Measurement of forces**

The setup is considered to be a cantilever, with the fixed end being the measuring end. As shown in Figure 46, the swab end was attached to the load cell plate. The load cell was held in position by means of a clamp. The load cell was connected to a bridge board which in turn was connected to the laptop. The swab tip was placed inside the vial with magnetic

particles. The device was connected to the motor and the rotational speed was increased from 100 to 500RPM. The reaction forces at the fixed end was measured under the influence of the impact forces at the tip by the magnetic particles. The values were recorded from the Bridge-full mode Phidget21 software.

The values of the forces were taken at the point of contact of the swab with the load cell plate. The forces were measured at the fixed end and the shear force ( $V$ ) is same throughout the entire length of the swab. This reflects the value of the operating force at the swab head tip to be exactly equal to the force applied at the free end. The impact of the rotating magnetic particles to the swab head produces dynamic forces applied to the free end. Hence the data rate was taken at 8/ms and averaged over the time period. Forces were calculated in kg-f at different rotational speeds and converted to N.

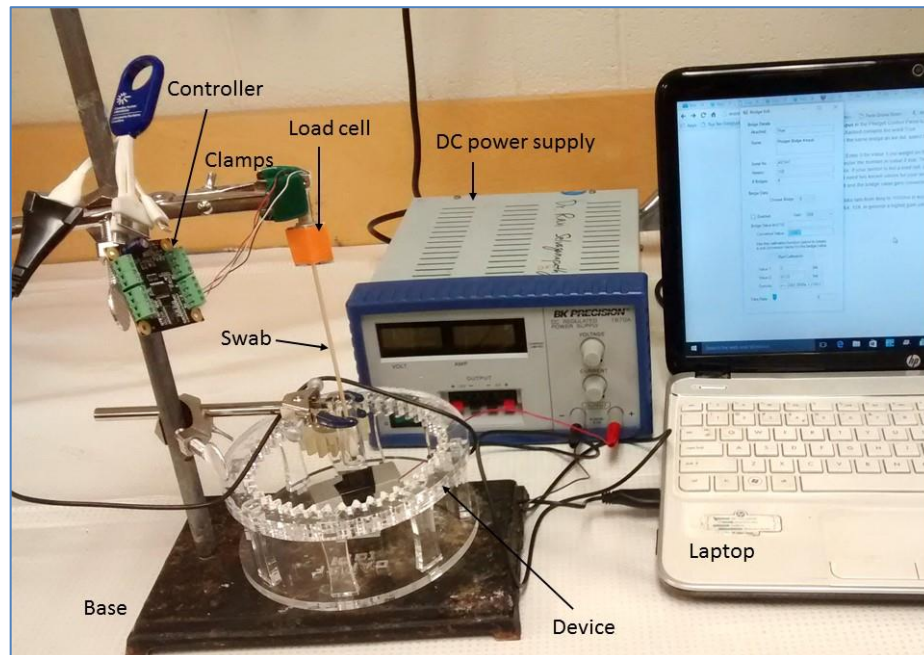


*Fig. 46 Experimental setup for measuring forces with load cell*

## **APPENDIX B**

### **Device design & fabrication**

The device, used in this thesis, consists of the following parts:

- Motor
- Support walls for motor
- Horizontal arm
- Planetary gear
- Ring gear
- Support walls
- Pillars
- Bearing
- Cylindrical placeholders

All these parts are made of acrylic and produced either by laser cutting or 3D micromachining as described in the next section. The device layouts and the description of the device has already been given in section 3.6. The device works with the principle of sun and planetary gear, where the planetary gear rotates around the static ring gear. In order to reduce the form factor of the device, the centre distance between the mating gears should be minimized. The centre distance is calculated after leaving sufficient space for the vial at the centre, the addendum diameter of the rotating gear and a clearance. The planetary rotation system is then designed with an inner planetary gear rotating around the teeth of an external fixed ring gear, the centre distance being 38.1mm. The device and its parts have been shown in Figure 47 and the exploded view is shown in Figure 48.

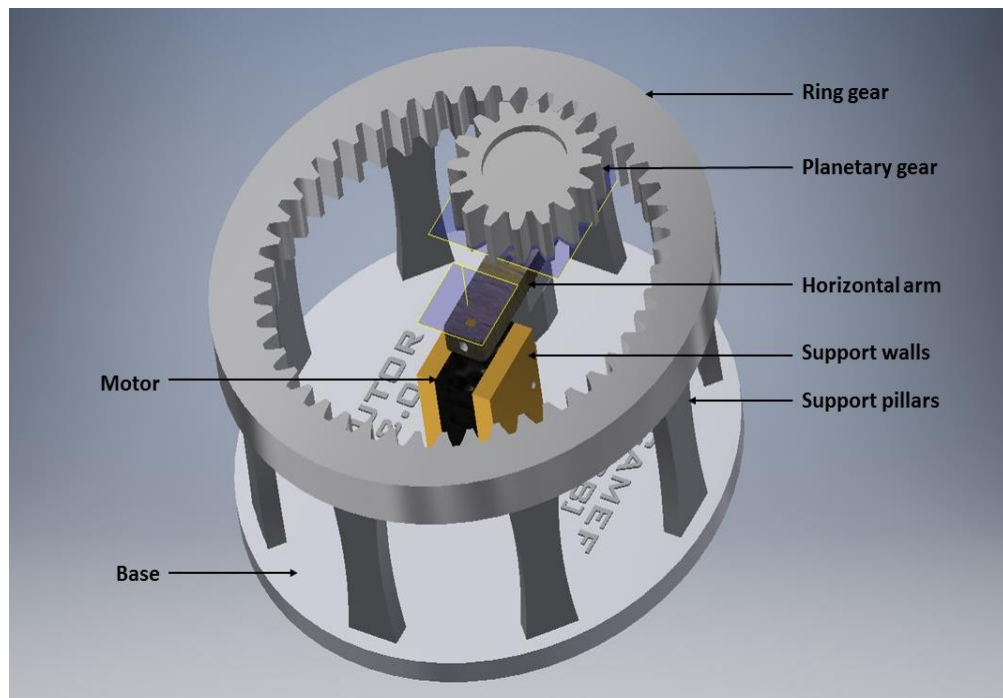


*Fig. 47 Device and its parts*

To make the device compact, the gear system has been designed on the basis of centre distance. In order to generate enough torque at higher speed requirements, the number of teeth in the planetary gear can't be less than 16. Also, to make the outer diameter of the device lower, as well as accommodate the planetary gear and the necessary clearance, the number of teeth on external ring should be optimized. This restricts the gear ratio to 2.88, above which the centre distance increases. The gear ratio between the mating gears was rounded to 2.9, with a module of 2.5 mm. The module was determined by the circular pitch, which again is a function of the number of teeth on the gear. The module is calculated from [102]

$$m = \frac{2a \cos\beta}{14i-9.77} \quad (16)$$

where,  $a$  is the centre distance and  $i$  is the gear ratio, and  $\beta$  is the helix angle (0).

The device is designed with 16 teeth on the planetary gear, 46 teeth on the outer ring gear and a facewidth of 12 mm on both structures to prevent gear failure. The number of teeth on inner gear was calculated from [102]

$$z_1 = \frac{2a \cos\beta}{m(i-1)} \quad (17)$$

The pressure angle was chosen to be 20° (Standard values are 14.5 and 20). Higher pressure angles tend to result in gear teeth with greater bending strength, lower efficiency, and lower contact ratios. But when the number of teeth becomes very small (less than 12), the pressure angle must be increased to prevent undercutting during manufacture.

Once the set of gears were designed, they were put together to assemble the device. The ring gear is held static by means of smaller pillars, while the planetary gear is connected to a horizontal arm. To maintain free rotation of the planetary gear, a bearing is placed in a slot at the bottom end, which in turn is connected to a small cylindrical placeholder and attached to the horizontal arm. The arm is connected to the motor shaft by means of a tightening screw. The device consists of a motor that rotates an arm which carries the magnet around. The magnet sits on the planetary gear which undergoes rotation and a circular translation around the vial which is placed at the centre.

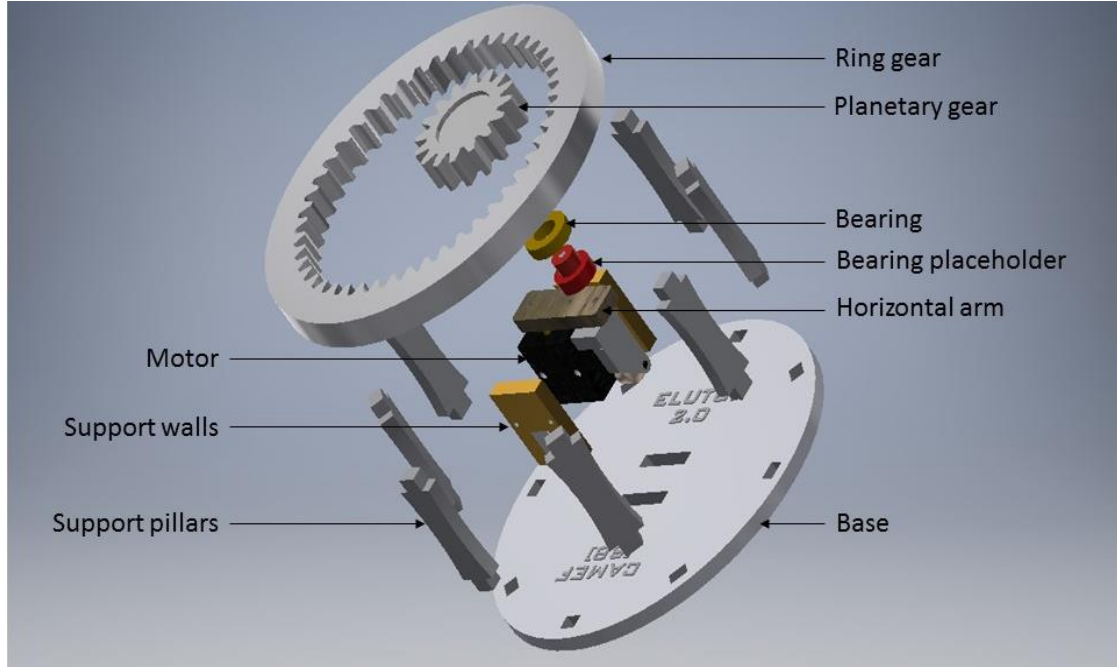


*Fig. 48 Exploded view of the device*

The device has been assembled in the following steps:

1. The base is placed on a flat surface first and eight support pillars are inserted inside in the slots and glued with the base.
2. The ring gear is placed on the top and the top of the pillars are inserted on to the slots present on the bottom of this gear.
3. The motor is placed on the base, in between the two support wall slots.
4. The support walls are placed in their respective slots and screwed with the motor to prevent any lateral movement.
5. The motor shaft is attached to a hole in the horizontal arm.
6. The other end of the horizontal arm is press fitted to a bearing by means of a cylindrical placeholder.

7. The bearing is attached to the base of the planetary gear, which holds the ring magnet.
8. The vial is placed at the middle of the device by means of a clamp.

### **MODIFICATIONS OF THE DEVICE**

A new compact design was developed in order to reduce the form factor of the device. This device also works on the same principle of sun and planetary gear combination. The device description and the working principle of the device has already been given in section 3.6.2. The different parts consisting of this modified device is shown in Figure 48 and the exploded view is shown in Figure 50.

The device consists of the following parts:

- Motor
- Support walls for motor
- Horizontal arms
- Sun gear
- Planetary gears
- Lower gears
- Bearings
- Cylindrical placeholders
- Central support
- Base

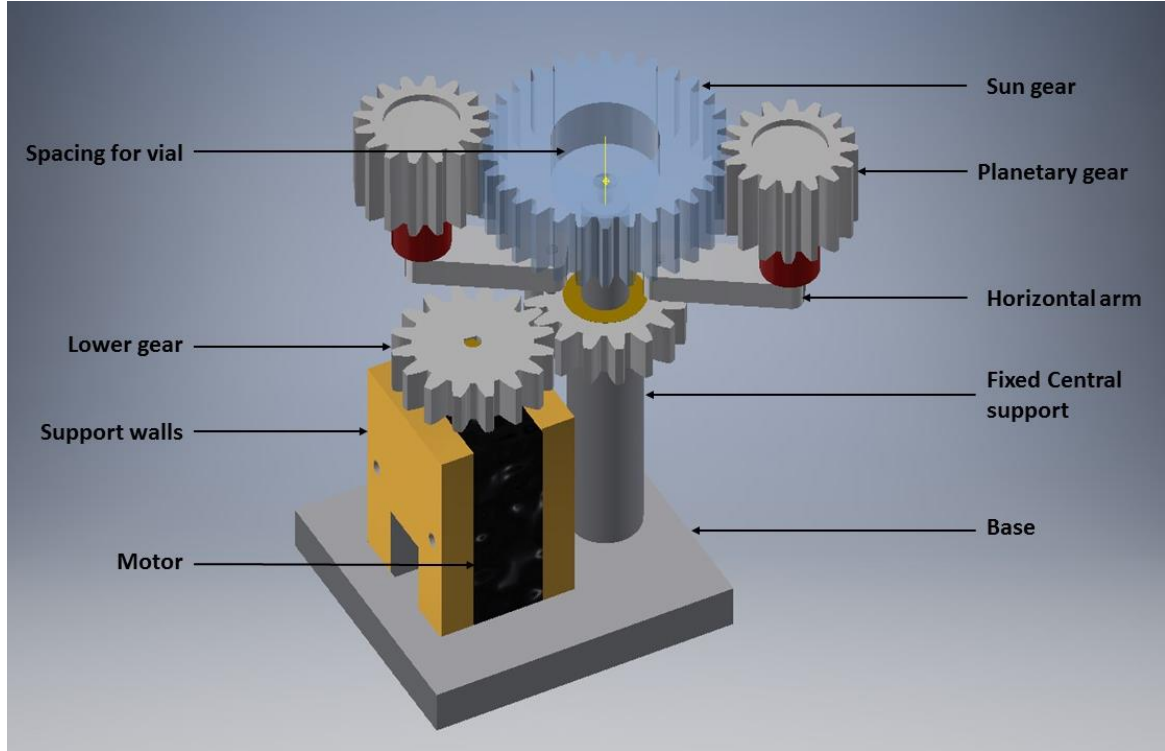


*Fig. 49 Schematic of the modified device and its parts*

The gear combination was designed on a centre design of 30mm at 20° pressure angle. The number of teeth on the central gear was 32 on a gear ratio of 2 and module 1.25mm. Higher facewidth of 15mm was provided to the central gear as compared to the external ones (10mm) to handle greater torque at high speeds. An extra pair of gears are introduced at the bottom. The horizontal arms are made to rotate by the help of these, which supports and aids the revolution of the top external gears around the static gear. The lower gear combination was designed on the basis of centre design, which was valued to 24mm. There are 16 teeth on each gear, with a gear ratio of 1 and module 1.5. The facewidth was chosen to be 10mm and the pressure angle was 20 degrees. These gear combinations now rotate at the same speed as that of the motor, when the central one is connected to the motor shaft.



6. Two small shafts on top of the left lower gear are attached to holes in the horizontal arms.
7. The other ends of the horizontal arms are press-fitted to bearings by means of bearing supports.
8. The bearings are attached to the base of the planetary gears, which holds the ring magnet. Two planetary gears are used to balance the horizontal force applied to the sun gear which mates with the planetary gear.
9. The central fixed gear is screwed on top of the central stand and has a central hole to place the customized vial described in section 3.6.2.

## **APPENDIX C**

### **Machining processes**

#### **Laser micro-machining**

Laser micro machining was used for most of the smaller parts like the base, the support walls, the support pillars and the horizontal arms from acrylic sheets. Acrylic sheets of 6mm thickness were cut into various shapes by laser using a Trotec Speedy 300 Laser engraving machine [103]. It has a 355 cm/second processing speed with an addressable accuracy of 5 $\mu$ m, which works on 12-120 Watts of sealed-off CO<sub>2</sub> laser. A Laser pointer allows precise positioning of the object at the start. A ferromagnetic stainless steel worktable is provided on a granite block to ensure a flat work surface. Honeycomb table insert is used while cutting, which reduces reflection of the beam from the Table and prevents melting of the back. A strong exhaust system and slight vacuum prevents slippage of materials.

The acrylic sheets were placed on the honeycomb table. The design, made in Autodesk Inventor, was exported to a .stl file and loaded to the JobControl software that managed the workflow in the laser cutter. All the required parts are crafted one by one and assembled together.

#### **3D printing**

For intricate parts, where higher resolution, accuracy, precision and surface finish are needed, 3D printing was used. All the gears and bearing supports were made by 3D

printing. The ProJet HD 3000 [104] was used for this purpose. It works on a Multi-Jet Modelling technology, which utilizes photo-curable acrylic. Multi-jet printing is a type of inkjet printing which deposits photo-curable plastic resin from a piezo printhead. The molten material ooze out of multiple nano-jets on the platform, and is cured layer-by-layer by UV light. The printer also provides automatic creation of wax support elements. Non-toxic wax materials provide easy melt away supports within an operating range of 18-28°C. Wax supports of such lower melting point melts away easily without affecting the cured acrylic.

The device has an ultra-high definition resolution of 656 x 656 x 800 DPI (x-y-z), with an accuracy of 25 µm. Higher resolution was required for the mating gears to avoid interference and hence 3D printers were used. Overheating and tooth damages were prevented by allowing for a backlash between all the gears. Allowing a 20° pressure angle provides a scope for ignoring the undercutting, although it requires a closer tolerance on gear-to-gear centre distance.

## APPENDIX D

### Ring Magnets vs Bar Magnets

The ring magnets used in the device is diametrically magnetized, which means that the north and south-seeking poles are on the opposite sides of the circular curvature. The magnetic field strength (H) is defined as the magnetizing force or the measure of the vector magnetic quantity that determines the ability of a magnet to induce a field at a given point. The magnetic field or the magnetic induction (B) induced by a field strength, H, at a point is the vector sum of the magnetic field strength and the resultant intrinsic induction (M). It is also defined as the flux per unit area normal to the direction of the magnetic path. The relation between B and H is given as,

$$B = \mu_0(H + M) \quad (18)$$

where, M is the magnetization of the material.  $\mu_0$  is the magnetic permeability. The radial field on the horizontal plane of the ring magnet is given as,

$$H_r(r, z) = \frac{\sigma}{2\pi\mu_0} \left( \tan^{-1} \left[ \frac{z}{r-r_1} \right] - \tan^{-1} \left[ \frac{z-h}{r-r_1} \right] \right) \quad (19)$$

where, a 2-D analytical approach is assumed with an infinite parallelepiped (Figure 51) whose height is h, z is the vertical height, r is the radius from centre,  $r_1$  is the inner radius and  $\sigma$  is the surface magnetic pole density. [88]

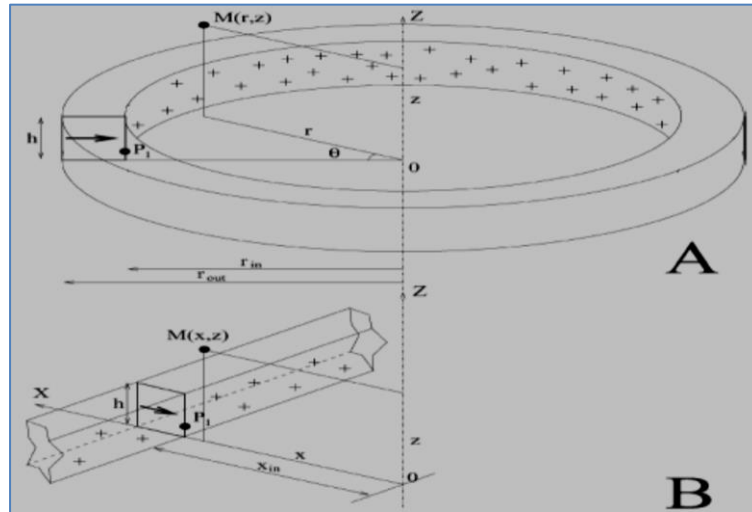


*Fig. 51 A) Ring with symmetric axis ( $z$ ) and radial polarization, B) Infinitely long parallelepiped approach. [88]*

A ring magnet of initial magnetic induction ( $M$ ) of 2.65T is used for the analysis. A ring magnet was chosen as compared to the more commonly available bar magnet in order to minimize the duration of time per rotation cycle when the magnetic field imposed by it is tangential to the surface of the swab. This phenomenon is described in Figures 52 and 53. A bar magnet is assumed that have the same magnetic remanence as that of the ring magnet and equal circumferential dimensions when rotated. The length of this bar magnet is considered to be equal to the diameter of the ring magnet. The rotating bar magnet is shown in Figure 52 (a) for different positions of the circumference from  $x=0$  at the left end to  $x=39.9\text{mm}$  after completing one full circle. The forces offered by the magnets along the circumference are shown in Figure 52 (b). Since the magnetic poles lie on the opposite ends only, the forces act at those two ends. This gives two distinct peaks of the maximum magnetic remanence, with a positive and negative value for either poles.

While rotating around the magnetic particles inside the vial, the bar magnet comes to certain positions when both of them are parallel to each other. This is shown in Figure 52 (c). the lines of forces acting on the magnetic particles unit is shown in red lines, emerging from north poles and ending in south poles. The forces are resolved into two directions: parallel and perpendicular to the magnets. The resultant force parallel to the magnets acts in one direction away from the north pole, while the forces perpendicular to the bar magnet balances each other. Hence, for each rotation of the bar magnet there are two situations when the resultant magnetic forces act parallel to the swab. To avoid this phenomenon, diametrically magnetized ring magnets are used.

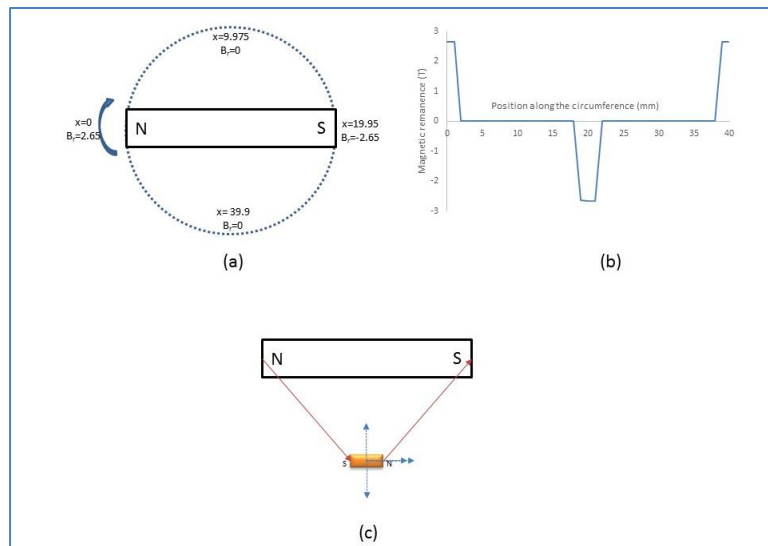


Fig. 52 a) Different positions of the rotating bar magnet along the outer circumference.

b) Magnetic remanence along the circular surface c) acting forces on the magnetic particles when they are placed parallel to each other.

The rotating ring magnet is shown in Figure 53 (a) for different positions on the circumference from  $x=0$  at the bottom to  $x=39.9$ mm, completing one full circle. The ring

magnet has a distinct magnetic distribution, where the north and south poles lies on the opposite curved surfaces. The polarity is maximum at two opposite poles and decreases smoothly to zero at the equator before reversal of polarity. This allows a uniform change in the magnetic field along the surface, which resembles a sinusoidal curve. The change in magnetic remanence along the circular surface is shown in Figure 53 (b). Due to the uniform decrease in pole strength, and their subsequent reversal, the magnetic force experience by the smaller magnets inside the vial never becomes tangential to the swab surface.

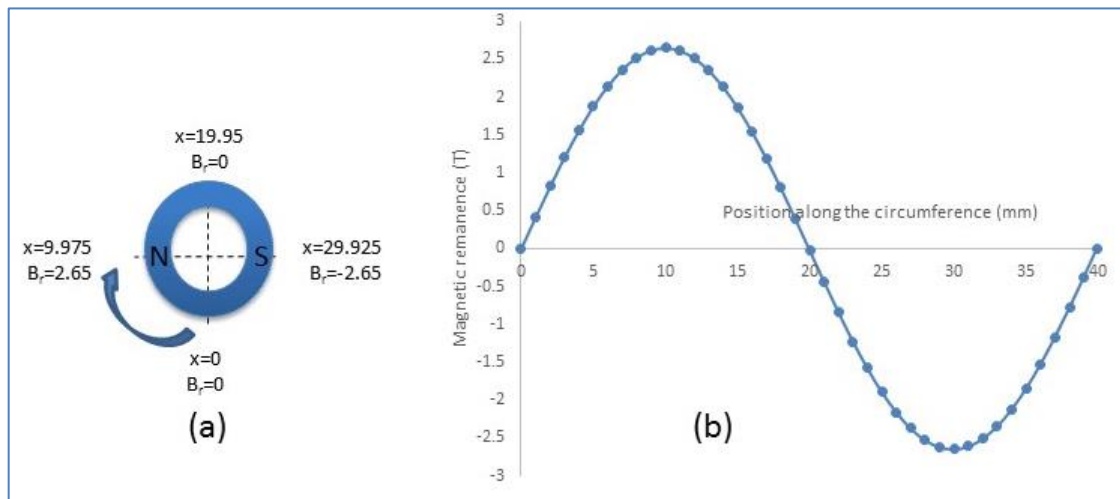


Fig. 53 a) Different positions of the rotating ring magnet along the outer circumference.

b) Magnetic remanence along the circular surface

## References

1. Pang, B. C. M., & Cheung, B. K. K. (2007). Double swab technique for collecting touched evidence. *Legal Medicine*, 9(4), 181-184.
2. Hodges, L. R., Rose, L. J., O'Connell, H., & Arduino, M. J. (2010). National validation study of a swab protocol for the recovery of *Bacillus anthracis* spores from surfaces. *Journal of microbiological methods*, 81(2), 141-146.
3. Dalmaso, G., Bini, M., Paroni, R., & Ferrari, M. (2008). Qualification of high-recovery, flocked swabs as compared to traditional rayon swabs for microbiological environmental monitoring of surfaces. *PDA Journal of Pharmaceutical Science and Technology*, 62(3), 191.
4. Rose, L. (2004). Swab Materials and *Bacillus anthracis* Spore Recovery from Nonporous Surfaces-Volume 10, Number 6—June 2004-Emerging Infectious Disease journal-CDC.
5. Stricklin, S. N. (2013). The Evaluation of Different Collection Methods for the Optimum Recovery of DNA from Bloodstains on Various Surfaces.
6. Chastre, J., Fagon, J. Y., Bornet-Lecso, M., Calvat, S., Dombret, M. C., al Khani, R. H. A. Y. D. A. H., Basset, F., Gibert, C. (1995). Evaluation of bronchoscopic techniques for the diagnosis of nosocomial pneumonia. *American journal of respiratory and critical care medicine*, 152(1), 231-240.
7. Najar, M. S., Saldanha, C. L., & Banday, K. A. (2009). Approach to urinary tract infections. *Indian journal of nephrology*, 19(4), 129.

8. Vinnerås, B., Nordin, A., Niwagaba, C., & Nyberg, K. (2008). Inactivation of bacteria and viruses in human urine depending on temperature and dilution rate. *Water research*, 42(15), 4067-4074.
9. Şahin, S., Saygun, I., Kubar, A., & Slots, J. (2009). Periodontitis lesions are the main source of salivary cytomegalovirus. *Oral microbiology and immunology*, 24(4), 340-342.
10. Voorhees, J. C., Ferrance, J. P., & Landers, J. P. (2006). Enhanced elution of sperm from cotton swabs via enzymatic digestion for rape kit analysis. *Journal of forensic sciences*, 51(3), 574-579.
11. Scherer, K., Mäde, D., Ellerbroek, L., Schulenburg, J., Johne, R., & Klein, G. (2009). Application of a swab sampling method for the detection of norovirus and rotavirus on artificially contaminated food and environmental surfaces. *Food and Environmental Virology*, 1(1), 42.
12. Carrera Fabra, J., Bru Gibert, R., & Comengés, C. A. (2013). *U.S. Patent No. 20,130,295,573*. Washington, DC: U.S. Patent and Trademark Office.
13. Pelssers, E. G. M., & Nieuwenhuis, J. H. (2014). *U.S. Patent No. 8,770,049*. Washington, DC: U.S. Patent and Trademark Office.
14. Biology Online. <http://www.biology-online.org/dictionary/Elution>. Accessed: 28-02-2017.
15. Roehm, N. W., Rodgers, G. H., Hatfield, S. M., & Glasebrook, A. L. (1991). An improved colorimetric assay for cell proliferation and viability utilizing the tetrazolium salt XTT. *Journal of immunological methods*, 142(2), 257-265.

16. Mosmann, T. (1983). Rapid colorimetric assay for cellular growth and survival: application to proliferation and cytotoxicity assays. *Journal of immunological methods*, 65(1-2), 55-63.
17. Riss, T. L., & Moravec, R. A. (2004). Use of multiple assay endpoints to investigate the effects of incubation time, dose of toxin, and plating density in cell-based cytotoxicity assays. *Assay and drug development technologies*, 2(1), 51-62.
18. Ngamwongsatit, P., Banada, P. P., Panbangred, W., & Bhunia, A. K. (2008). WST-1-based cell cytotoxicity assay as a substitute for MTT-based assay for rapid detection of toxigenic *Bacillus* species using CHO cell line. *Journal of microbiological methods*, 73(3), 211-215.
19. Twentyman, P. R., & Luscombe, M. (1987). A study of some variables in a tetrazolium dye (MTT) based assay for cell growth and chemosensitivity. *British journal of cancer*, 56(3), 279.
20. Scudiero, D. A., Shoemaker, R. H., Paull, K. D., Monks, A., Tierney, S., Nofziger, T. H., Currens, M. J., Seniff, D., Boyd, M. R. (1988). Evaluation of a soluble tetrazolium/formazan assay for cell growth and drug sensitivity in culture using human and other tumor cell lines. *Cancer research*, 48(17), 4827-4833.
21. *Back to Basics: What is an immunoassay? ImmunoChemistry Technologies*. <https://immunochemistry.com/2016/07/07/back-basics-immunoassay/>. Accessed: 28-02-2017.
22. Tijssen, P. (1985). *Practice and theory of enzyme immunoassays* (Vol. 15). Elsevier.

23. Pradelles, P., Grassi, J., & Maclouf, J. (1985). Enzyme immunoassays of eicosanoids using acetylcholine esterase as label: an alternative to radioimmunoassay. *Analytical Chemistry*, 57(7), 1170-1173.
24. Ishikawa, E., Imagawa, M., Hashida, S., Yoshitake, S., Hamaguchi, Y., & Ueno, T. (1983). Enzyme-labeling of antibodies and their fragments for enzyme immunoassay and immunohistochemical staining. *Journal of Immunoassay and Immunochemistry*, 4(3), 209-327.
25. Hall, M., Kazakova, I., & Yao, Y. M. (1999). High sensitivity immunoassays using particulate fluorescent labels. *Analytical biochemistry*, 272(2), 165-170.
26. Palecek, E., & Foita, M. (2001). Detecting dna hybridization and damage. *Analytical chemistry*, 73(3), 74A-83A.
27. Diamandis, E. P. (1990). Analytical methodology for immunoassays and DNA hybridization assays—current status and selected systems—critical review. *Clinica Chimica Acta*, 194(1), 19-50.
28. Freeman, W. M., Robertson, D. J., & Vrana, K. E. (2000). Fundamentals of DNA hybridization arrays for gene expression analysis. *Biotechniques*, 29(5), 1042-1055.
29. Zhang, Y., & Ozdemir, P. (2009). Microfluidic DNA amplification—a review. *Analytica chimica acta*, 638(2), 115-125.
30. Gill, P., & Ghaemi, A. (2008). Nucleic acid isothermal amplification technologies—a review. *Nucleosides, Nucleotides, and Nucleic Acids*, 27(3), 224-243.
31. Morisset, D., Stebih, D., Cankar, K., Zel, J., & Gruden, K. (2008). Alternative DNA amplification methods to PCR and their application in GMO detection: a review. *European Food Research and Technology*, 227(5), 1287-1297.

32. Zhang, C., Xu, J., Ma, W., & Zheng, W. (2006). PCR microfluidic devices for DNA amplification. *Biotechnology advances*, 24(3), 243-284.
33. Lab test online: Explaining pathology. <http://www.labtestsonline.org.au/learning/test-index/bone-marrow>. Accessed: 28-02-2017.
34. Myles, M. H. (2015). *U.S. Patent No. 20,150,233,923*. Washington, DC: U.S. Patent and Trademark Office.
35. Shirtcliff, E. A., Granger, D. A., Schwartz, E., & Curran, M. J. (2001). Use of salivary biomarkers in biobehavioral research: cotton-based sample collection methods can interfere with salivary immunoassay results. *Psychoneuroendocrinology*, 26(2), 165-173.
36. Weaver, B. A., Feng, Q., Holmes, K. K., Kiviat, N., Lee, S. K., Meyer, C., ... & Koutsky, L. A. (2004). Evaluation of genital sites and sampling techniques for detection of human papillomavirus DNA in men. *Journal of Infectious Diseases*, 189(4), 677-685.
37. Puritan. Swab Handle Materials & Tip Materials. <http://www.puritanmedproducts.com/resources/swab-handle-tip-materials>. Accessed: 28-02-2017.
38. Giles, R. C. (2008). Improved methods for the elution and extraction of spermatozoa from sexual assault swabs. *Forensic Magazine*, 5(2), 14-21.
39. Lincoln, P. J., & Dodd, B. E. (1973). An evaluation of factors affecting the elution of antibodies from bloodstains. *Journal of the Forensic Science Society*, 13(1), 37-45.

40. Deshpande, A., & White, P. S. (2012). Multiplexed nucleic acid-based assays for molecular diagnostics of human disease. *Expert review of molecular diagnostics*, 12(6), 645-659.
41. Hindiyeh, M., Acevedo, V., & Carroll, K. C. (2001). Comparison of three transport systems (Starplex StarSwab II, the new Copan Vi-Pak Amies Agar Gel collection and transport swabs, and BBL Port-A-Cul) for maintenance of anaerobic and fastidious aerobic organisms. *Journal of clinical microbiology*, 39(1), 377-380.
42. Barber, S., Lawson, P. J., & Grove, D. I. (1998). Evaluation of bacteriological transport swabs. *Pathology*, 30(2), 179-182.
43. Texwipe. Cotton & Cotton / Foam Swabs. <https://www.texwipe.com/products/swabs/high-sorption-cotton.aspx>. Accessed: 28-02-2017.
44. Medical Wire. Dry swabs: Cotton swabs, Rayon swabs, Dacron swabs. <http://www.mwe.co.uk/microbiology-lab-supplies/dry-swabs-cotton-swabs-rayon-swabs-dacron-swabs/> Accessed: 28-02-2017.
45. Puritan™ Calcium Alginate Swabs. <https://www.fishersci.ca/shop/products/puritan-medical-calcium-alginate-swabs-5/p-183523>. Accessed: 28-02-2017.
46. Sherlock, O., Dolan, A., & Humphreys, H. (2010). MRSA screening: can one swab be used for both culture and rapid testing? An evaluation of chromogenic culture and subsequent Hain GenoQuick PCR amplification/detection. *Clinical Microbiology and Infection*, 16(7), 955-959.

47. 3M Enviro swabs.  
[http://solutions.3m.com/wps/portal/3M/en\\_WW/Food\\_Safety/home/Products/one/?PC\\_Z7\\_RJH9U52308M770IC4G5E581080000000\\_nid=VR6MKCBFQNbWGVF7JCOXJgl](http://solutions.3m.com/wps/portal/3M/en_WW/Food_Safety/home/Products/one/?PC_Z7_RJH9U52308M770IC4G5E581080000000_nid=VR6MKCBFQNbWGVF7JCOXJgl) Accessed: 28-02-2017.
48. Copan FLOQ Swabs. <http://www.copanusa.com/products/collection-transport/floqswabs-flocked-swabs/>. Accessed: 28-02-2017.
49. Puritan swabs. <http://www.puritanmedproducts.com/products/P12> Accessed: 28-02-2017.
50. Perry, J. L., Ballou, D. R., & Salyer, J. L. (1997). Inhibitory properties of a swab transport device. *Journal of clinical microbiology*, 35(12), 3367.
51. Quality control of microbiology transport systems; approved Standard. NCCLS document M-40-A, NCCLS, Wayne, PA (2003)
52. Virkler, K., & Lednev, I. K. (2009). Analysis of body fluids for forensic purposes: from laboratory testing to non-destructive rapid confirmatory identification at a crime scene. *Forensic Science International*, 188(1), 1-17.
53. Animireddy, D., Bekkem, V. T. R., Vallala, P., Kotha, S. B., Ankireddy, S., & Mohammad, N. (2014). Evaluation of pH, buffering capacity, viscosity and flow rate levels of saliva in caries-free, minimal caries and nursing caries children: An in vivo study. *Contemporary clinical dentistry*, 5(3), 324-328.
54. Sugano, N., Ikeda, K., Oshikawa, M., Idesawa, M., Tanaka, H., Sato, S., & Ito, K. (2004). Relationship between *Porphyromonas gingivalis*, Epstein-Barr virus infection and reactivation in periodontitis. *Journal of oral science*, 46(4), 203-206.

55. Raggam, R. B., Wagner, J., Michelin, B. D., Putz-Bankuti, C., Lackner, A., Bozic, M., Stauber, R. E., Santner, B. I., Marth, E., Kessler, H. H. (2008). Reliable detection and quantitation of viral nucleic acids in oral fluid: Liquid phase-based sample collection in conjunction with automated and standardized molecular assays. *Journal of medical virology*, 80(9), 1684-1688.
56. Furuta, Y., Aizawa, H., Sawa, H., Ohtani, F., & Fukuda, S. (2004). Varicella-zoster virus DNA level and facial paralysis in Ramsay Hunt syndrome. *Annals of Otolaryngology & Rhinology*, 113(9), 700-705.
57. Lopez-Vidriero, M. T., Charman, J., Keal, E., De Silva, D. J., & Reid, L. (1973). Sputum viscosity: correlation with chemical and clinical features in chronic bronchitis. *Thorax*, 28(4), 401-408.
58. Majima, Y., Harada, T., Shimizu, T., Takeuchi, K., Sakakura, Y., Yasuoka, S., & Yoshinaga, S. (1999). Effect of biochemical components on rheologic properties of nasal mucus in chronic sinusitis. *American journal of respiratory and critical care medicine*, 160(2), 421-426.
59. Gwaltney Jr, J. M. (1996). Acute community-acquired sinusitis. *Clinical Infectious Diseases*, 1209-1223.
60. Smith, J. J., Travis, S. M., Greenberg, E. P., & Welsh, M. J. (1996). Cystic fibrosis airway epithelia fail to kill bacteria because of abnormal airway surface fluid. *Cell*, 85(2), 229-236.
61. Cardiovascular Physiology Concepts. Richard E. Klabunde. <http://www.cvphysiology.com/Hemodynamics/H011.htm>. Accessed: 28-02-2017

62. Greisen, K., Loeffelholz, M., Purohit, A., & Leong, D. (1994). PCR primers and probes for the 16S rRNA gene of most species of pathogenic bacteria, including bacteria found in cerebrospinal fluid. *Journal of clinical microbiology*, 32(2), 335-351.
63. Wain, J., Diep, T. S., Ho, V. A., Walsh, A. M., Hoa, N. T. T., Parry, C. M., & White, N. J. (1998). Quantitation of bacteria in blood of typhoid fever patients and relationship between counts and clinical features, transmissibility, and antibiotic resistance. *Journal of clinical microbiology*, 36(6), 1683-1687.
64. Healthline. Urine pH level. <http://www.healthline.com/health/urine-ph>. Accessed: 28-02-2017.
65. Nakamura, N., Shigematsu, A., & Matsunaga, T. (1991). Electrochemical detection of viable bacteria in urine and antibiotic selection. *Biosensors and Bioelectronics*, 6(7), 575-580.
66. Vasan, S. S. (2011). Semen analysis and sperm function tests: How much to test?. *Indian journal of urology: IJU: journal of the Urological Society of India*, 27(1), 41.
67. Centola, G. M., & Eberly, S. (1999). Seasonal variations and age-related changes in human sperm count, motility, motion parameters, morphology, and white blood cell concentration. *Fertility and sterility*, 72(5), 803-808.
68. Fredricks, D. N., Fiedler, T. L., Thomas, K. K., Mitchell, C. M., & Marrazzo, J. M. (2009). Changes in vaginal bacterial concentrations with intravaginal metronidazole

- therapy for bacterial vaginosis as assessed by quantitative PCR. *Journal of clinical microbiology*, 47(3), 721-726.
69. Dauphin, L. A., Marston, C. K., Bhullar, V., Baker, D., Rahman, M., Hossain, M. J., Chakraborty, A., Khan, S. U., Hoffmaster, A. R. (2012). Swab protocol for rapid laboratory diagnosis of cutaneous anthrax. *Journal of clinical microbiology*, 50(12), 3960-3967.
70. Hulme, P., Lewis, J., & Davidson, G. (2013). Sperm elution: an improved two phase recovery method for sexual assault samples. *Science & Justice*, 53(1), 28-33.
71. Allard, J. E., Baird, A., Davidson, G., Jones, S., Lewis, J., McKenna, L., ... & Teppett, G. (2007). A comparison of methods used in the UK and Ireland for the extraction and detection of semen on swabs and cloth samples. *Science & Justice*, 47(4), 160-167.
72. Lutz, J. K., Crawford, J., Hoet, A. E., Wilkins, J. R., & Lee, J. (2013). Comparative performance of contact plates, electrostatic wipes, swabs and a novel sampling device for the detection of *Staphylococcus aureus* on environmental surfaces. *Journal of applied microbiology*, 115(1), 171-178.
73. Walker, R. E., Petersen, J. M., Stephens, K. W., & Dauphin, L. A. (2010). Optimal swab processing recovery method for detection of bioterrorism-related *Francisella tularensis* by real-time PCR. *Journal of microbiological methods*, 83(1), 42-47.
74. Brown, G. S., Betty, R. G., Brockmann, J. E., Lucero, D. A., Souza, C. A., Walsh, K. S., Boucher, R. M., Tezak, M. S., Wilson, M. C., Rudolph, T., Lindquist, H. D. A. (2007). Evaluation of rayon swab surface sample collection method for *Bacillus* spores from nonporous surfaces. *Journal of applied microbiology*, 103(4), 1074-1080.

75. McDonnell, G. E. (2007). *Antisepsis, disinfection, and sterilization: types, action and resistance*. ASM press.
76. Katharia, R., & Chaudhary, R. K. (2013). Removal of antibodies from red cells: Comparison of three elution methods. *Asian journal of transfusion science*, 7(1), 29.
77. Elutions Prior to Antibody Identification. <https://sites.ualberta.ca/~pletendr/tm-modules/methods/70met-elute-ab.html>. Accessed: 28-02-2017.
78. Kuttath, V. (2015). Removal of Antibodies from Direct Antiglobulin Test Positive Red Blood Cells-A comparison of three elution methods. *Academic Medical Journal of India*, 3(2), 51-54.
79. Roberts, G. H. (2006). Elution Techniques in Blood Bank. *Continuing Education Topics & Issues*. Article 301.
80. Nason, F. L. (1990). *U.S. Patent No. 4,978,504*. Washington, DC: U.S. Patent and Trademark Office.
81. Fleming, B. M. (1988). *U.S. Patent No. 4,789,639*. Washington, DC: U.S. Patent and Trademark Office.
82. Shah, T. M. (2008). *U.S. Patent No. 7,337,907*. Washington, DC: U.S. Patent and Trademark Office.
83. Tuite, J., & Andreotti, P. (2004). *U.S. Patent Application No. 10/866,135*.
84. Asplen, C. H., Gaffney, M. J., Hurst, L. H., Johnson, C. L., Lovrich, N. P., Pratt, T. C., & Schellberg, T. M. (2003). National forensic DNA study report. *National Institute of Justice, Washington, DC*.

85. Gill, P., Jeffreys, A. J., & Werrett, D. J. (1985). Forensic application of DNA 'fingerprints'. *Nature*, 318(6046), 577-579.
86. Tereba, A., Flanagan, L., Mandrekar, P., & Olson, R. (2004). A new, rapid method to separate sperm and epithelial cells. *Profiles in DNA*, 7(2), 8-10.
87. Norris, J. V., Manning, K., Linke, S. J., Ferrance, J. P., & Landers, J. P. (2007). Expedited, chemically enhanced sperm cell recovery from cotton swabs for rape kit analysis. *Journal of forensic sciences*, 52(4), 800-805.
88. Fujita, Y., & Kubo, S. I. (2006). Application of FTA® technology to extraction of sperm DNA from mixed body fluids containing semen. *Legal medicine*, 8(1), 43-47.
89. Lounsbury, J. A., Nambiar, S. M., Karlsson, A., Cunniffe, H., Norris, J. V., Ferrance, J. P., & Landers, J. P. (2014). Enhanced recovery of spermatozoa and comprehensive lysis of epithelial cells from sexual assault samples having a low cell counts or aged up to one year. *Forensic science international: genetics*, 8(1), 84-89.
90. Hucker, G. J., Emery, A. J., & Winkel, E. (1951). The relation of soil film buildup and low surface wetting properties to plastic and china surfaces. *Journal of Milk and Food Technology*, 14, 95-7.
91. Ravaud, R., Lemarquand, G., Lemarquand, V., & Depollier, C. (2008). Analytical calculation of the magnetic field created by permanent-magnet rings. *IEEE Transactions on Magnetics*, 44(8), 1982-1989.
92. Harry, K. H., Turner, J. C., & Madhusudhan, K. T. (2013). Comparison of physical characteristics and collection and elution performance of clinical swabs. *African Journal of Microbiology Research*, 7(31), 4039-4048.

93. All About Magnetization Direction. All about magnetization direction. <https://www.kjmagnetics.com/blog.asp?p=magnetization-direction> Accessed: 28-02-2017.
94. FluoSpheres Fluorescent Microsph. <https://tools.thermofisher.com/content/sfs/manuals/mp05000.pdf>. Accessed: 28-02-2017.
95. Richards, B., Skoletsky, J., Shuber, A. P., Balfour, R., Stern, R. C., Dorkin, H. L., Parad, R. B., Witt, D., Klinger, K. W. (1993). Multiplex PCR amplification from the CFTR gene using DNA prepared from buccal brushes/swabs. *Human molecular genetics*, 2(2), 159-163.
96. Dissolution (chemistry). [https://en.wikipedia.org/wiki/Dissolution\\_\(chemistry\)](https://en.wikipedia.org/wiki/Dissolution_(chemistry)).
97. Freundlich equation. [https://en.wikipedia.org/wiki/Freundlich\\_equation](https://en.wikipedia.org/wiki/Freundlich_equation).
98. M7027 SIGMA. Methyl cellulose. <http://www.sigmaaldrich.com/catalog/product/sigma/m7027?lang=en&region=CA>. Accessed: 28-02-2017.
99. Si, F., Li, B., Margolin, W., & Sun, S. X. (2015). Bacterial growth and form under mechanical compression. *Scientific reports*, 5, 11367. DOI: 10.1038/srep11367.
100. Rojas, E., Theriot, J. A., & Huang, K. C. (2014). Response of Escherichia coli growth rate to osmotic shock. *Proceedings of the National Academy of Sciences*, 111(21), 7807-7812.
101. Ong, Y. L., Razatos, A., Georgiou, G., & Sharma, M. M. (1999). Adhesion Forces between E. coli bacteria and biomaterial surfaces. *Langmuir*, 15(8), 2719-2725.

102. Autodesk Inventor. Design Formulas for Spur Gear Modules and Tooth Numbers.

<https://knowledge.autodesk.com/support/inventor-products/learn-explore/caas/CloudHelp/cloudhelp/2016/ENU/Inventor-Help/files/GUID-A5988CE7-3F46-43F1-A223-502527EDBDC1-htm.html>. Accessed: 28-02-2017.

103. Trotec Laser Engraving Machines.

[https://www.troteclaser.com/fileadmin/content/images/Laser\\_Machines/Speedy\\_Series/laser-engraver-speedy-brochure.pdf](https://www.troteclaser.com/fileadmin/content/images/Laser_Machines/Speedy_Series/laser-engraver-speedy-brochure.pdf). Accessed: 28-02-2017.

104. Visijet EX200.

[http://www.3dsystems.com/products/datafiles/visijet/datasheets/Visijet\\_EX200\\_Info\\_0509.pdf](http://www.3dsystems.com/products/datafiles/visijet/datasheets/Visijet_EX200_Info_0509.pdf). Accessed: 28-02-2017.